AD-A065 566 HUGHES AIRCRAFT CO FULLERTON CALIF GROUND SYSTEMS GROUP F/G 9/5
PHOTOLITHOGRAPHIC TECHNIQUES FOR SURFACE ACOUSTIC WAVE (SAW) DE--ETC(U)
DEC 78 A W DOZIER, W R SMITH DAAB07-75-C-0044
UNCLASSIFIED FR-79-12-40-VOL-2 DELET-TR-75-0044-F-V-2 NL

1 OF 2
AD A065566

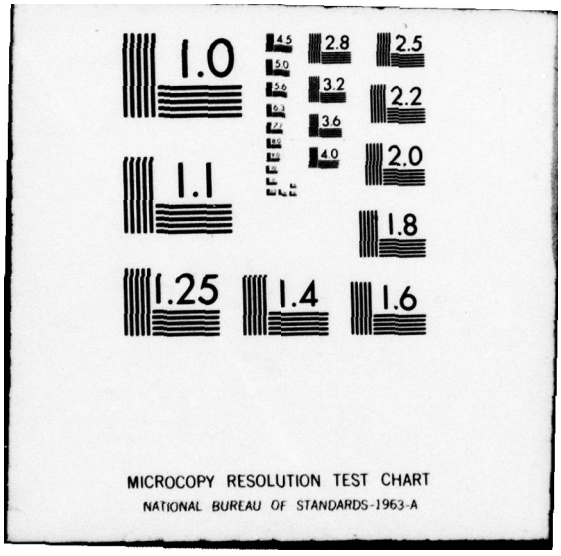
1.0
1.1
1.25
1.4
1.6
1.8
2.0
2.2
2.5
2.8
3.2
3.6
4.0
4.5
5.0
5.6
MICROCOPY RESOLUTION TEST CHART
NATIONAL BUREAU OF STANDARDS-1963-A

LEVEL II

12

10

AD A064197

Research and Development Technical Report
DELET-TR-75-0044-F

AD A065566

# PHOTOLITHOGRAPHIC TECHNIQUES FOR SURFACE ACOUSTIC WAVE (SAW) DEVICES

W.R. SMITH
A.W. DOZIER

GROUND SYSTEMS GROUP
HUGHES AIRCRAFT COMPANY
FULLERTON, CALIFORNIA 92634



July 1975 to 31 December 1978

Final Report: Volume 2 – Technical and Operational Parts 1 and 2





ERADCOM
US ARMY ELECTRONICS RESEARCH AND DEVELOPMENT COMMAND
FORT MONMOUTH, NEW JERSEY 07703

# NOTICES

## Acknowledgements

This project has been accomplished as part of the US Army Manufacturing and Technology Program, which has as its objective the timely establishment of manufacturing, processes, techniques or equipment to insure the efficient production of current or future defense programs.

## Disclaimers

The findings in this report are not be be construed as an official Department of the Army position, unless so designated by other authorized documents.

The citation of trade names and names of manufacturing in this report is not to be constructed as official Government endorsement or approval of commercial products or services referenced herein.

## Disposition

Destroy this report when it is no longer needed. Do not return it to the originator.

(14) FR-79-12-40-VOL-2

UNCLASSIFIED

SECURITY CLASSIFICATION OF THIS PAGE (When Data Entered)

| REPORT DOCUMENTATION PAGE | READ INSTRUCTIONS BEFORE COMPLETING FORM |
|---|---|
| 1. REPORT NUMBER (19) (18) DELET-TR-75-0044-F-V-2 | 2. GOVT ACCESSION NO. (9) 3. RECIPIENT'S CATALOG NUMBER |
| (6) Photolithographic Techniques for Surface Acoustic Wave (SAW) Devices. Volume 2, Technical and Operational Parts 1 and 2. | 5. TYPE OF REPORT & PERIOD COVERED Final rept. 1 Jul 75 - 31 Dec 78 |
| | 6. PERFORMING ORG. REPORT NUMBER FR 79-12-40 |
| 7. AUTHOR(s) Volume 2 – Technical and Operational (Parts 1 and 2) (10) A.W. Dozier W.R. Smith | 8. CONTRACT OR GRANT NUMBER(s) (15) DAAB07-75C-0044 |
| 9. PERFORMING ORGANIZATION NAME AND ADDRESS Hughes Aircraft Company Ground Systems Group Fullerton, California 92634 | 10. PROGRAM ELEMENT, PROJECT, TASK AREA & WORK UNIT NUMBERS 62705A |
| 11. CONTROLLING OFFICE NAME AND ADDRESS Electronics Technology & Devices Laboratory (DELET-MM) USAERADCOM Fort Monmouth, New Jersey 07703 | (11) 12. REPORT DATE Dec 1978 13. NUMBER OF PAGES 128 |
| 14. MONITORING AGENCY NAME & ADDRESS(if different from Controlling Office) (12) 127p. | 15. SECURITY CLASS. (of this report) UNCLASSIFIED 15a. DECLASSIFICATION/DOWNGRADING SCHEDULE |

16. DISTRIBUTION STATEMENT (of this Report)

Approved for puplic release, distribution unlimited.

17. DISTRIBUTION STATEMENT (of the abstract entered in Block 20, if different from Report)

Vol I
AD64197

18. SUPPLEMENTARY NOTES

19. KEY WORDS (Continue on reverse side if necessary and identify by block number)

Surface Acoustic Wave Devices
Bandpass Filters
Tapped Delay Line Filters
Pulse Compression Filters
SAW Processing
SAW Packaging

20. ABSTRACT (Continue on reverse side if necessary and identify by block number)

The object of the program was the establishment of a production capability for surface acoustic wave devices of varied design and material for the purpose of meeting estimated military needs for a period of two years after the completion of the contract, and to establish a base and plans which may be used to meet expanded requirements. The primary requirement was the pilot line production of devices that are reliable, reproducible, and low cost.

DD FORM 1 JAN 73 1473 EDITION OF 1 NOV 65 IS OBSOLETE

UNCLASSIFIED

SECURITY CLASSIFICATION OF THIS PAGE (When Data Entered)

172 370

The first phase of this program required the design, fabricat ion and testing of a total of 60 prototype bandpass, tapped delay line and pulse compression SAW filters on both lithium niobate and ST-quartz. The First Engineering Phase (Phase I) clerical testing demonstrated that the device designs generally met the specifications imposed by the program. Deviations from specification, which required additional test to optimize the levels of padding and/or shunt resistance and capacitance, were resolved during the Second Engineering Phase (Phase II) for the PC-Q, PC-LN and TDL-200. Deviations from the insertion loss specification occurred with the BP-LN and TDL-100 designs. In the former case, a redesign excluding the program-specified multi-strip coupler, was theoretically evaluated, In the latter case, as pointed out in the Hughes proposal, a theoretical analysis precluded the possibility of a specification accommodation. It was necessary to revise the specification for both designs since the customer insisted on utilization of the multistrip coupler in the BP-LN.

Testing of modified semiconductor pin packages during Phase II demonstrated these to be suitable, cost-effective replacements for the machined chassis employed for Phase I. A Quartz orientation problem was highlighted in Phase I and negotiated during Phase II. The quartz vendor implemented an effective screening procedure for the off-orientation problem. However, problems with this vendor continued in the form of substrate surface defects. Other major yield problems encountered during these portions of the program resulted from the dicing and mask making operations. The Phase I and Phase II efforts resulted in a finalized layout, electrical specifications and test procedure for the Third Engineering Phase (Phase III).

Phase III involved fabrication of a larger quantity (50 ea.) of confirmatory devices which were sampled at a high rate and subjected to rigorous life and environmental testing. Phase III was successfully completed with delivery and acceptance of the confirmatory samples. The device configuration is detailed as it existed for Phase III along with assembly details, results and conclusions from the Confirmatory Sample production run (Phase III).

The Fourth Engineering Phase (Phase IV) of the program was pilot line production effort of 150 each of the devices scheduled to be delivered. Solder scaling was identified as a problem area during Phase IV for SAW devices in Phase III packages. New solder seal screening and processing procedures were investigated. In addition, alternative sealing approaches were evaluated. These procedures, Tungsten Inert Gas (TIG) and projection and seam welding were demonstrated to be more compatible with SAW processing. They are especially suitable for high volume production.

Phase IV pilot line production was completed with the delivery of approximately 150 of each of the device types. Some devices were shipped short due to the inability to locate a second source for projection welding, and the extended lead time in reprocurement of packages capable of being sealed by alternate procedures.

Data from Phases I through IV are presented in the Technical and Operational volume of the Final Report. Pilot Line process flow and related documentation are presented in the Process Specification Volume of the Final Report. All inspection positions, pilot run yields, and quality control procedures for Phase IV are presented in the Quality Control Volume of the Final Report. Cost analysis and labor distribution for all facets of the program are covered in a non-distributable volume of the final report.

The program will include preparation of a General Report, which will consist of an analysis of equipment and facilities required to produce SAW devices of the type produced in the Pilot Run at a rate of 500 per month. In addition, an Industry Demonstration was prepared which verbally and visually presented all facets of the MMT program through the Pilot Run.

CONTENTS

## APPENDICES



## LIST OF FIGURES

LIST OF FIGURES (Continued)

## LIST OF TABLES

## PURPOSE

This report presents the results of the three year effort in satisfying the requirements of a Manufacturing Methods and Technology Program devoted to a representative range of surface acoustic wave (SAW) device designs.

The objective of this program was to establish a production capability for the purpose of meeting estimated military needs for a period of two years after the completion of the contract, and to establish a base and plans which may be used to meet expanded requirements. The manufacturing method emphasized the photolithographic fabrication of SAW devices that are reliable and reprodicible at low cost.

Specific tasks included establishing and demonstrating a capability to manufacture the six SAW device designs on a pilot line basis using methods and processes suitable for a production rate of 150 devices per month for each type. In addition, engineering analysis and planning remains to be accomplished for expansion of the manufacturing capability which could accommodate the production of such devices at a rate of 500 each per month. This analysis and planning will be delivered in the General Report.

The program was divided into four phases. The first (Phase I First Engineering Sample) addressed the design, fabrication and analytical testing of six prototype SAW devices that are representative of the major current and potential application of the technology. While these device requirements did not represent the state-of-the-art in an R & D sense, they were of such complexity as to require a serious design effort in each case.

The second phase (Phase II – Second Engineering Samples) was performed to redesign those devices that failed the intended design specification. The net result of this effort was to be functional electrical specification adherence, based on a cost effective packaging commitment.

The third phase (Phase III – Confirmatory Samples) was to test and conform to specification for both the electrical and environmental commitment of the various devices. The final phase (Phase IV – Pilot Run) was to test the reproducibility of those predetermined electrical and environmental requirements in a high volume (500 per month) production environment. A key result of this phase was the establishment of meaningful manufacturing cost data on each device as well as a comparison of this data to the prior low volume efforts of the earlier phases. These data will then be extrapolated to a production rate of 500 per month with assumptions regarding facilities and equipment in the General Report.

## GLOSSARY

| | | |
|---|---|---|
| SAW | – | Surface Acoustic Wave |
| BP-Q | – | Bandpass Filter – ST Quartz Substrate |
| BP-LN | – | Bandpass Filter – Lithium Niobate Substrate |
| TDL-100 | – | Tapped Delay Line Filter – 100 MHz – ST Quartz Substrate |
| TDL-200 | – | Tapped Delay Line – 200 MHz – ST Quartz Substrate |
| PC-Q | – | Pulse Compression Filter – ST Quartz Substrate |
| PE-Q | – | Pules Expansion Filter – ST Quartz Substrate |
| PC-LN | – | Pulse Compression Filter – Lithium Niobate Substrate |
| PE-LN | – | Pulse Expansion Filter – Lithium Niobate Substrate |
| ST | – | Quartz orientation, ST cut ($42^{o}$ 45'), X propagating |
| YZ | – | Lithium Niobate orientation, Y cut Z propagating |
| TIG | – | Tungsten Inert Gas Welding |
| MSC | – | Multistrip Coupler |
| $K^2$ | – | Electromechanical Coupling Constant |
| $f_o$ | – | Center frequency |
| B | – | Bandwidth |
| T | – | Time Delay |
| TXB | – | Time Bandwidth Product |
| VSWR | – | Voltage Standing Wave Ratio |
| DUT | – | Device Under Test |
| $L_{INS}$ | – | Insertion Loss |
| $S_{S.L.}$ | – | Sidelobe Suppression |
| $S_{f.t.}$ | – | Feedthrough Suppression |
| $S_{Spur}$ | – | Spurious Suppression |
| TTS | – | Triple Transit Signal |

# 1.0.0
# STATE OF THE ART IN SAW MANUFACTURING TECHNIQUES AT PROGRAM INITIATION

## 1.0.0 STATE OF THE ART IN SAW MANUFACTURING TECHNIQUES AT PROGRAM INITIATION

Prior to the initiation of this MMT program, devices with electrical performance characteristics comparable to those described herein had been developed in the Hughes R&D laboratory. Particularly in the case of pulse compression filters, devices with even higher center frequencies and time-bandwidth products had been demonstrated. However, there did not exist facilities or techniques for batch-processing any of the devices; they were produced and tested on a one-at-a-time basis. Since the majority of these devices were developed on R&D programs and were not yet installed in deliverable systems, process specifications and SAW crystal documentation procedures had not been developed.

Hughes' first system requirement for a hermetically sealed SAW filter arose at about the same time as the MMT program began. Up to that time, SAW packaging consisted of non-hermetic, machined boxes with slots for the SAW crystals and often with separate compartments for matching circuit elements. While packages of this type are amenable to good suppression of spurious electromagnetic feedthrough, their non-hermeticity and high machining expense render them unsuitable for military systems especially at the higher production levels.

The MMT program and other concurrent Hughes' programs provided the vehicles for developing packaging techniques using commercially available platform and butterfly type packages, and dealing with the increased difficulty of suppressing electromagnetic feedthrough in these packages. It was also the first program where serious consideration was given to multiple-crystal photomask layouts for optimum usage of the crystal substrates whose sizes were determined by availability from the vendors. Other developments which are direct outgrowths of the MMT program included the modification of Hughes' SAW device computer simulation program to output detailed data on transducer geometry, and a study of the inherent limitations in trading off insertion loss, bandwidth, triple transit suppression, and VSWR.[1]

[1] W.R. Smith, "Key Tradeoffs in SAW Transducer Design and Component Specification" 1976 IEEE Ultrasonics Symposium Proceedings, pp 547-552.

# 2.0.0
# SAW DEVICE DESIGN-FIRST ENGINEERING SAMPLES (PHASE I)

## 2.0.0 SAW DEVICE DESIGN-FIRST ENGINEERING SAMPLES (PHASE I)

Phase I of this program was intended to perform the design and electrical test of ten each of the devices outlined in Appendix I. Emphasis was placed on determination of compliance of the designed crystals to the specification in Appendix I. As a result, machined aluminum packages were used in Phase I to eliminate any variables which might result from the package. Emphasis was placed on timely delivery, hence electrical tests were performed in the R&D laboratory where the devices were fabricated. As a result, equipment utilized for this phase was not that which would be utilized to build devices at the production rates required in Phase IV, the pilot run. Electrical test procedures were identical to those utilized for test of devices fabricated under Phase II, Second Engineering Phase. As a result, electrical test procedures will be covered in the section on Phase II.

# 2.1.0
# LINEAR-PHASE BANDPASS FILTER-QUARTZ SUBSTRATE (BP-Q) DESIGN AND EVALUATION

## 2.1.0 QUARTZ LINEAR PHASE BANDPASS FILTER (BP-Q) DESIGN AND EVALUATION

### 2.1.1 Transducer Geometry and Predicted Performance

The quartz bandpass filter (BP-Q) is designed for a 2 MHz, 3 dB bandwidth at a center frequency of 100 MHz. It employs a conventional, in-line transducer configuration with one transducer unapodized and one transducer apodized, as shown schematically in Figure 2.1-1.

a. Unapodized Source – Withdrawal Transducer

The unapodized transducer contains 134 double electrodes, with only the first and last pairs of double electrodes being shown in Figure 2.1-1. This transducer does not have a uniformly alternating electrode polarity sequence but is a "source withdrawal" transducer. The source withdrawal transducer concept is similar to "finger withdrawal" except that no metal fingers are actually omitted from the transducer.[2] Instead, a double electrode appears at every position throughout the transducer, but the polarities sometimes deviate from the normal sequence. When successive double electrodes (4 or more consecutive metal stripes) are connected to the same transducer sum bar, as in the regions denoted "missing or withdrawn sources" in Figure 2.1-2, a region of nearly zero electric field exists and little acoustic excitation occurs. This is in contrast to the regions marked "ordinary sources" between adjacent double electrodes of opposite polarity. Note that an odd number of consecutive missing sources causes a reversal in the polarity sequence of the surrounding ordinary sources, while an even number of consecutive missing sources preserves the polarity sequence.

Source withdrawal is used to implement a desired bandshape by considering the associated impulse response. One adds or deletes sources so that the cumulative number of sources, measured from the beginning of the transducer, is proportional to the integral of (area under) the impulse response, also measured from the beginning of the transducer. When the impulse response function is everywhere positive, only even numbers of consecutive sources are withdrawn; odd numbers of consecutive sources are withdrawn at a point where an impulse response function with negative sidelobes changes sign. The advantage of source withdrawal over conventional finger withdrawal is that a uniform grating of double electrodes is preserved, thus affording maximum suppression of mass/electrical loading reflections.

Note that source withdrawal provides a "staircase approximation" to the continuous impulse response function and is analogous to performing numerical integration by the rectangular approximation. In the present implementation of Hughes' source withdrawal synthesis, a

---

[2] C.S. Hartmann, "Weighting Interdigital Surface Wave Transducers by Selective Withdrawal of Electrodes," 1973 IEEE Ultrasonics Symposium Proceedings, pp 423 – 426.

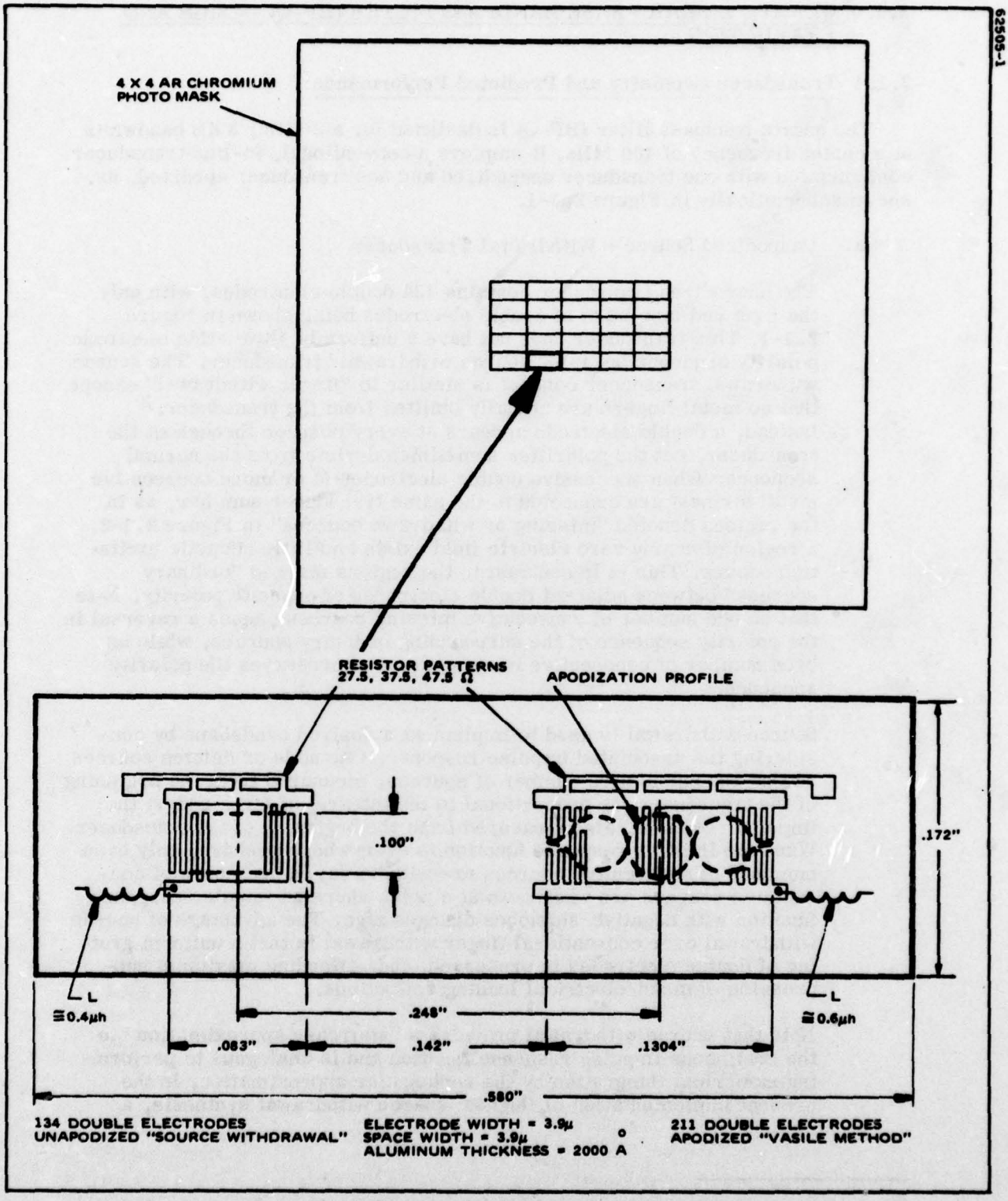


Figure 2.1-1. Schematic of BP-Q Layout

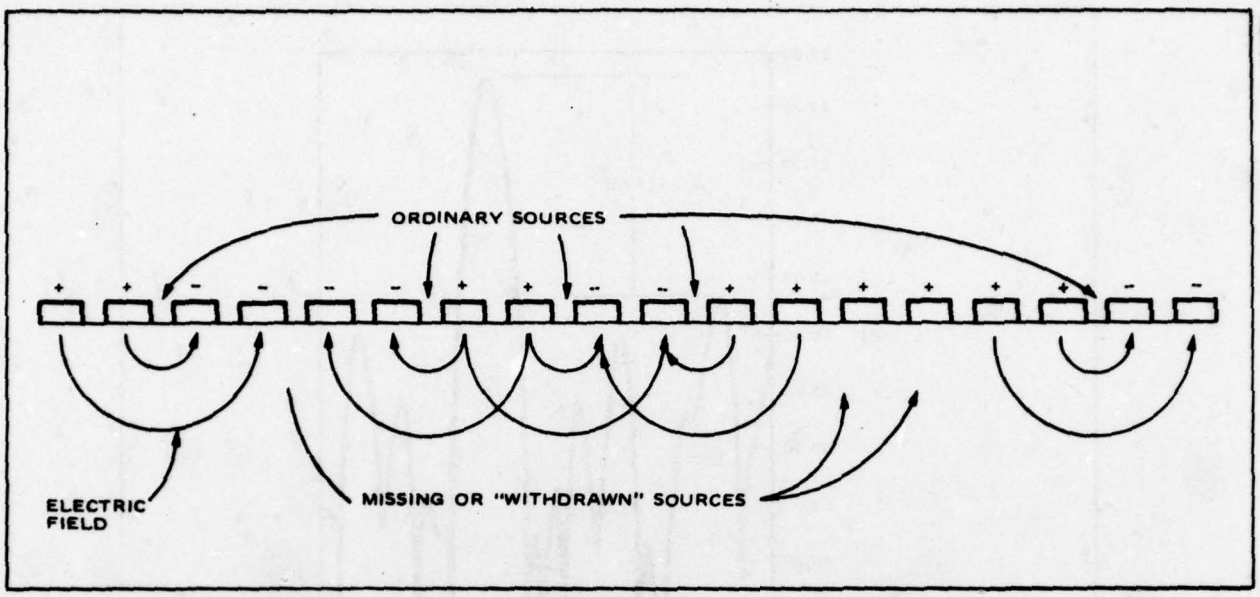


Figure 2.1-2. Example of a Series of Double Electrodes, Nonstandard Polarity Sequence, Illustrating the "Source Withdrawal" Concept

delta-function model[3] is assumed wherein missing sources have strength zero and ordinary sources have strength ±1. The designs are checked by analysis using Hughes' newest, much more accurate circuit model analysis[4] which accounts for the actual electric field distribution under each electrode. It is planned eventually to refine the synthesis procedure to take into effect the results of that circuit model analysis but the present form of synthesis is more than adequate for the BP-Q filter specifications.

For the BP-Q filter, the impulse response for the unapodized, source-withdrawal transducer was chosen as a cosine-squared on a pedestal (Hamming) function since the largest sidelobe in the associated frequency response has a level of -43 dB. Thus, the unapodized transducer is designed to provide considerably more stopband suppression than an ordinary periodic transducer whose (sin X/X) type response would have a near-in, -13 dB sidelobe.

In the BP-Q device, the 134 double electrode source withdrawal transducer has the insertion loss function, (exclusive of electrical tuning and matching) shown in Figure 2.1-3. The highest sidelobe is at -18 dB, much higher than the ideal -43 dB because of the discrete approximation to the desired impulse response. Nevertheless, this

[3] R.H. Tancrell and M.G. Holland, "Acoustic Surface Wave Filters," Proc IEEE, Vol 59, pp 393 – 409, March 1971.
[4] W.R. Smith and W.F. Pedler, "Fundamental – and Harmonic – Frequency Circuit Model Analysis of Interdigital Transducers with Arbitrary Metallization Ratios and Polarity Sequences," IEEE Trans MTT-23, November 1975.

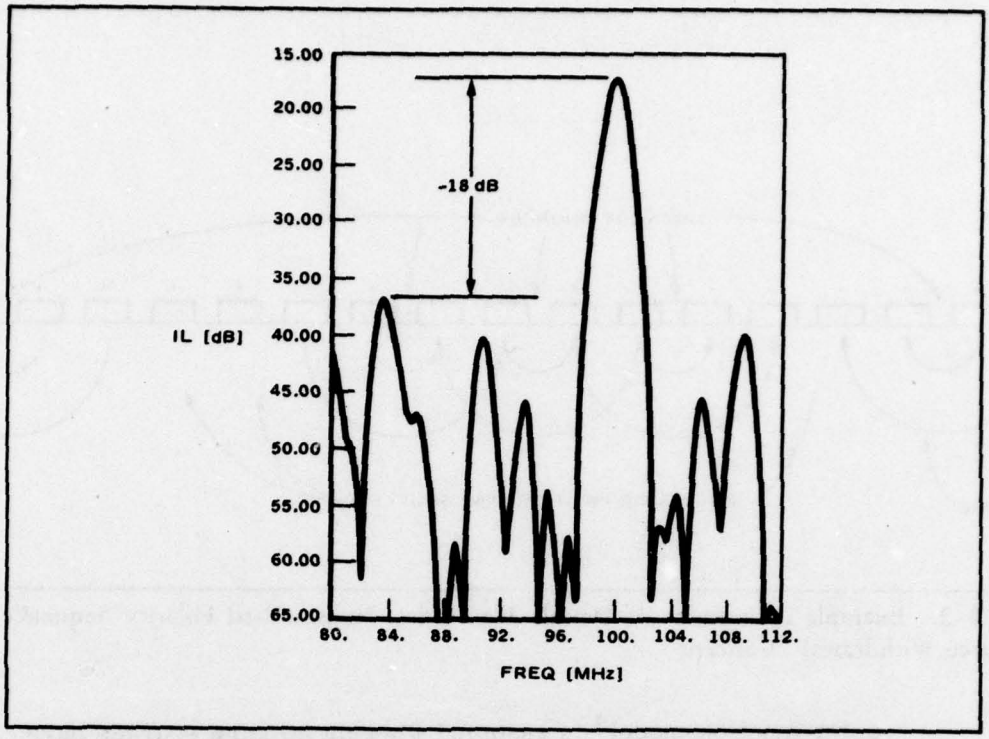


Figure 2.1-3. Predicted Untuned Insertion Loss of the Unapodized Transducer in the BP-Q Filter

double electrode source withdrawal response is superior to the (sin x/x) response of a periodic transducer, not only because the -18 dB sidelobe is lower than the first -13 dB sidelobe of a (sin x/x) periodic transducer, but also because the -18 dB sidelobe is farther from the center frequency and can be suppressed with electrical tuning. In addition, the source-withdrawal transducer has more capacitance than a (sin x/x) periodic transducer of comparable bandwidth and is, therefore, easier to tune inductively.

b. Apodized Transducer

The apodized transducer in the BP-Q contains 211 double electrodes and was designed according to the frequency-eigenfunction method described by Vasile[5]. The apodization profile contains one sidelobe on each side of the main or center lobe. The theoretical insertion loss of this transducer (before tuning) is shown in Figure 2.1-4. The predicted stopband suppression for the apodized transducer exceeds 50 dB so that the stopband suppression of the filter (both transducers combined with series inductive tuning on each) is well in excess of 70 dB exclusive of spurious signals such as bulk waves and feedthrough.

---

[5] C. F. Vasile, "A Numerical Fourier Transform Technique and its Application to Acoustic-Surface-Wave Bandpass Filter Synthesis and Design." IEEE Trans SU-21, pp 7 – 11, January 1974.

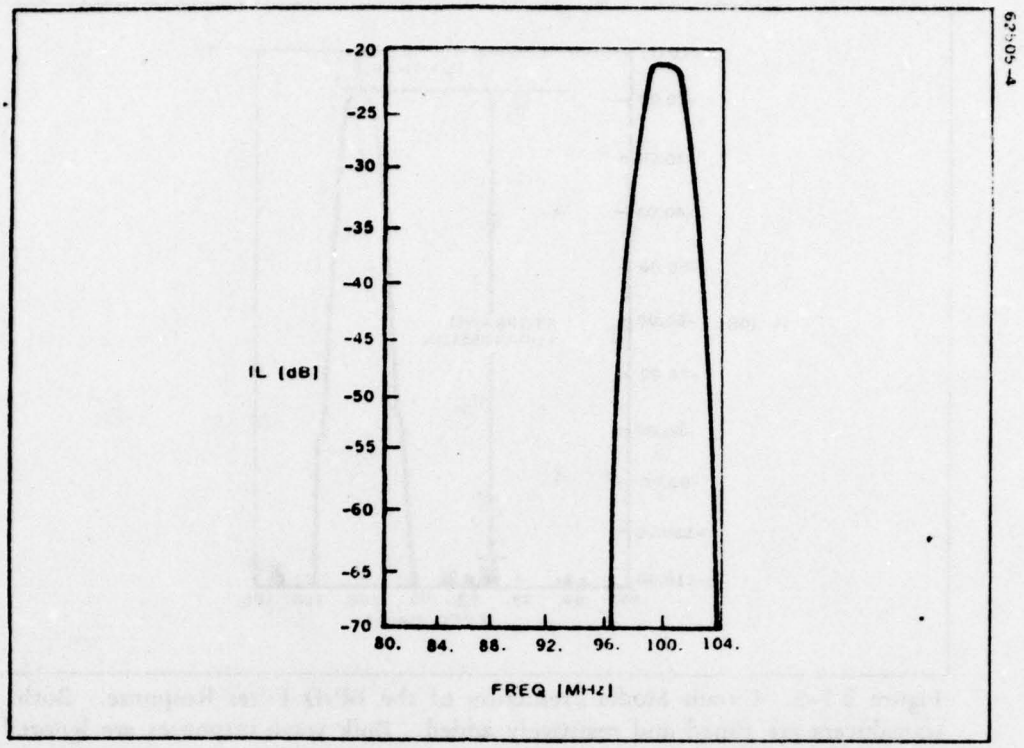


Figure 2.1-4 Predicted Untuned Insertion Loss of the Apodized Transducer in the BP-Q Filter

An alternate design which was considered for the apodized transducer had an additional apodization sidelobe on each end and more than 500 electrodes total. This design would have allowed the apodized transducer to have a response with a dip at the center frequency and two surrounding maxima. When combined with the unapodized source withdrawal transducer, whose response is rounded, this would have provided a net passband shape which is nearly rectangular with a low (40 dB/3 dB) shape factor. The alternate design was not adopted because of the increase in fabrication complexity and substrate area required for a 500 + electrode transducer; also, no particular requirement for the shape factor was specified.

The theoretical response of the filter (surface wave response exclusive of spurious feedthrough and bulk wave signals) was calculated by circuit model analysis. Included in the analysis was series inductive tuning and series padding resistors of 37.5 Ω to lower the VSWR and also the electric Q so that the series-resonant tuning of the transducers does not excessively narrowband the filter. The padding resistors were incorporated in the device by aluminum film strips with three taps to allow adjustment to 27.5, 37.5 or 47.5 ohms, as shown in Figure 2.1-1. Figure 2.1-5 shows the resultant response as predicted by circuit model analysis. The predicted insertion loss is 18 dB, the 3 dB bandwidth is 2 MHz, and the stopband suppression exceeds 80 dB everywhere except for a small knee at -50 dB below midband. The VSWR from impedance calculation (not shown) is less than 1.5. All relevant dimensions

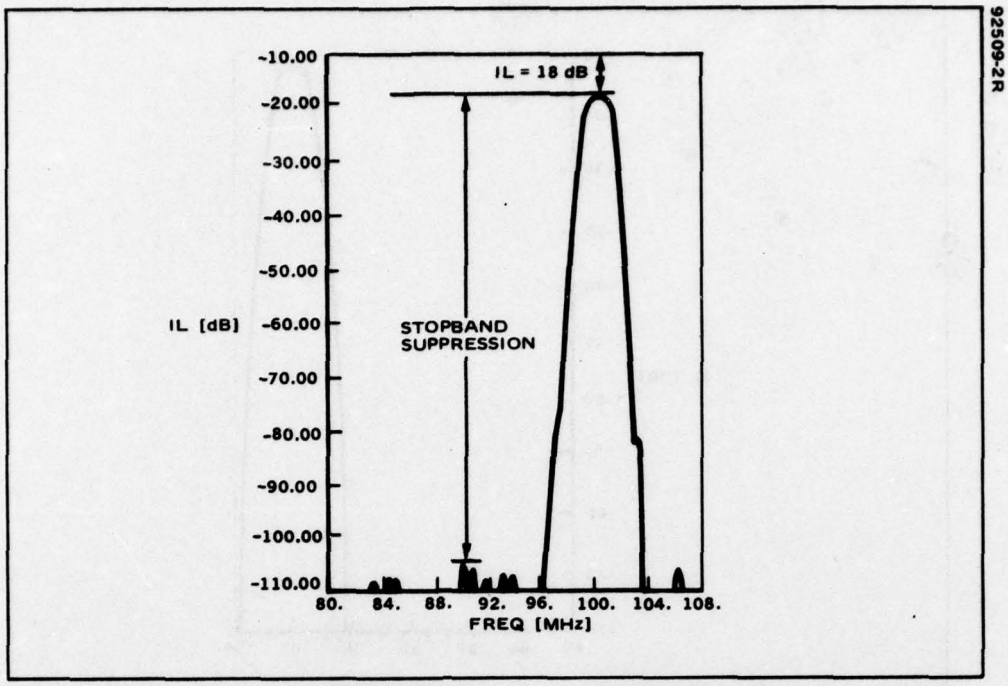


Figure 2.1-5. Circuit Model Prediction of the BP-Q Filter Response. Both transducers are tuned and resistively added. Bulk wave responses are ignored in this calculation

of a single filter structure are shown in the bottom portion of Figure 2.1-1; the center-to-center spacing between transducers is set for 2.0 μs nondispersive delay. The upper portion of Figure 2.1-1 shows the 5 x 5 die layout of the photomask, designed for fabricating 15 filters on a single substrate before dicing. Given the 3 x 0.75 inch substrate, the mask contains redundant patterns to replace those damaged in processing. All the design parameters and circuit model predictions meet the required specifications. The entire design is well within the state-of-the-art for surface wave bandpass filters.

## 2.1.2 Measured Performance

A prototype BP-Q filter was series tuned with variable inductors adjusted for maximum response at 100 MHz and the first tap of the three-tap resistor pattern was broken to achieve the nominal value of 37.5 Ω series padding resistance provided by the center tap. Smith chart impedance plots of the tuned and padded transducers are shown in Figure 2.1-6, where the full sweep range is 10 MHz centered at 100 MHz. For both transducers, the VSWR is well under 1.5 over the 2 MHz operating band.

The measured insertion loss is shown in Figure 2.1-7. The minimum insertion loss is 21 dB, within the specification of 20 dB ± 2 dB. The center frequency is about 100.3 MHz, or 0.3 MHz above the design goal but well within the specification of 100 ± 2 MHz. This slight error in the center frequency is the result of using an ST-X quartz velocity for much thicker metal electrodes than actually used in the design. The 3 dB bandwidth is 2 MHz and the stopband rejection

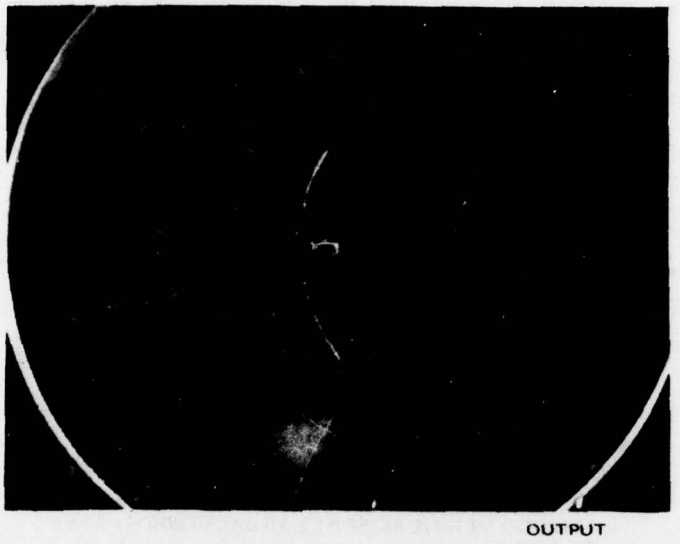


(a) UNAPODIZED TRANSDUCER


(b) APODIZED TRANSDUCER

**Figure 2.1-6. Smith Chart Impedance Plots for the BP-Q Transducers with Series Tuning Inductors and Padding Resistors**

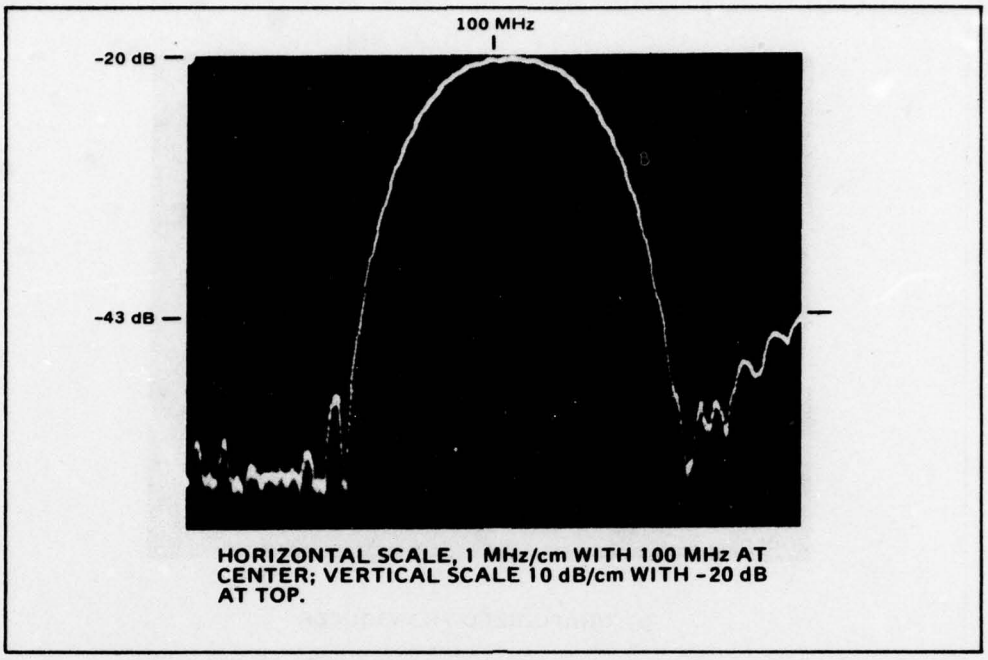


Figure 2.1-7. Measured Insertion Loss of the BP-Q Filter with Series Tuning Inductors and Padding Resistors

exceeds 35 dB everywhere in spite of the spurious bulk wave response which has reached the -43 dB level at 105 MHz, the upper frequency limit of Figure 2.1-7.

Measured parameters for the ten BP-Q filters fabricated for Phase I are compared with SCS 476 (Appendix I) in Table 2.1-1. All the specifications were met by each of the BP-Q devices delivered in Phase I.

TABLE 2.1-1. COMPARISON OF MEASURED PARAMETERS AND SPECIFICATIONS FOR BP-Q FILTERS

| SCS 476 Para No. | Parameter | SCS 476 Dec. 9, 74 | Average of Measured Parameter |
|---|---|---|---|
| 3.10.1.2a | fo (MHz) | 100 ± 2 | 100.2 |
| 3.10.2.2a | $\beta$ at -3 dB (MHz) | 2 ± 0.04 | 2.04 |
| 3.10.3.2a | $\tau$ ($\mu$sec) | 2 ± 0.01 | 1.995* |
| 3.10.4.2a | $\tau$ x $\beta$ | 4:1 | 4.07:1 |
| 3.10.5.2a | Insertion Loss (dB) | 20 ± 2 | 22 |
| 3.10.6.2a | Sidelobe supp (dB) | ≥ 35 | 40 |
| 3.10.7 | Feedthrough supp (dB) | > 50 | 58 |
| 3.10.8 | Spurious supp (dB) | > 35 | 43 |
| 3.10.9 | VSWR | < 1.5:1 | < 1.2:1 |

*See Appendix II for a description of the measurement technique.

# 2.2.0
# LITHIUM NIOBATE LINEAR PHASE BANDPASS FILTER (BP-LN) DESIGN AND EVALUATION

## 2.2.0 LITHIUM NIOBATE LINEAR PHASE BANDPASS FILTER (BP-LN) DESIGN AND EVALUATION

### 2.2.1 Transducer Geometry and Predicted Performance

The lithium niobate bandpass filter is designed for a 30 MHz, 3 dB bandwidth at a center frequency of 150 MHz, and utilizes two apodized transducers with an intervening multistrip coupler (MSC) so that the transducer transfer functions can be multiplied. The unique feature of the Hughes design approach for this type of filter is the use of different center frequencies for the two transducers. In the case of the BP-LN, one transducer operates at a center frequency of 148.0 MHz, and the other at 152.0 MHz, which provides a net center frequency of 150 MHz and staggers the individual transducer responses just enough for maximum ripple cancellation. As indicated schematically in Figure 2.2-1, the amplitude peaks for one transducer are aligned with the amplitude

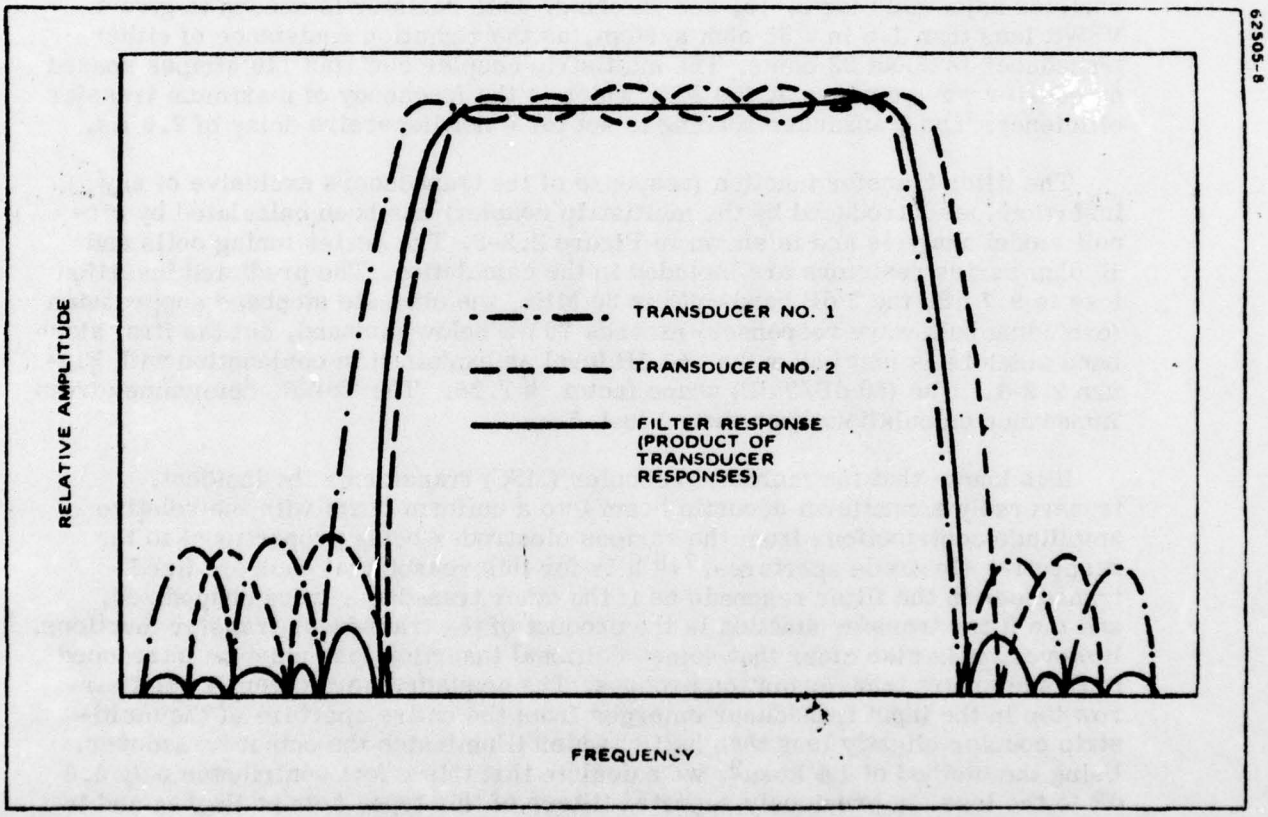


Figure 2.2-1. Schematic of Individual Transducer Responses and Overall Filter Response in a Bandpass Filter with Staggered Transducer Center Frequencies

minima of the other transducer so as to provide a product response (solid line) with a smaller ripple amplitude than that of either transducer alone. The same general type of ripple cancellation occurs for the phase transfer function also. One relatively minor disadvantage of this staggering scheme is that the first stopband ripple on either side of the passband is larger than the remaining stopband ripples because the first stopband ripple is actually in the stopband of one transducer only and just within the passband of the other transducer.

Both transducers in the BP-LN were synthesized using the equiripple or Chebyshev computer[6] program furnished to Hughes by McClellan and Parks of Rice University. In this procedure, one specifies for each transducer a fractional bandwidth, shape factor, number of electrodes, and relative weight factor for trading off passband versus stopband ripple amplitudes. The program then generates the optimum set of tap weights (i.e., the apodization) for a transducer having a uniform ripple amplitude in the passband and a different uniform stopband ripple amplitude. The passband and stopband ripple amplitudes are in the ratio specified and are the minimum possible for the specified number of electrodes, fractional bandwidth, and shape factor.

The geometrical layout of the BP-LN is shown in Figure 2.2-2 (bottom portion), with the top portion showing the 5 x 12 die array on the complete photomask which is used to fabricate 20 BP-LN filters on a single substrate before dicing. The 148 MHz center frequency transducer contains 86 double electrodes and the 152 MHz center frequency transducer contains 88 double electrodes. Both transducers have series inductive tuning and a three-tap, aluminum film resistor adjustable for 5, 10, and 15 ohms. This resistor is needed to give a VSWR less than 1.5 in a 50 ohm system, as the radiation resistance of either transducer is about 22 ohms. The multistrip coupler contains 140 stripes spaced on quarter wave centers at 150 MHz which is the frequency of maximum transfer efficiency. The transducer spacing is set for a nondispersive delay of 2.0 $\mu$s.

The filter transfer function (response of the transducers exclusive of any insertion loss introduced by the multistrip coupler) has been calculated by circuit model analysis and is shown in Figure 2.2-3. The series tuning coils and 10 ohm series resistors are included in the calculation. The predicted insertion loss is 9.7 dB, the 3 dB bandwidth is 30 MHz, the ultimate stopband suppression (excluding bulk wave responses) exceeds 70 dB below midband, but the first stopband sidelobe is just below the -40 dB level as explained in conjunction with Figure 2.2-1. The (40 dB/3 dB) shape factor is 1.28. The VSWR, determined from impedance calculations (not shown) is 1.5.

It is known that the multistrip coupler (MSC) transforms the incident, transversely nonuniform acoustic beam into a uniform beam with the relative amplitude contributions from the various electrodes being proportional to the respective electrode apertures.[7,8] It is for this reason that each apodized transducer in the filter responds as if the other transducer were unapodized, and the filter transfer function is the product of the transducer transfer functions. However, it is also clear that some additional insertion loss must be introduced in this aperture transformation process. The acoustic energy from a very narrow tap in the input transducer emerges from the entire aperture of the multistrip coupler slightly less than half of which illuminates the output transducer. Using the method of La Rosa[9], we calculate that this effect contributes only 0.6 dB to the loss. In previously reported filters of this type, both at Hughes and in

---

[6] J.H. McClellan, T.W. Parks, and L.R. Rabiner, "A Computer Program for Designing Optimum FIR Linear Phase Digital Filters." IEEE Trans AU-21, pp 506 – 526, December 1973.

[7] R.H. Tancrell and H. Engan, "Design Considerations for SAW Filters," 1973 IEEE Ultrasonics Symposium Proceedings, pp 419 – 422.

[8] Hughes Technical Proposal for Acoustic Multistrip Device Techniques, Document #RP73-14-67, pp 2-6 to 2-7a, April 30, 1973.

[9] R. La Rosa and S.J. Karbel, "Equivalent Circuit Representation of Interacting SAW Transducers," 1976 IEEE Ultrasonics Symposium Proceedings, pp 558-563.

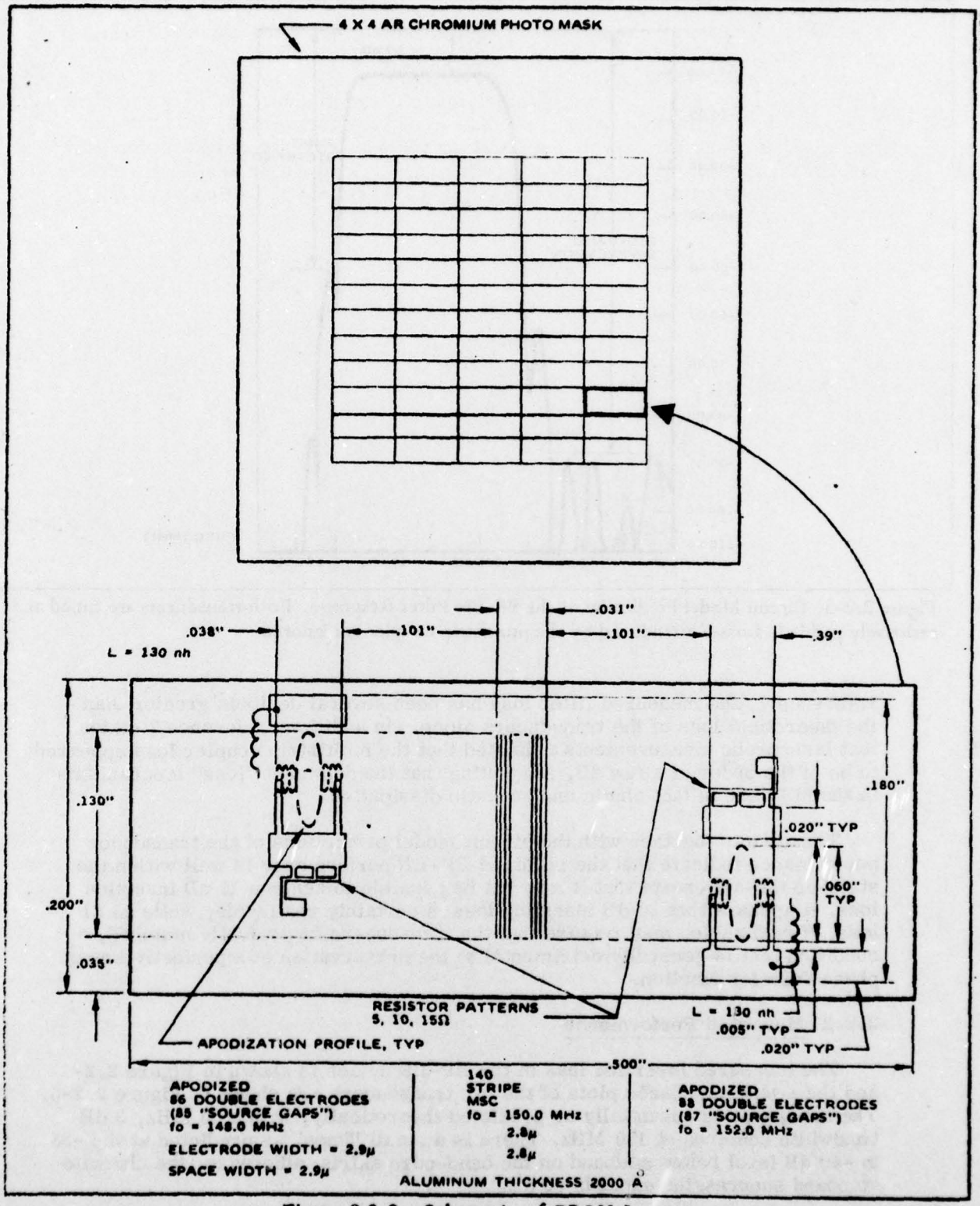


Figure 2.2-2. Schematic of BP-LN Layout

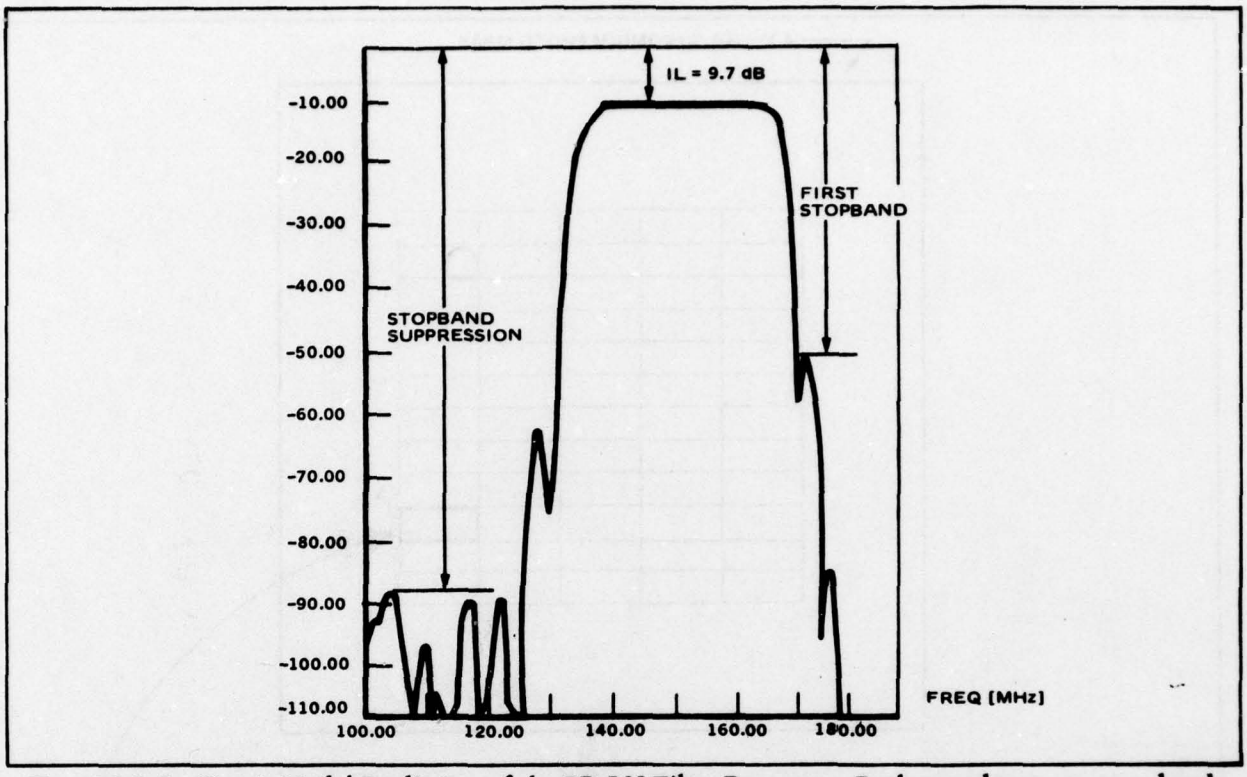


Figure 2.2-3. Circuit Model Prediction of the BP-LN Filter Response. Both transducers are tuned and resistively padded. Losses introduced by the multistrip coupler are ignored.

reference 7, the measured filter loss has been several decibels greater than the theoretical loss of the transducers alone. In addition, reference 7 states that laserprobe measurements indicated that the multistrip coupler loss appeared to be of the order of a few dB, suggesting that the dominant "loss" mechanisms in the MSC are in fact ohmic and acoustic dissipation.

These facts together with the circuit model predictions of the transducer performance indicate that the required BP-LN performance is well within the state-of-the-art except that it may not be possible to achieve 15 dB insertion loss. It appears that 20 dB insertion loss is certainly realizable, while 15 dB loss, if realizable, may require that the transducers be perfectly matched, a condition that is generally detrimental to the preservation of a perfectly linear phase transfer function.

### 2.2.2 Measured Performance

The measured insertion loss of the BP-LN device is shown in Figure 2.2-4 and the swept impedance plots of the two transducers are shown in Figure 2.2-5. The bandshape is essentially as predicted theoretically, with a 30 MHz, 3 dB bandwidth centered at 150 MHz. There is a small "knee" as predicted at the -35 to -40 dB level below midband on the band-edge skirts; otherwise, the ultimate stopband suppression exceeds 50 dB.

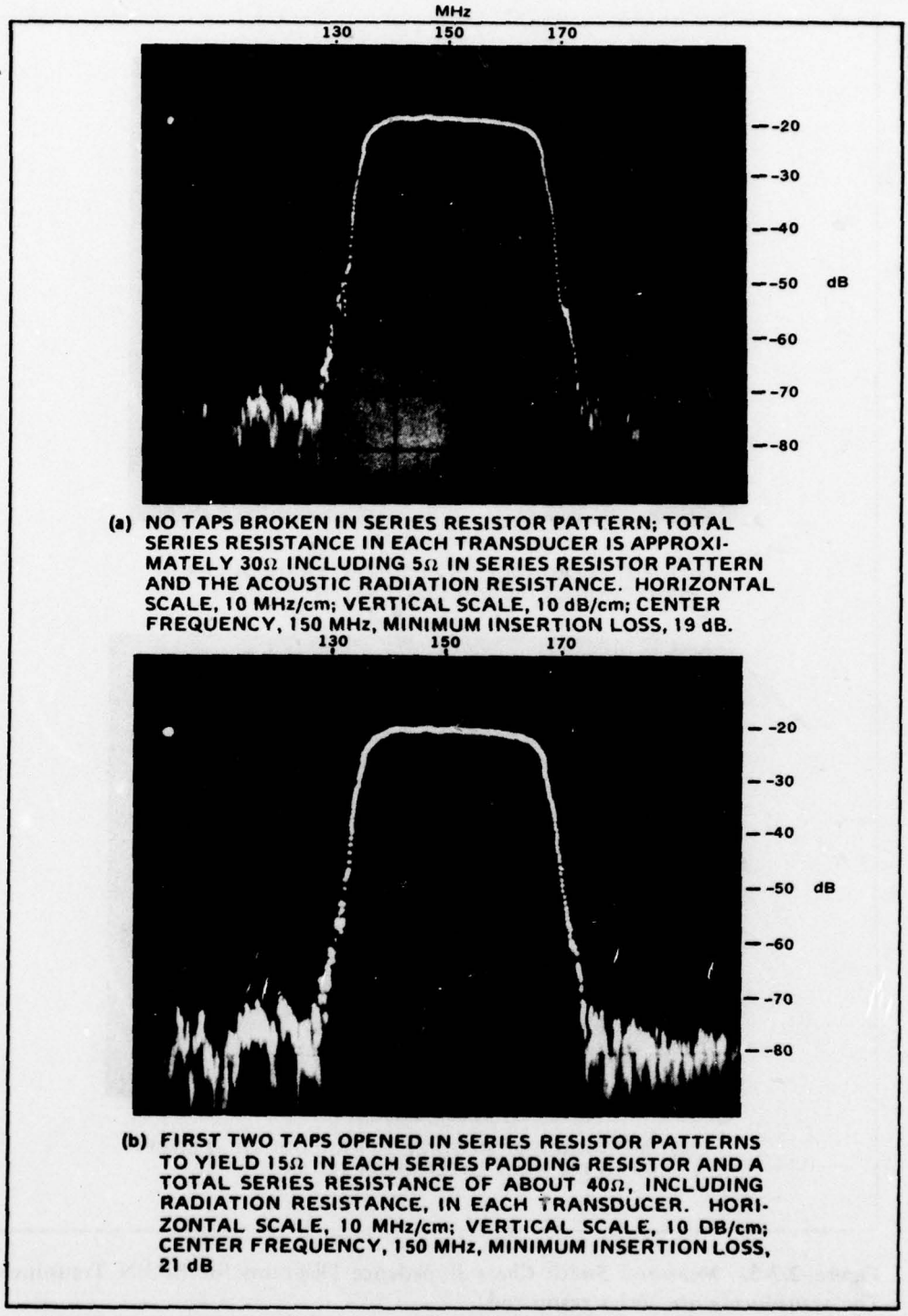


(a) NO TAPS BROKEN IN SERIES RESISTOR PATTERN; TOTAL SERIES RESISTANCE IN EACH TRANSDUCER IS APPROXIMATELY 30Ω INCLUDING 5Ω IN SERIES RESISTOR PATTERN AND THE ACOUSTIC RADIATION RESISTANCE. HORIZONTAL SCALE, 10 MHz/cm; VERTICAL SCALE, 10 dB/cm; CENTER FREQUENCY, 150 MHz, MINIMUM INSERTION LOSS, 19 dB.

(b) FIRST TWO TAPS OPENED IN SERIES RESISTOR PATTERNS TO YIELD 15Ω IN EACH SERIES PADDING RESISTOR AND A TOTAL SERIES RESISTANCE OF ABOUT 40Ω, INCLUDING RADIATION RESISTANCE, IN EACH TRANSDUCER. HORIZONTAL SCALE, 10 MHz/cm; VERTICAL SCALE, 10 DB/cm; CENTER FREQUENCY, 150 MHz, MINIMUM INSERTION LOSS, 21 dB

**Figure 2.2-4.** Measured Insertion Loss of BP-LN Filter with Minimum and Maximum Padding Resistance

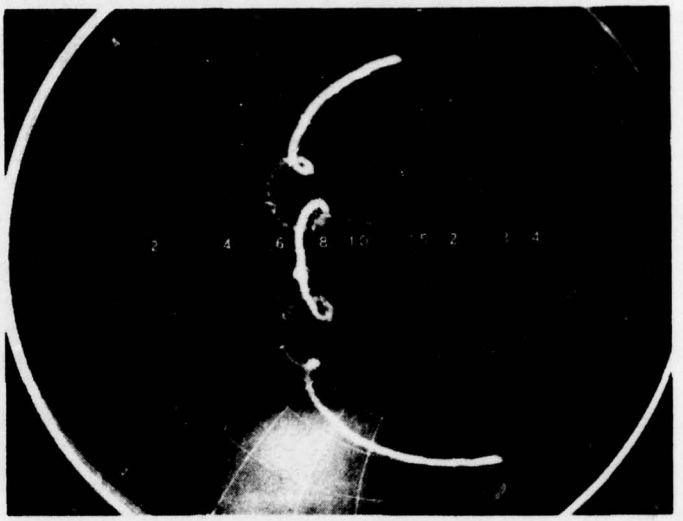

IMPEDANCE

(a) INPUT IMPEDANCE OF APODIZED TRANSDUCER #1 SWEPT OVER 100 MHz CENTERED AT 150 MHz

IMPEDANCE

(b) IMPEDANCE OF APODIZED TRANSDUCER #2 SWEPT OVER 100 MHz CENTERED AT 150 MHz

Figure 2.2-5. Measured Smith Chart Impedance Diagrams for BP-LN Transducers. The transducers are series resonated.

Before opening any taps in the series padding resistor patterns, the insertion loss is 19 dB as shown in Figure 2.2-4(a). In this case, the theoretical transducer radiation resistances are about 22Ω, the resistance in each padding resistor is 5Ω, and it was assumed that there is a remaining parasitic resistance (electrodes, bonds, coils) of about 5Ω when calculating the corresponding loss for the two transducers at 10 dB as shown in Figure 2.2-3.

In order to minimize the VSWR, the first two taps in each padding resistor were opened, raising the built-in padding resistors from 5Ω to 15Ω. The insertion loss is increased by 2 dB (as expected) and the resultant impedance plots for the two transducers are shown in Figure 2.2-4(b). The measured insertion loss is now 21 dB. The total out-of-band resistance, from the impedance plots of Figure 2.2-5, averages about 24Ω, slightly greater than the design estimates of 15Ω in the pad resistor plus 5Ω in the wires, bonds, and coils. More significant is the fact that the effective radiation resistance of the transducers averages about 14Ω rather than the theoretical value of 22Ω. This reduction is due to parasitic capacitance between ground and the transducer with its tuning coil. We can therefore identify from these impedance plots that 15 dB of the total filter loss is in the transducers. Over half of the remaining 6 dB loss must be due to dissipative effects in the MSC, since only 0.6 dB was identified as being due to the transversely nonuniform intensity pattern of the incident acoustic beam. The VSWR is less than 1.5 at the center frequency and over at least most of the passband; unfortunately, there are no frequency markers in Figure 2.2-4 to indicate the -3 dB points. The full sweep width is 100 MHz. A VSWR of 1.5 at the center frequency could have just been realized by opening only one tap on each series resistor pattern, making each padding resistor a 10 ohm resistor (the design value), and the associated insertion loss would be 20 dB.

The performance of this line is essentially as desired except that the insertion loss is 5 dB too high as was anticipated might be the case. Whether or not this can be overcome can be answered only in the light of a theoretical and/or experimental analysis of the MSC operation in this type of filter. Averages of measured parameters for the ten BP-LN filters fabricated for Phase I are compared with SCS 476 (Appendix I) in Table 2.2-1. These devices met most requirements of Appendix I, but failed to meet two performance specifications. First, the VSWR was excessive. However, by increasing the series padding resistance so

TABLE 2.2-1. COMPARISON OF MEASURED PARAMETERS AND SPECIFICATIONS FOR BP-LN FILTER

| SCS 476 Para No. | Parameter | SCS 476 Dec. 9, 74 | Average of Measured Parameter |
|---|---|---|---|
| 3.10.1.2b | fo (MHz) | 150 ± 3 | 150.0 |
| 3.10.2.2b | $\beta$ at -3 dB (MHz) | 30 ± 0.6 | 30.0 |
| 3.10.3.2b | $\tau$ ($\mu$sec) | 2 ± 0.01 | 2.00* |
| 3.10.4.2b | $\tau \times \beta$ | 60:1 | 60:1 |
| 3.10.5.2b | Insertion Loss (dB) | 15 ± 1.5 | 21 |
| 3.10.6.2b | Sidelobe supp (dB) | ≥35 | 40 |
| 3.10.7 | Feedthrough supp (dB) | >50 | 53 |
| 3.10.8 | Spurious supp (dB) | >35 | 39 |
| 3.10.9 | VSWR | <1.5:1 | <2.3:1 |

*See Appendix II for a description of the measurement technique.

that the total input resistance is 50 ohms, at midband, a VSWR of 1.5:1 can just be achieved over the operating band. The second specification deviation is more serious. The use of a multistrip coupler (MSC), as required in Appendix I, results in an insertion loss of up to 6 dB in addition to the usual losses due to transducer mismatch, bidirectionality, and propagation effects. While this effect has been observed previously,[10] it was not attributed to the MSC until after the beginning of the program. The only possible way to comply with the insertion loss requirement is to implement a new design without the MSC. Hughes modelled the BP-LN minus the MSC in order to evaluate the feasibility of meeting the required 15 dB insertion loss. These data will be discussed under Phase II.

---

[10] R.H. Tancrell and H. Engan "Design Considerations for SAW Filters," 1973 IEEE Ultrasonics Symposium Proceedings, pp 419 – 422.

# 2.3.0
# QUARTZ BIPHASE CODED TAPPED DELAY LINE FILTERS (TDL-100 AND TDL-200) DESIGN AND EVALUATION

## 2.3.0 QUARTZ BIPHASE CODED TAPPED DELAY LINE FILTERS (TDL-100 AND TDL-200) DESIGN AND EVALUATION

The two quartz biphase tapped delay lines are so similar that they are both described in this section. They both contain 127 taps coded according to the biphase code which was found to have the lowest sidelobe level.[11] In each case, the total length of the code is 12.7 $\mu$s and the chip rate (bandwidth) is 10 MHz. The only difference is in the center or carrier frequency; the line at 200 MHz requires twice the electrode line resolution as the 100 MHz lines, while the 100 MHz line, having a 10% fractional bandwidth, is harder to match for low insertion loss on low-coupling ST-X quartz.

### 2.3.1 Transducer Geometry and Predicted Performance

The design of the biphase coded tapped delay lines was largely fixed by the specification (Appendix I). The design process is essentially reduced to choosing the number of electrodes per tap and an aperture which allows optimum input transducer matching and insertion loss minimization. An unapodized tapping array has been specified along with the chip rate and code length; the code mentioned above is an obvious choice from the results of a previous ECOM program.

The criteria for choosing the number of electrodes per tap are (1) limiting "mass/electrical loading" reflections as described below; (2) keeping the taps as short as possible so that they are broadband compared to a chip and resemble infinite-bandwidth ideal samplers, while on the other hand, (3) using enough electrodes to minimize insertion loss.

The impact of the number of electrodes on the insertion loss is described in reference 12, where the aperture is also found to be an important factor. The insertion loss is minimized when the capacitive susceptance of the complete 127 tap array equals the 20 millimho load admittance – a general rule for untuned unmatched transducers. This is the case for the 127 tap arrays; only the input transducers are tuned and matched for a VSWR of 1.5. Reference 12 also gives the level of spurious "regenerated" signals in the output tap array which are driven by the voltage that the transducer delivers to the electric load. This spurious signal increases as the insertion loss is reduced and it is sometimes necessary to deliberately trade off insertion loss to reduce the spurious. However, it is found in the quartz tapped delay line designs described below that regenerated signals are not a limiting factor and the tap arrays have thus been designed to minimize insertion loss.

Another important consideration is spurious acoustic reflections caused by electrode mass/electrical loading. Because of the low coupling constant of ST-X quartz, acoustic reflections caused by electrical loading (i.e., shorting of the tangential electric field by the electrodes) are much smaller than those on lithium niobate. It is also found that, by limiting the electrode thickness to about 1250 angstroms, mass loading reflections can be kept acceptably low. It was found in the ASPD study[12] that a convenient "rule of thumb" criterion for adequate

---

[11] P.H. Carr, P.A. DeVito, T.L. Szabo, "The Effect of Temperature and Doppler Shift on the Performance of Elastic Surface Wave Encoders and Decoders," IEEE Trans. Sonics and Ultrasonics, SU-19:3, 357-67 (7/72).

[12] G. Judd, F. Morse, and W.R. Smith "Acoustic Signal Processing Devices" (First Interim Report), Technical Report ECOM-0023-1, Section 3.3.

reflection suppression is established by looking at the pulse train which is acoustically transmitted through the tap array when it is excited with one chip.[13] The performance of a coded line will generally be acceptable if the first transmitted echo (triple transit echo two chip lengths after the main transmitted pulse) is suppressed below the main transmitted pulse by at least the required sidelobe suppression.

Inasmuch as the size of the reflection from one tap increases as the number of "single electrodes" in the tap, this criterion will determine whether single electrodes are acceptable instead of requiring the double electrode taps with interspersed dummy gratings described in reference 13, Section 2.5, Case 2. It is found that ordinary single electrodes are acceptable provided that the number of taps is limited as in the designs adopted below. This is advantageous from the point of view of fabrication simplicity as well as eliminating the higher propagation loss associated with the intertap dummy gratings.

### 2.3.1.1 TDL-100 Design

The TDL-100 geometry is shown in Figure 2.3-1. Assuming 1250 Å aluminum and single electrodes in the taps, it was determined that seven electrodes per tap should give a -27 dB first transmitted echo in the transmission test for mass/electrical loading reflections, or some 5 dB below the theoretical sidelobe level for the chosen code. Mass loading is the dominant source of these reflections. With seven single electrodes in each tap, and aperture of 0.125 inches is predicted for a total capacitive susceptance of 20 millimuo, which minimizes the insertion loss of the untuned, unmatched tap array. The predicted insertion loss of the output tap array alone, neglecting propagation loss, is 23 dB measured to the highest point on the smooth envelope to the insertion loss function whose fine structure is rapidly-varying with narrow peaks above, and nulls below, the envelope.

The input transducer is periodic with 21 double electrodes. It is series-tuned and a series padding resistor is included to lower the VSWR and also the electric Q of the series resonant circuit so that it does not seriously narrowband the desired chip waveform. Double electrodes were chosen in order to increase the transducer capacitance so that the series tuning inductor can be held down to around 1 $\mu$h; larger inductors would suffer a self-resonance problem. The predicted radiation resistance is 15$\Omega$; with a series padding resistor of 45$\Omega$, the input VSWR is 1.2, the input transducer insertion loss is 9 dB and the resonant electric Q is 8.4. Thus, the expected insertion loss for the TDL-100 device is around 35 dB when propagation loss is included.

### 2.3.1.2 TDL-200 Design

The TDL-200 layout is shown in Figure 2.3-2. Each tap contains four single electrodes, which results in a transmitted echo about 25 dB below the main pulse in the transmission criterion for assessing mass/electrical loading reflections. Again, this is lower than the theoretical maximum sidelobe for this code. The predicted insertion loss of the output tap array again measured to the envelope of the insertion loss function with fine structure, is 27 dB.

---

[13] G. Judd, F. Morse, W.R. Smith, and L. Templin, "Acoustic Signal Processing Devices," (Final Report), Technical Report ECOM-0023-F, Section 2.5.

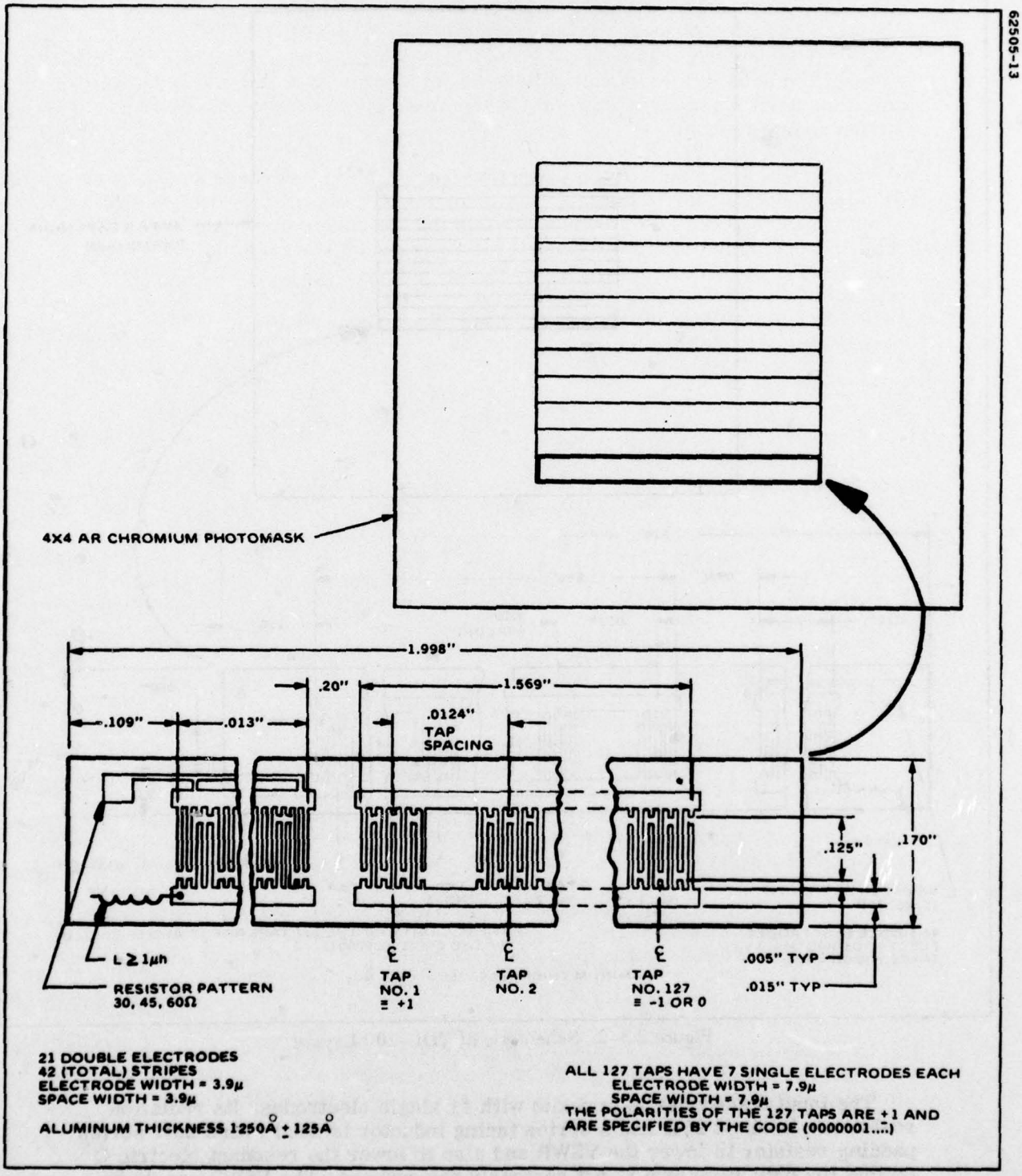


**Figure 2.3-1. Schematic of TDL-100 Layout**

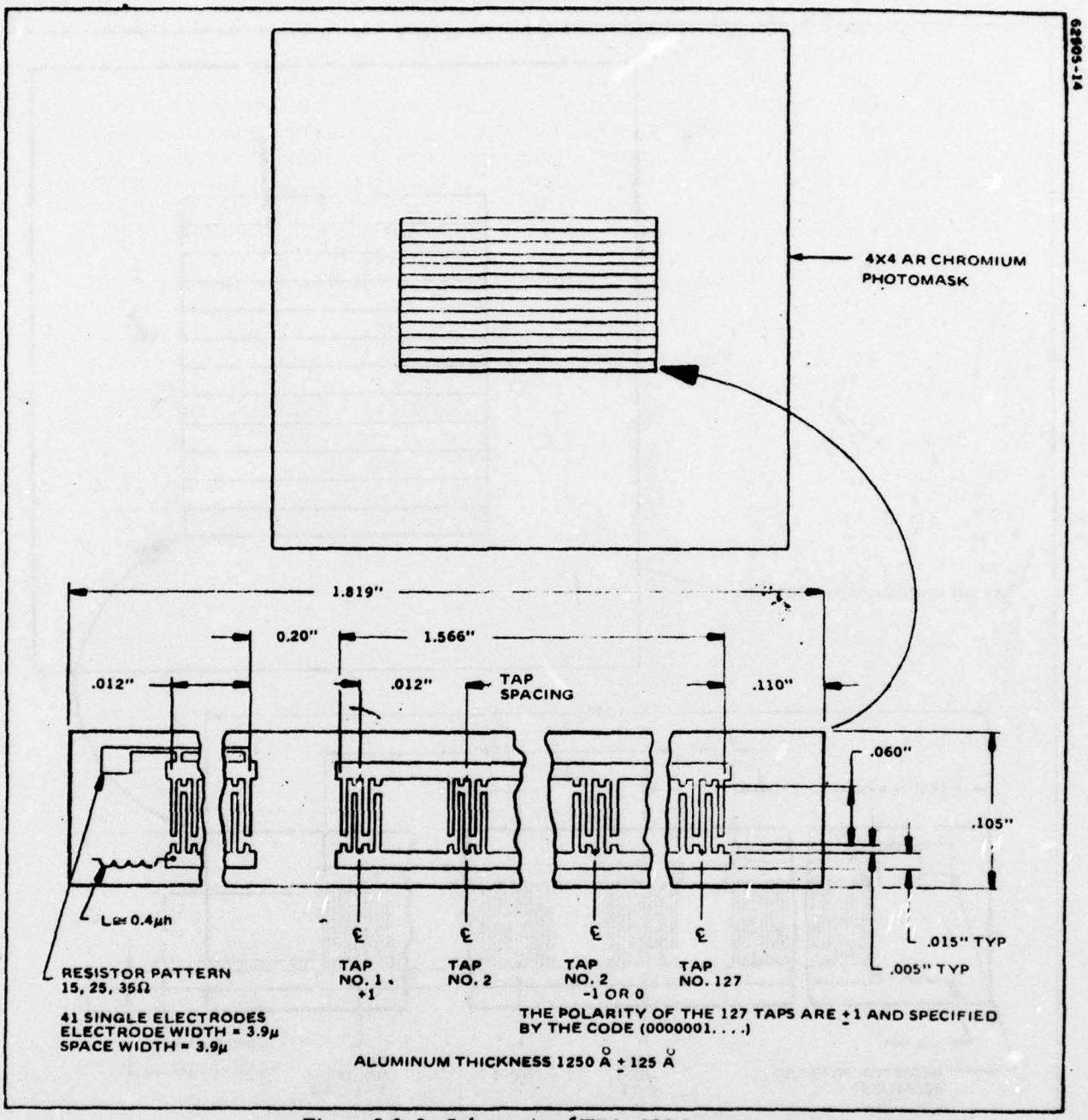


Figure 2.3-2. Schematic of TDL-200 Layout

**The input transducer is periodic with 41 single electrodes. Its radiation resistance is about 25Ω and a series tuning inductor is used with a 25Ω series padding resistor to lower the VSWR and also to lower the resonant electric Q so that the chip waveform is not seriously narrowband. The VSWR should be 1.0 at the center frequency of 200 MHz, with an insertion loss of 6 dB and a resonant electric Q or 4.2. The total insertion loss should be around 35 dB.**

Predicted device performance is largely as desired except that the insertion loss is expected to be at least 35 dB. There are two fundamental reasons why this loss must be accepted, both of which ultimately rooted in the low $k^2$ of ST-X quartz. First, the number of electrodes per tap is limited by the need to avoid large spurious reflections. Second, extra loss must be incurred for use of padding resistors in the input transducers in order to achieve the required bandwidth (especially for the TDL-100) on ST-X quartz. In fact, the resonant electric Q is just barely low enough to prevent narrowbanding in the present designs. Therefore, three effects in the present designs are potentially detrimental to the sidelobe levels: (1) distortion due to electric narrowbanding on the input transducers, (2) acoustic reflections in the tap arrays and (3) failure to apodize the tap arrays to compensate for propagation loss as described in reference 12, Section 3.4. It is hoped that all these effects will result in sufficiently small sidelobe degradation that the sidelobes, although raised above the ideal level of -22.8 dB, will not exceed a level of -19 dB. If the electrical tuning on the input transducers is too narrowband, it can be improved with more series padding resistance, but at a slight additional penalty in insertion loss.

## 2.3.2 Measured Performance

### 2.3.2.1 Impulse Response – TDL-100 and TDL-200

Impulse response data for the TDL-100 and TDL-200 lines can be seen in Figures 2.3-3 through 2.3-5. Series inductive tuning was applied to the input transducers, but the series padding resistors were not adjusted. Swept insertion loss measurements were not made in Phase I, because suitable packaging for suppression of electromagnetic feedthrough was not yet available. In addition, the output tap arrays had a dc-resistance of the order of 100 ohms rather than open circuit, suggesting a possible defect (short) in the arrays.

The impulse response of the TDL-100, before applying series inductive tuning to the input transducer, is shown in Figure 2.3-3. An encouraging feature was the lack of appreciable roll-off due to propagation loss. The insertion loss was lowered some 15 dB by series inductive tuning, resulting in the impulse response shown in Figure 2.3-4. The apparent amplitude is comparable to that shown in Figure 2.3-3 since a 15 dB attenuator was inserted in the test circuit. Note, however, that there is appreciable narrowbanding due to the series inductive tuning, resulting in distortion at the phase-reversals of the code. This problem could be alleviated by opening one or both taps in the series padding resistor to lower the electric Q; however, there may not be sufficient padding resistance in the present design to overcome this narrowbanding effect. The nominal electric Q is about 8, which is rather high for use with an input transducer whose acoustic fractional bandwidth is 0.1.

The impulse response of the TDL-200, with series inductive tuning, is shown in Figure 2.3-5. Here, electrical narrowbanding was not a major problem inasmuch as the nominal series resonant electric Q of the input transducer was less than 5 while the acoustic fractional bandwidth is only 0.05. The principal problem evident in the preliminary TDL-200 measurement is a roll-off of about 10 dB from the first to last tap. Because the taps are not apodized to compensate for propagation loss, some roll-off was anticipated although it was not expected to exceed 3 to 5 dB. A first attempt to reduce the roll off consisted of bonding the output leads near the far end of the tap array. This resulted in reduction of the roll-off to about 5 dB. Increased compensation could be achieved by using

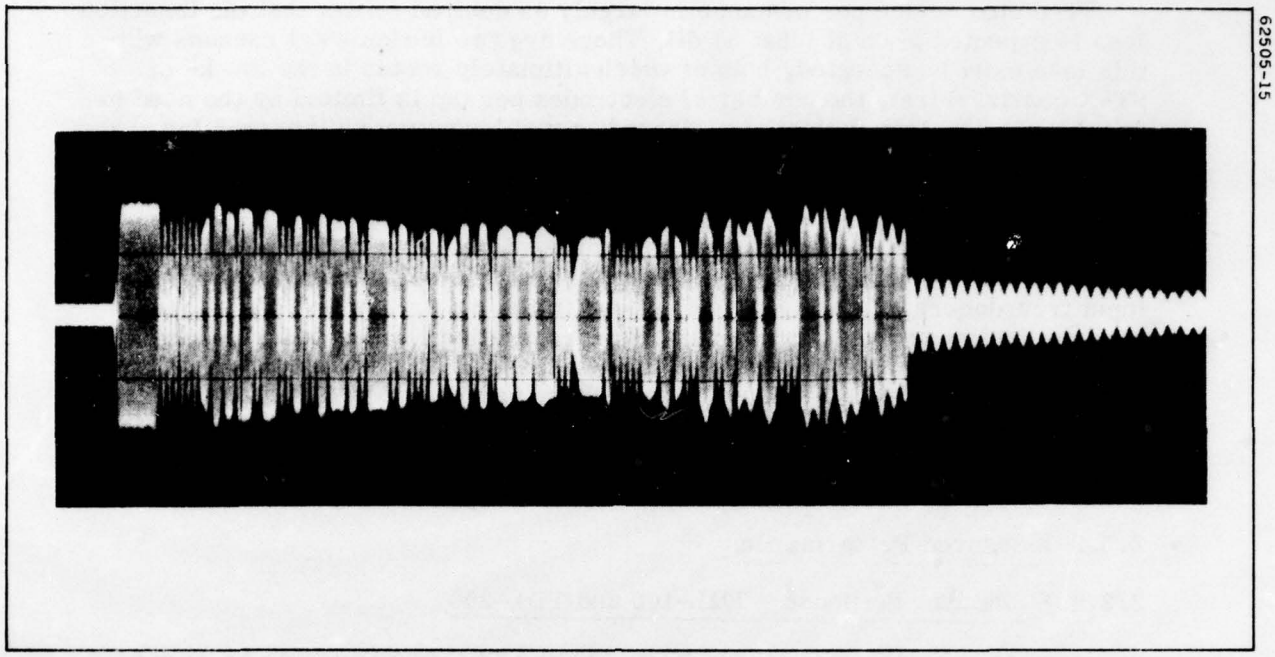


Figure 2.3-3. Short Pulse Response of the TDL-100 Prior to Transducer Tuning. Horizontal scale 1.0 μs/cm, vertical scale 0.05 volt/cm.

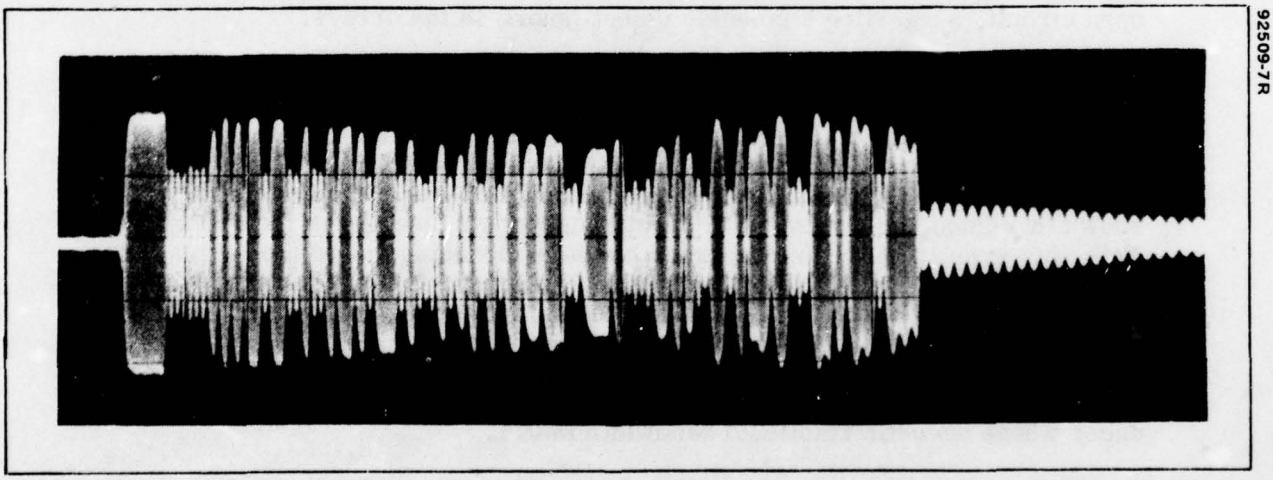


Figure 2.3-4. Short Pulse Response of the TDL-100 After Transducer Tuning. Horizontal scale 1.0 μs/cm, vertical scale 0.05 volt/cm. A 15 dB attenuator was inserted in the test circuit.

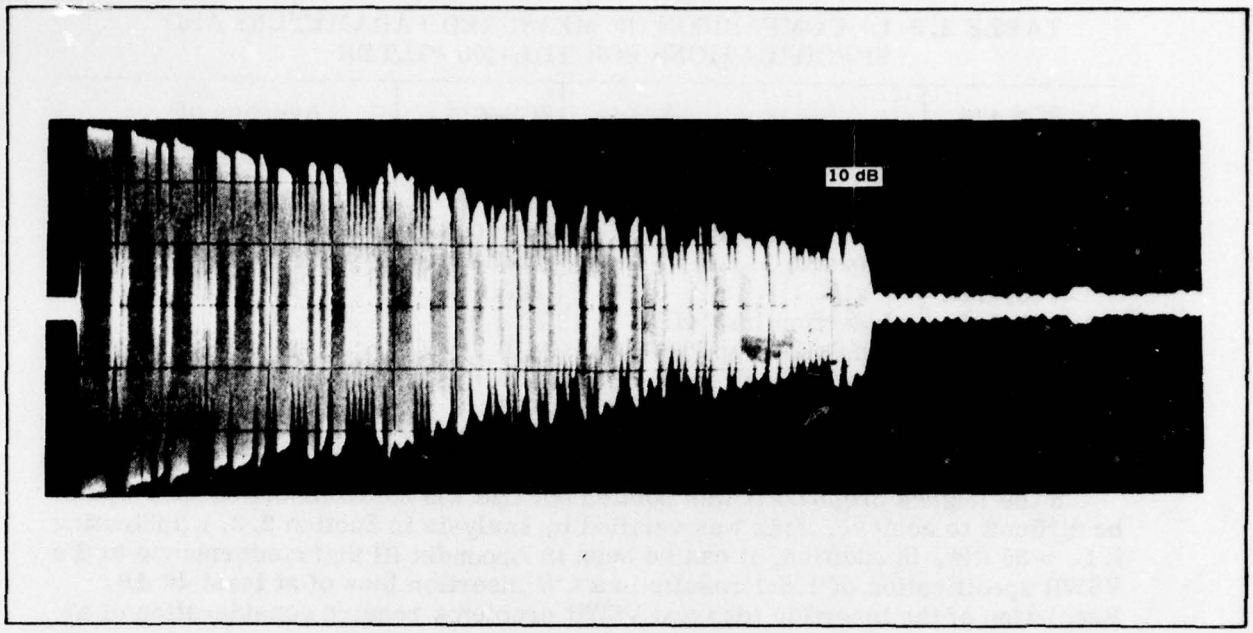


Figure 2.3-5. Response of the Tuned TDL-200 to a 0.1 μsec, 200.086 MHz pulse. Horizontal scale 1.0 μs/cm, Vertical scale 0.05 volt/cm.

more electrodes in the "late" taps than in the "early" taps, since apodization is prohibited in the program specification.

In each of the TDL impulse response photographs (Figures 2.3-3, -4, -5) a series of trailing sidelobes is seen following the main output signal of duration 12.7 μs. These sidelobes are caused by acoustic reflections within the tap array. The dominant type of spurious reflected output signal is a double transit echo (once-reflected, backward acoustic wave) detected by an "earlier" output tap than the one causing the reflection. Each sidelobe is the sum of all double transit echos having the same value of delay; the (n+1) sidelobe corresponds to double transit signals whose backward travel distance is one tap-spacing more than those producing the n-th sidelobe. It was confirmed that the TDL devices are operating with the correct code, center frequencies, and signal time-duration.

2.3.2.2 Measured Performance – TDL-100 (100 MHz Lines)

Average measured parameters of the Phase I TDL-100 filters are compared with SCS 476 (Appendix I) in Table 2.3-1. Typical Smith chart impedance plots for the transducers are shown in Figure 2.3-6. Typical swept frequency response (99.5 – 100.5 MHz) and response to a 50 nanasecond pulse are shown in Figure 2.3-7, while the recompressed pulse (amplified to show sidelobes) and the swept frequency response (75 – 125 MHz) are shown in Figure 2.3-8.

The following parameters complied with the following specified values: center frequency ($f_o$), bandwidth ($\beta$), time delay ($\tau$), time-bandwidth product ($\tau \times \beta$), and feed-through suppression. Discrepancies were as follows: insertion loss is 18 dB instead of the specified 19 dB, spurious echo suppression is typically 28 dB rather than exceeding 35 dB, and the input transducer VSWR varies over the passband so as to be <6:1 everywhere (<3:1 at midband) as compared to specification of <1.5:1.

TABLE 2.3-1. COMPARISON OF MEASURED PARAMETERS AND SPECIFICATIONS FOR TDL-100 FILTER

| SCS 476 Para No. | Parameter | SCS-476 Dec. 9, 74 | Average of Measured Parameter |
|---|---|---|---|
| 3.10.1.3a | fo (MHz) | 100 ± 2 | 100.0 |
| 3.10.2.3a | $\beta$ at -3 dB (MHz) | 10 ± 0.2 | 10.0 |
| 3.10.3.3a | $\tau$ ($\mu$sec) | 12.7 ± 0.01 | 12.7 |
| 3.10.4.3a | $\tau$ x $\beta$ | 127:1 | 127:1 |
| 3.10.5.3a | Insertion loss (dB) | 30 ± 3 | 40 |
| 3.10.6.3a | Sidelobe supp (dB) | ≥19 | 15 to 18 |
| 3.10.7 | Feedthrough supp (dB) | >50 | 60 |
| 3.10.8 | Spurious supp (dB) | >35 | 28 |
| 3.10.9 | VSWR | <1.5:1 | <6:1 |

In the Hughes proposal it was pointed out that the 30 dB insertion loss would be difficult to achieve. This was verified by analysis in Section 2.3.1 (indicating I. L. = 35 dB). In addition, it can be seen in Appendix III that conformance to the VSWR specification of 1.5:1 results in a CW insertion loss of at least 46 dB. Resolution of the insertion loss and VSWR problems require consideration of a number of interrelated parameters.

1. The VSWR specification for the input transducer cannot be met using the selected series L-R matching technique without incurring significant increases in insertion loss. The theoretical basis for this conclusion is presented in Appendix III. This tradeoff can be improved somewhat by using L-C matching networks such as quarter wave transformers and J-inverter networks. However, Hughes feels these are unacceptable because of their complexity and cost. Rather than constrain the VSWR, Hughes recommends that the matching be designed to optimize the tradeoff between insertion loss and biphase-coded waveform distortion. The effect of increased VSWR on system performance is discussed in Appendix IV.

2. Even when this optimum tradeoff is obtained, the specified insertion loss cannot be achieved. In fact, a better method of specifying the loss should be developed. The insertion loss spectrum of a typical biphase coded TDL fluctuates rapidly about a $(\sin x/x)^2$ function. Measurement of the average loss function would be prohibitively complex, and Hughes has arbitrarily chosen to use the minimum insertion loss value as the specification. Unfortunately, this value depends on the selected code and is therefore not useful for arbitrary codes. A more meaningful specification would be to operate the TDL as a matched filter and to measure the level of the correlation peak relative to the level of a conjugate-coded input waveform. This value would correspond to the sum of the insertion loss from the input transducer to an individual output tap and the correlation gain, which for both of the TDL's is $20 \log_{10} 127 = 42.1$ dB. The advantages of this method are that it provides a direct measure of the parameter which is detected in a typical receiver application and that the measurement depends only on N, the number of code chips, and not on the code sequence. The actual specification will have to be developed during Phase II (Second Engineering Phase).

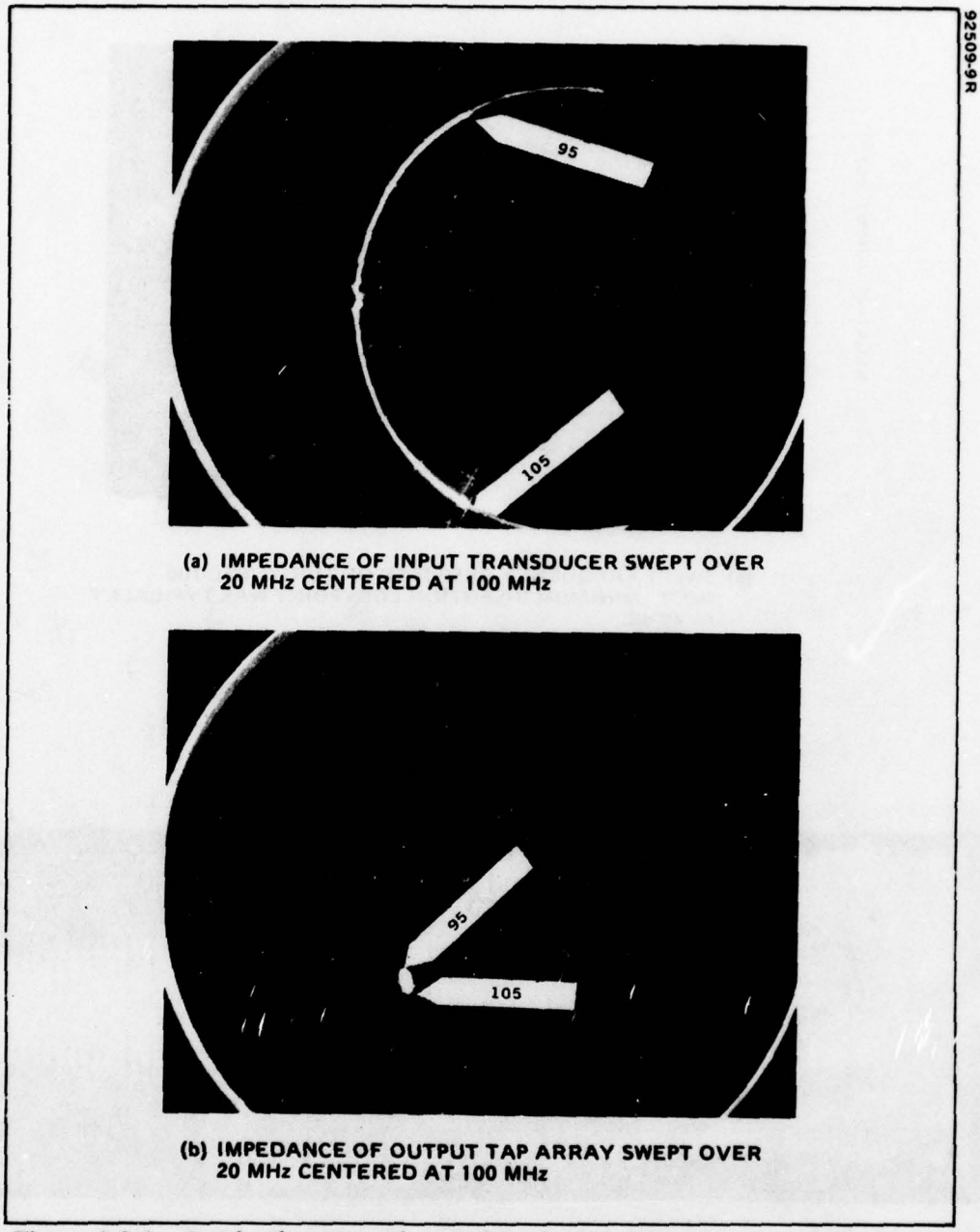


Figure 2.3-6. Smith Chart Impedance Plots for the TDL-100 Transducers, with Series Tuning Inductor and Padding Resistor on the Input Transducer, No Matching on the Output Tapping Array

92509-10R

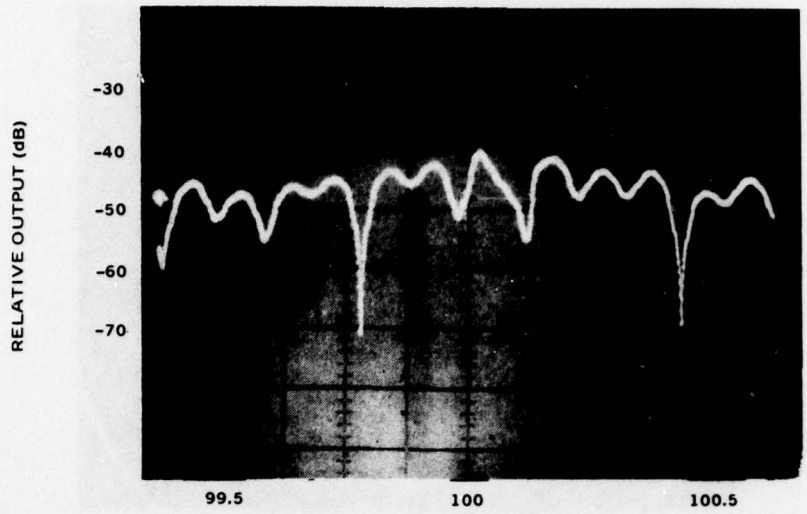


(a) SWEPT FREQUENCY RESPONSE OF TUNED TDL-100 NO. 1. MINIMUM INSERTION LOSS POINT WAS TYPICALLY 40-42 dB.

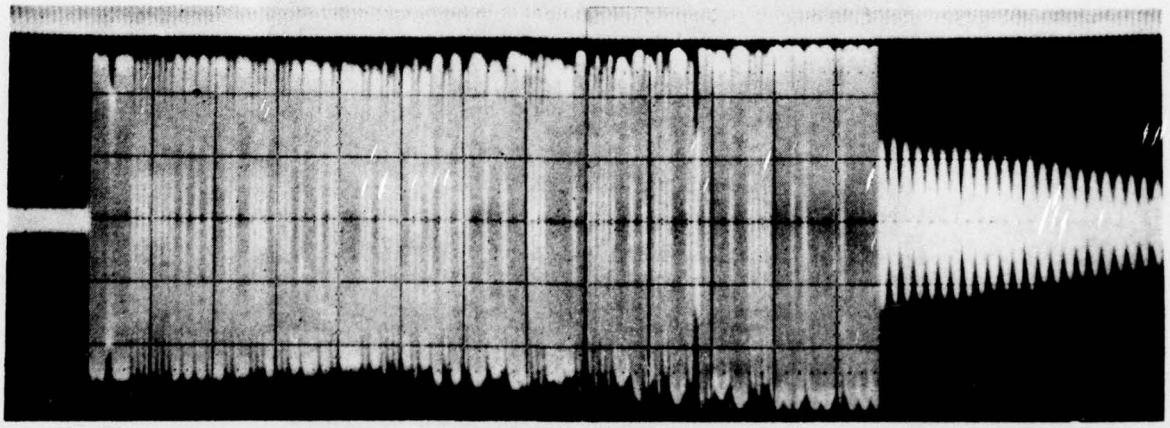

(b) RESPONSE OF THE TDL-100 NO. 1 TO A 50 ns PULSE AT 100 MHz AFTER APPLICATION OF SERIES INDUCTIVE TUNING. VERTICAL SCALE, 50 MV/DIV. HORIZONTAL SCALE 1 μS/DIV.

Figure 2.3-7. Midband Frequency Response and Expanded Pulse for TDL-100 #1

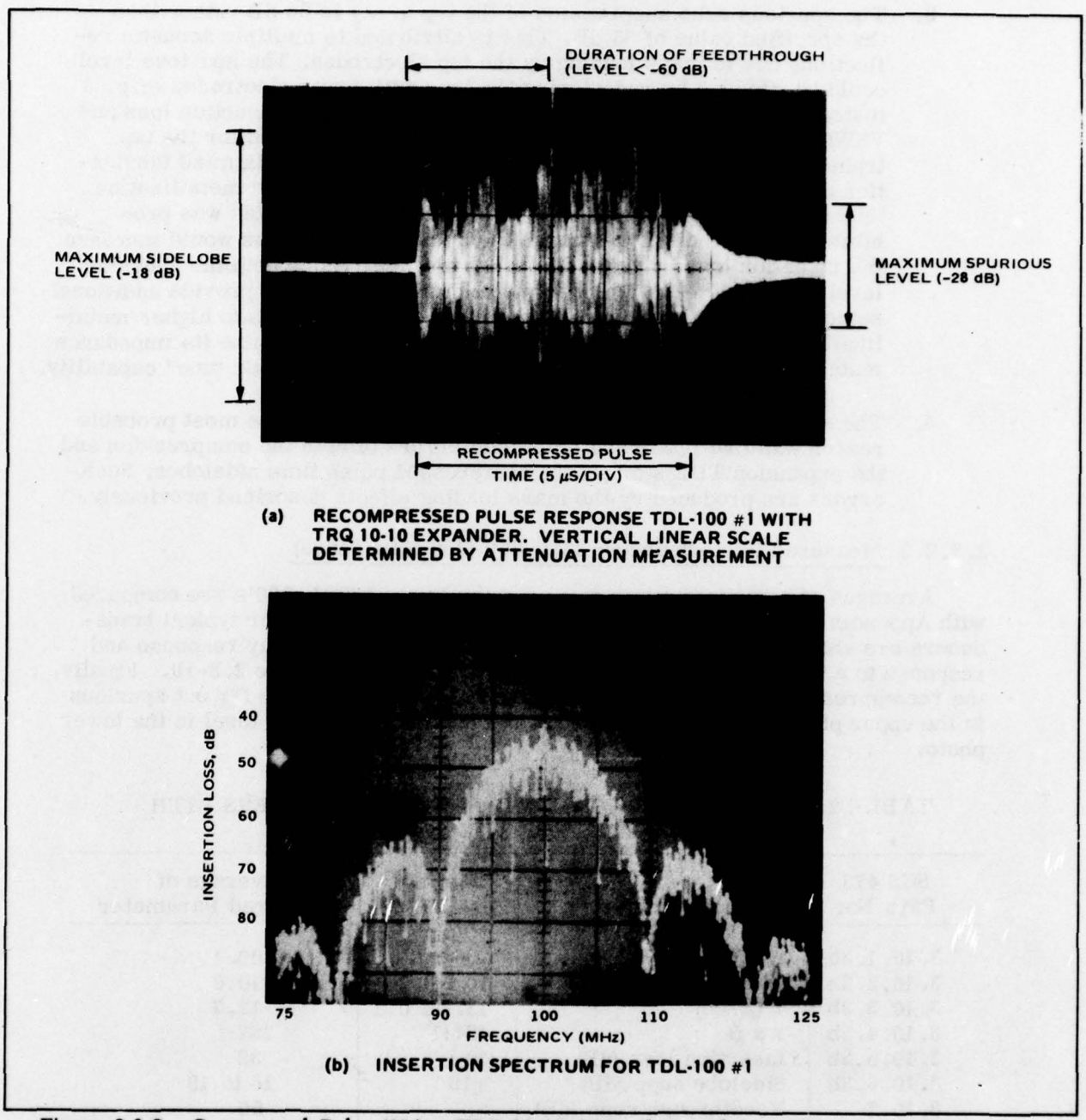


Figure 2.3-8. Compressed Pulse (Using TRQ-10-10 Expander) and Insertion Loss Spectrum for TDL-100 #1

3. The spurious echo suppression of the tap array is 28 dB rather than the specified value of 35 dB. This is attributed to multiple acoustic reflections due to mass loading by the tap electrodes. The spurious level could be reduced by redesigning the taps with fewer electrodes (e.g. 3 instead of 6). However, this would increase both the insertion loss and VSWR of the tap array. Double electrodes could be used for the tap transducers but this should be avoided if possible to minimize fabrication costs. The recommended approach is to reduce the metallization thickness by roughly a factor of two (1500 to 700 Å). This was prohibited by Appendix I. Although the decreased thickness would increase the insertion loss by a few decibels, it would reduce both the spurious level and the VSWR. Thinner metallization would also provide additional series electrode resistance in the input transducer (due to higher metallization sheet resistivity), which was required to optimize its impedance matching network in lieu of a mask change or a "dynamic tune" capability.

4. The specified time sidelobe level was not achieved. The most probable reason was that phase and amplitude errors of both the compression and the expansion TDL's affect the compressed pulse time sidelobes. Such errors are produced by the mass loading effects described previously.

2.3.2.3 Measured Performance – TDL-200 (200 MHz Lines)

Averages of measured parameters for the Phase I TDL-200's are compared with Appendix I in Table 2.3-2. Smith chart impedance plots for typical transducers are shown in Figure 2.3-9, while typical swept frequency response and response to a 0.1 μsec, 200.086 MHz pulse are shown in Figure 2.3-10. Finally, the recompressed pulse is shown in Figure 2.3-11, showing the far out spurious in the upper photo and amplified to show the maximum sidelobe level in the lower photo.

TABLE 2.3-2. COMPARISON OF MEASURED PARAMETERS WITH SPECIFICATIONS FOR TDL-200 FILTER

| SCS 476 Para No. | Parameter | SCS 476 Dec. 9, 74 | Average of Measured Parameter |
|---|---|---|---|
| 3.10.1.3b | fo (MHz) | 200 ± 4 | 200.1 |
| 3.10.2.3b | $\beta$ at -3 dB (MHz) | 10 ± 0.2 | 10.0 |
| 3.10.3.3b | $\tau$ (μsec) | 12.7 ± 0.1 | 12.7 |
| 3.10.4.3b | $\tau \times \beta$ | 127:1 | 127:1 |
| 3.10.5.3b | Insertion loss (dB) | 30 ± 3 | 38 |
| 3.10.6.3b | Sidelobe supp (dB) | ≥19 | 16 to 19 |
| 3.10.7 | Feedthrough supp (dB) | >50 | 50 |
| 3.10.8 | Spurious supp (dB) | >35 | 34 |
| 3.10.9 | VSWR | <1.5:1 | <3.5:1 |

The following parameters comply with the specified values: center frequency ($f_o$), bandwidth ($\beta$), time delay ($\tau$), time-bandwidth product ($\tau \times \beta$), and feedthrough suppression. Furthermore, the spurious echo suppression is within 1 dB of specification and can be improved, for example, by the use of thinner electrode

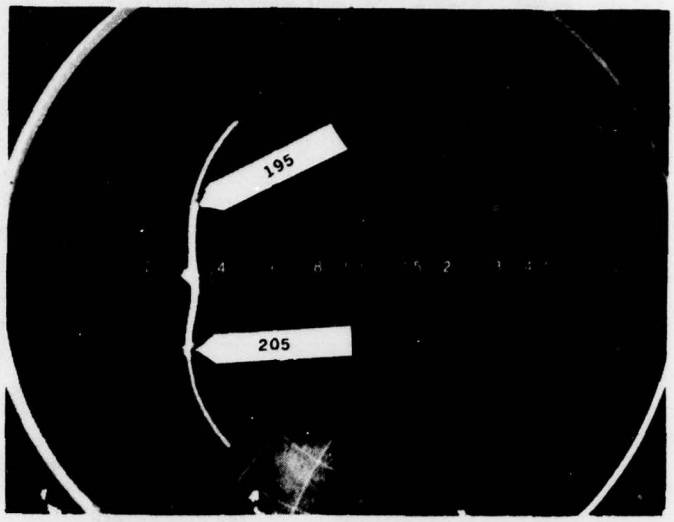


(a) IMPEDANCE OF INPUT TRANSDUCER SWEPT OVER 20 MHz CENTERED AT 200 MHz

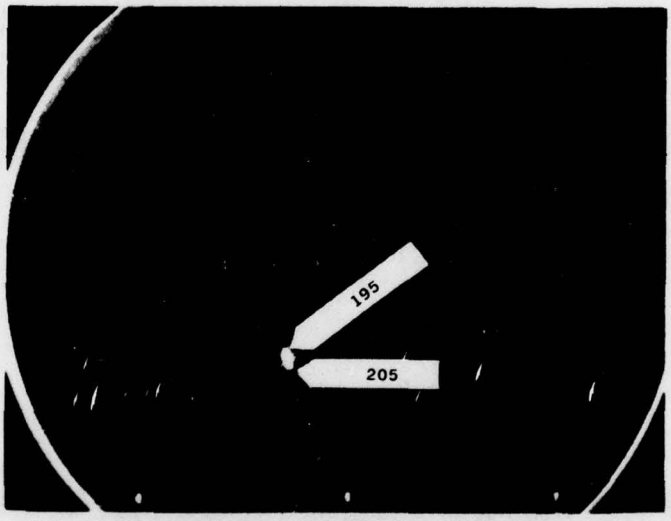


(b) IMPEDANCE OF OUTPUT TAP ARRAY SWEPT OVER 20 MHz CENTERED AT 200 MHz

92509-12R

Figure 2.3-9. Smith Chart Impedance Plots for the TDL-200 #1 Transducers, with Series Inductor Tuning on the Input Transducer, No Matching on the Output Tapping Array

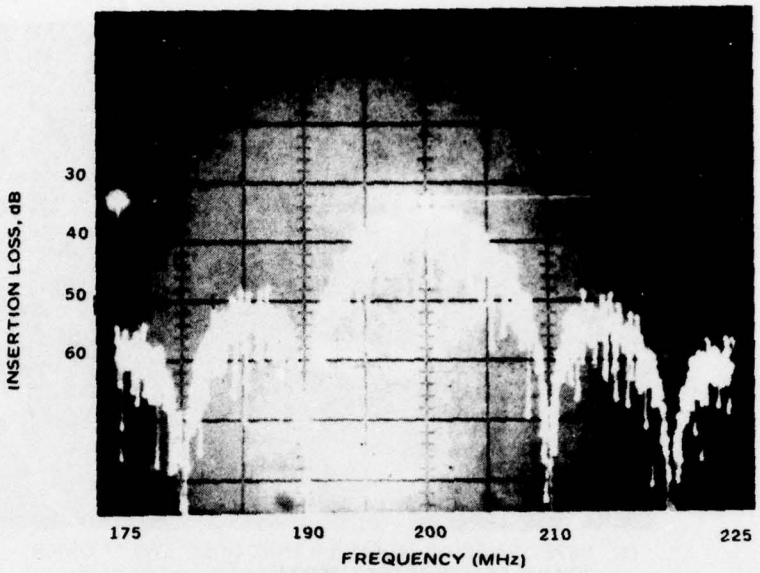


92509-13R

(a) SWEPT FREQUENCY RESPONSE OF TUNED TDL-200 NO. 1. MINIMUM INSERTION LOSS POINT WAS TYPICALLY 32 dB FOR TUNING BETWEEN TRANSDUCER AND GROUND (PREFERRED APPROACH) BUT 38 dB FOR TUNING BETWEEN TRANSDUCER AND SOURCE, BECAUSE OF PARASITIC CAPACITANCE.

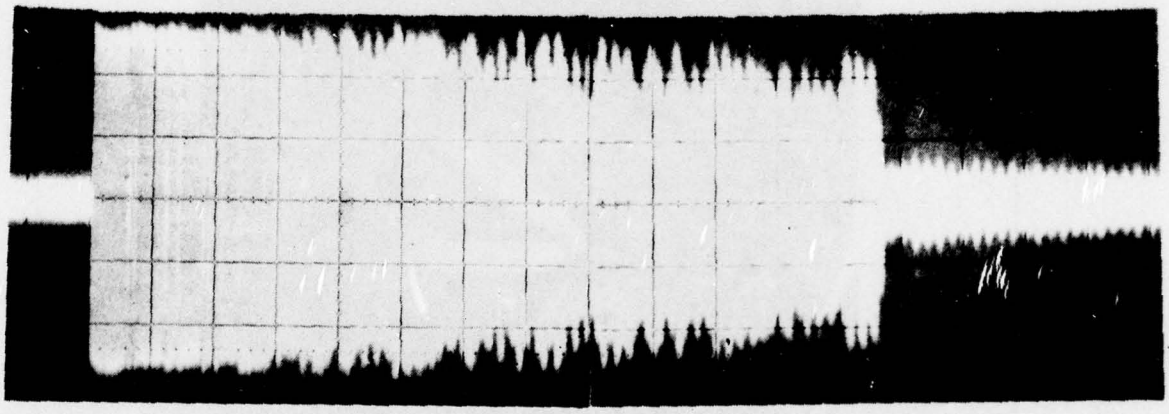

(b) RESPONSE OF THE TDL-200 NO. 1 TO A 0.1 μSEC, 200.086 MHz PULSE, WITH SERIES INDUCTIVE TUNING ON THE INPUT TRANSDUCER. VERTICAL SCALE 50 MV/DIV. LOSS TAPER WAS APPROXIMATELY 5 dB OVER THE EXPANDED PULSE LENGTH. HORIZONTAL SCALE 1 μS/DIV.

Figure 2.3-10. Swept Frequency Response and Expanded Pulse for TDL-200 #1

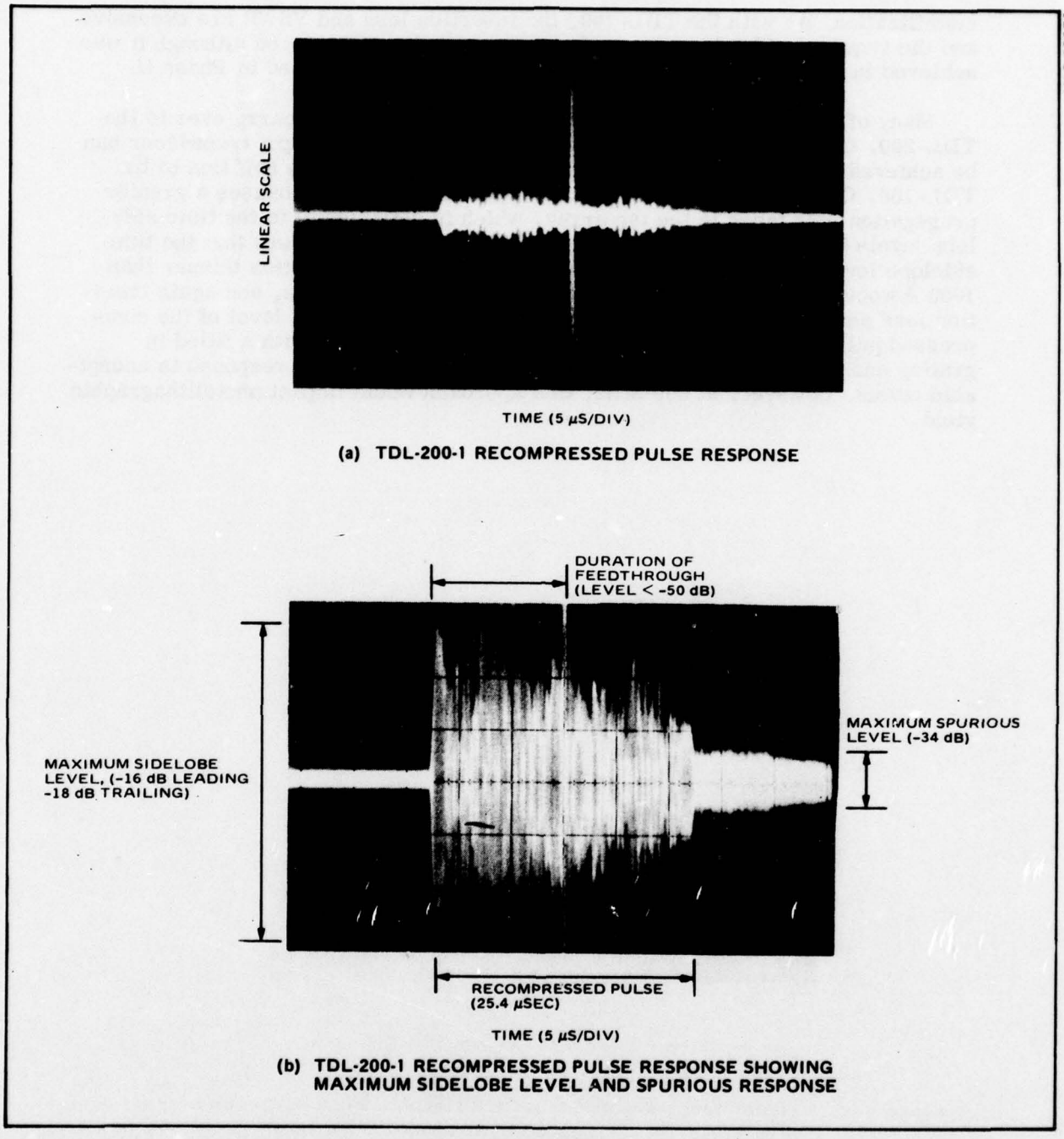


Figure 2.3-11. Recompressed Pulse Response for TDL-200 #1 on Normal and Expanded Amplitude Scales. Vertical linear scale determined by attenuation measurement.

metallization. As with the TDL-100, the insertion loss and VSWR are excessive and the required sidelobe suppression was typically not achieved although it was achieved in some samples. This discrepancy will be discussed in Phase II.

Many of the recommendations applicable to the TDL-100 carry over to the TDL-200. One exception is that the required VSWR for the input transducer can be achieved for the TDL-200 since the fractional bandwidth is half that of the TDL-100. On the other hand, the higher operating frequency causes a greater propagation loss taper in the tap array, which is detrimental to the time sidelobe levels in the recompressed pulse. Consequently, it appears that the time sidelobe levels better than -17 dB are not feasible. Metallization thinner than 1000 Å would improve the marginal spurious echo suppression, and again insertion loss should be redefined in terms of the correlation peak level of the compressed pulse. An alternate design using double electrodes with a filled in grating and apodization could decrease sidelobe and spurious response to acceptable levels. However, at 200 MHz, this approach would impact photolithographic yield.

# 2.4.0
# PULSE COMPRESSION AND EXPANSION FILTER DESIGN AND EVALUATION (PC-Q, PE-Q, PC-LN, PE-LN)

## 2.4.0 PULSE COMPRESSION AND EXPANSION FILTER DESIGN AND EVALUATION (PC-Q, PE-Q, PC-LN, PE-LN)

Because the quartz and lithium niobate pulse compression filters are designed similarly, they will both be described in this section. In reality, there are four separate filter designs because the quartz and lithium niobate pulse compression filters (PC-Q and PC-LN) require companion pulse expansion test filters (PE-Q and PE-LN) in order to demonstrate pulse compression.

Each of the filters is composed of one apodized transducer and one unapodized transducer. For simplicity of design, each transducer has electrodes positioned according to the classical FM law and the electrode widths vary throughout the transducer so as to be everywhere equal to the adjacent gap width. Strictly speaking, the transfer function of a filter containing two linear FM transducers is only approximately a linear FM filter. The ideal design procedure calls for dividing the transfer function of the unapodized transducer into the desired linear FM transfer function, thus obtaining the (somewhat nonlinear) FM transfer function for which the apodized transducer should be synthesized[14,15]. This procedure is rather lengthy, however, and it is found that the simpler, approximate design procedure in which both transducers are linear FM results in a design error sufficiently small that time sidelobes below -30 dB are realized. It turns out that the most severe limitation on the time sidelobe suppression is caused by electric circuit loading in the PC-LN.

In the expansion/compression filter designs described in this section, the "unapodized" transducer has a dispersive delay of 1.40 $\mu$s/1.06 $\mu$s, and is unapodized over the central 1.0 $\mu$s/0.94 $\mu$s, but has a short "tail" of length 0.2 $\mu$s/0.06 $\mu$s on each end where the electrode apertures taper smoothly to zero to suppress Fresnel ripple (and consequently time sidelobes). The apodized transducers in the two pulse expansion test lines also contain "tail" regions of length 0.2 $\mu$s on each end for the same purpose; however, these tail regions are not needed in the apodized transducers of the compression lines since the built-in Hamming weighting already causes the electrode apertures to taper smoothly to nearly zero at the transducer ends.

### 2.4.1 Quartz Pulse Compression and Expansion Filter Design (PC-Q and PE-Q)

The geometrical layout of the quartz pulse expansion test filter (PE-Q) is shown in Figure 2.4-1. This is an up-chirp filter since the low-frequency ends of the transducers face each other. Each transducer contains 421 double electrodes and the "apodization profiles" shown in Figure 2.4-1 show the tail regions on the ends of each transducer.

In the "apodized" transducer, in its central region, the apertures vary directly as the electrode spacing or, equivalently, as the reciprocal of the local

---

[14] W.R. Smith, Jr., "Acoustic Surface Wave Filters for Multichannel Linear FM Operation." Section 2, Unpublished Hughes Final Report for contract sponsored by the Mitre Corporation. October 9, 1974.

[15] W.M. Bridge "The Development of Surface Wave Dispersive Filters for Use in a Multichannel Pulse Compression System," Mitre Corporation Technical Report MTR-2921, June 30, 1974.

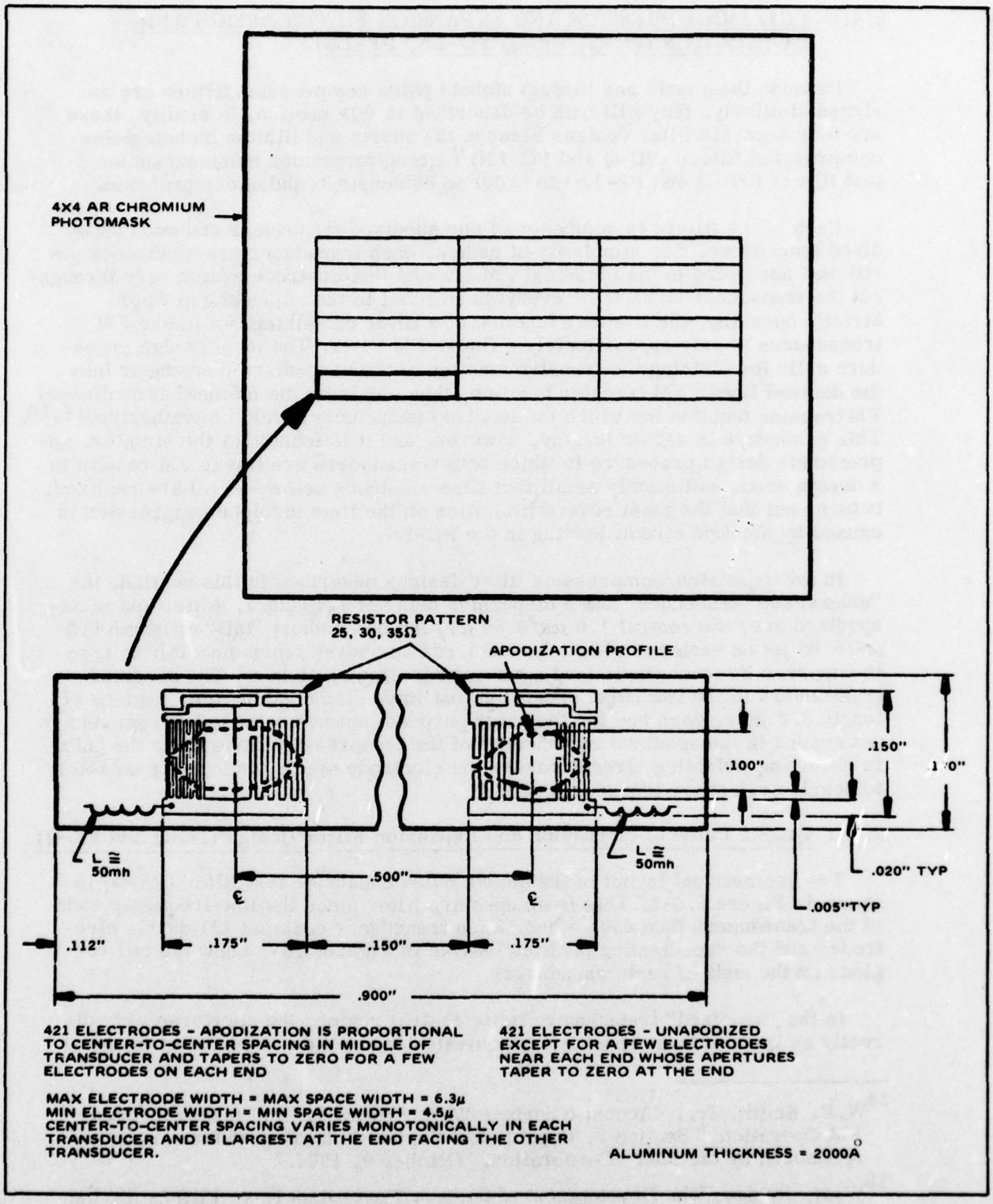


Figure 2.4-1. Schematic of PE-Q Layout

electrode synchronous frequency. This apodization law is used because each transducer is tuned with a series inductor and is in contrast with the $F^{-3}$ apodization law that is used for untuned or shunt tuned transducers. The transducers in the quartz filters must be series tuned because the low dielectric constant and $k^2$ of quartz dictate, for reasonable apertures, that the series radiation resistance is large enough for the required insertion loss, while the shunt radiation conductance is not.

The series radiation resistance of the "unapodized" transducer varies directly as frequency while that of the apodized transducer varies inversely as frequency, so that the product (filter transfer function) is flat. That is shown in the circuit model prediction of the expansion line insertion loss function, given in Figure 2.4-2. The predicted insertion loss is 48 dB, including the effect of series inductive tuning and the 30 ohm series padding resistors on each transducer which are used to lower the VSWR below 1.5.

The design of the quartz pulse compression filter is in many ways similar to that of the expansion test filter. The principal differences are that it is a down-chirp filter (the high-frequency ends of the transducers face each other) and the apodized transducer contains built-in Hamming weighting. Figure 2.4-3 (bottom) shows the layout of this filter, while the upper portion shows the 3x6 die layout of the photomask. The "unapodized" transducer contains 319 double electrodes; its apodized tails which suppress Fresnel ripple are much shorter than those in the pulse expansion filter because the Hamming weighting in the apodized transducer also suppresses Fresnel ripple.

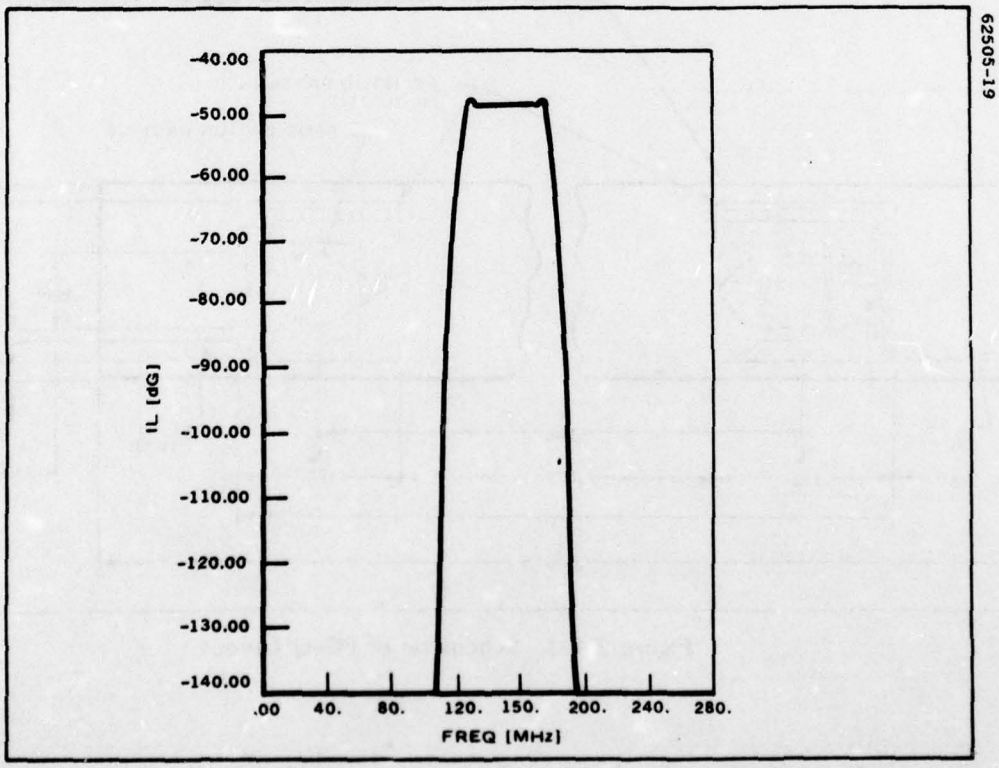


Figure 2.4-2. Predicted Insertion Loss of the PE-Q Filter. Both transducers are tuned and resistively padded.

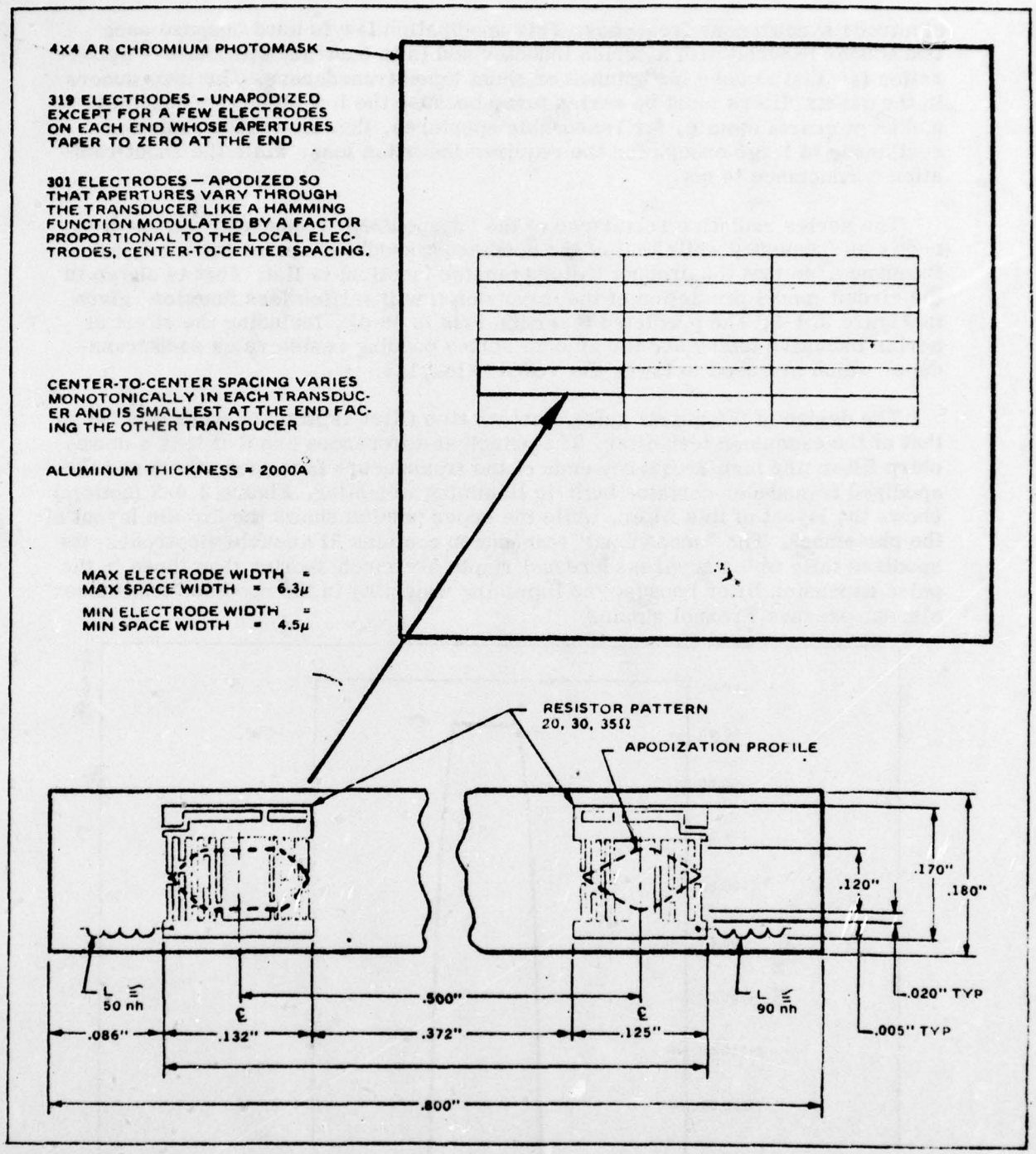


Figure 2.4-3. Schematic of PC-Q Layout

The apodization function of the apodized transducer is a Hamming (cosine squared on a pedestal) function modulated by a factor proportional to the electrode spacing (i.e., to the reciprocal of the local instantaneous frequency). This is appropriate so that the transfer function of the filter, whose transducers are series tuned, will have a Hamming-shaped amplitude response without superimposed roll-up or roll-off. The same 30 ohm series resistors as in the expansion filter are used to lower the VSWR and also to lower the resonant electric Q and prevent narrowbanding.

The circuit model prediction of the compression filter insertion loss is shown in Figure 2.4-4, which clearly exhibits the Hamming response from built-in weighting, with a center frequency insertion loss of 44 dB. The VSWR, from impedance data (not shown) is less than 1.5. The predicted compressed pulse, obtained from the responses of both the PE-Q and PC-Q filters, is shown in Figure 2.4-5. All sidelobes are below a level of -36 dB.

The circuit model predictions indicate that all specifications can be met and this filter is well within the state-of-the-art for surface wave pulse compression filters. Batch-producing the relatively large number of double electrodes without defects is the principal new area to be explored for these filters, but the filter performance is expected to be relatively insensitive to small numbers of defects.

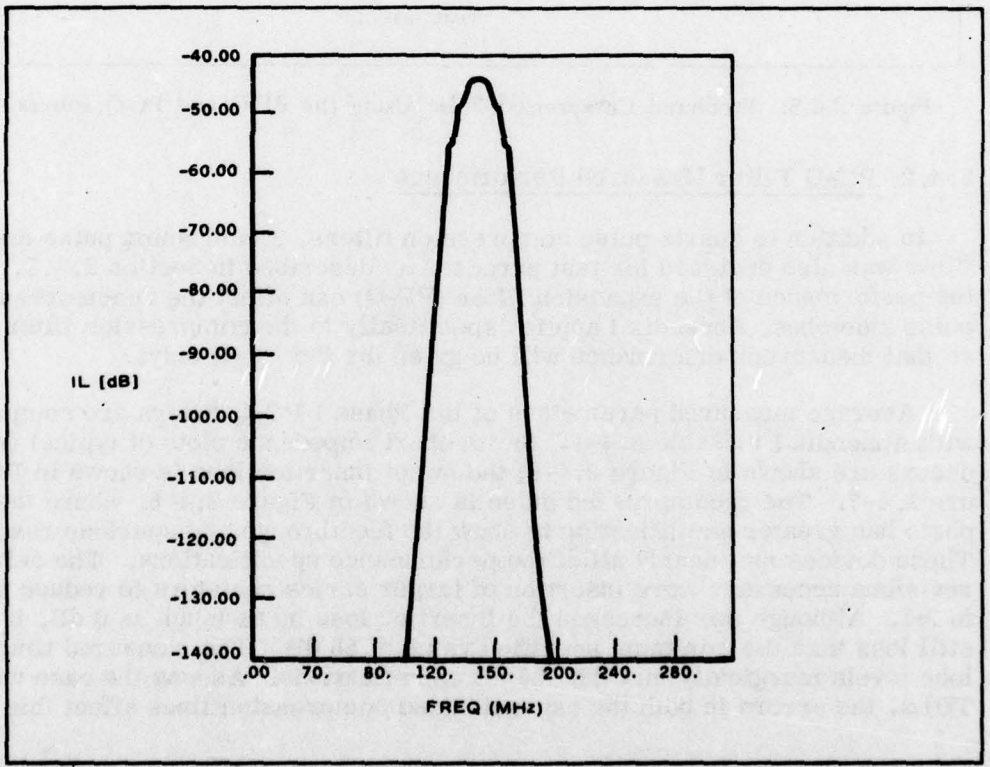


Figure 2.4-4. Predicted Insertion Loss of the PC-Q Filter. Both transducers are tuned and resistively padded.

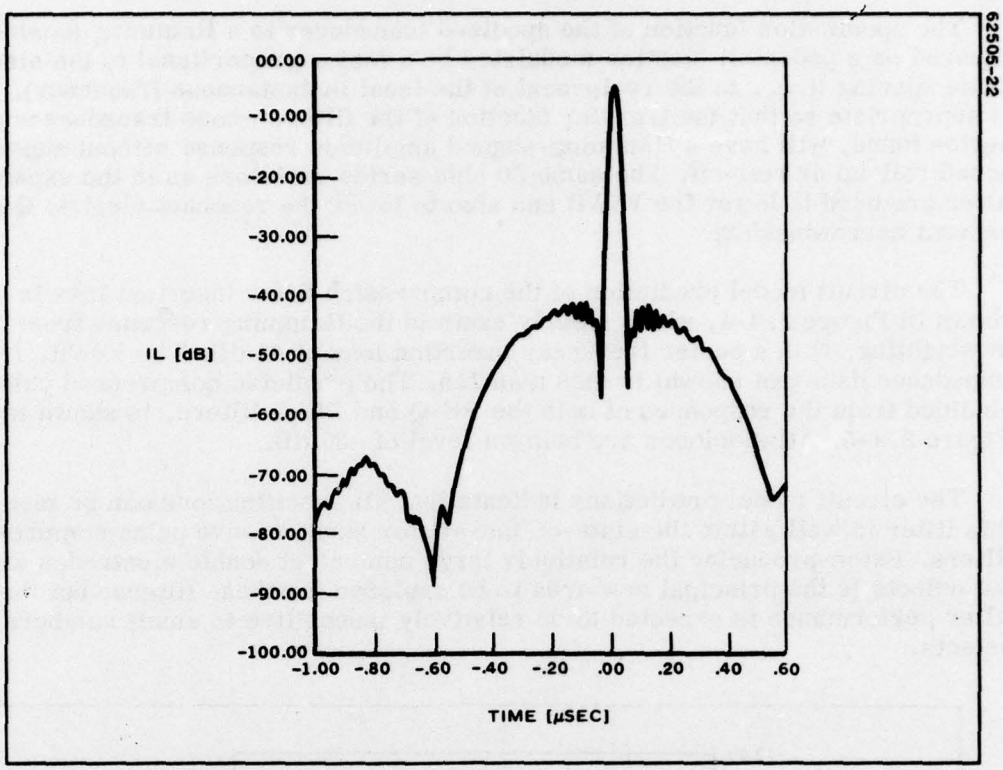


Figure 2.4-5. Predicted Compressed Pulse Using the PE-Q and PC-Q Filters

## 2.4.2 PC-Q Filter Measured Performance

In addition to quartz pulse compression filters, a companion pulse expansion filter was also designed for test purposes as described in Section 2.4.1. While the performance of the expansion filter (PE-Q) can affect the recompressed pulse sidelobes, Appendix I applies specifically to the compression filter (PC-Q), so that measured performance will be given for the PC-Q only.

Average measured parameters of the Phase I PC-Q filters are compared with Appendix I in Table 2.4-1. Smith chart impedance plots of typical transducers are shown in Figure 2.4-6; the swept insertion loss is shown in Figure 2.4-7. The recompressed pulse is shown in Figure 2.4-8, where the upper photo has greater amplification to show the feedthrough and spurious responses. These devices met nearly all of the performance specifications. The only device revisions necessary were insertion of larger series resistors to reduce VSWR to 2:1. Although this increased the insertion loss by as much as 6 dB, it was still less than the minimum specified value of 55 dB. The measured time sidelobe levels marginally met the -25 dB specifications. As was the case with the TDLs, the errors in both the expansion and compression lines affect this result.

TABLE 2.4-1. COMPARISON OF MEASURED PARAMETERS TO SPECIFICATIONS FOR PC-Q FILTER

| SCS-476 Para No. | Parameter | SCS-476 Dec. 9, 74 | Average of Measured Parameter |
|---|---|---|---|
| 3.10.1.1a | fo (MHz) | 150 ± 3 | 149.5 |
| 3.10.2.1a | $\beta$ (MHz) | 50 ± 1* | 50.0 |
| 3.10.3.1a | $\tau$ ($\mu$sec) | 2 ± 0.02 | 2 |
| 3.10.4.1a | $\tau$ x $\beta$ | 100 | 100 |
| 3.10.5.1a | Insertion loss (dB) | 55 ± 5 | 39 to 48 |
| 3.10.6.1a | Sidelobe supp. (dB) | ≥25 | 19 to 28 |
| 3.10.7 | Feedthrough supp. (dB) | >50 | 70 |
| 3.10.8 | Spurious supp. (dB) | >35 | 49 |
| 3.10.9 | VSWR | <1.5:1 | 2:1 |

*Interpreted to be -6 dB bandwidth of unweighted linear FM waveform and the -28 dB bandwidth of the Hamming-Weighted pulse compression filter. See Appendix V.

### 2.4.3 Lithium Niobate Pulse Compression and Expansion Filter Design (PC-LN and PE-LN)

The lithium niobate pulse expansion and compression filters are designed much like the quartz filters and employ the same number of double electrodes and electrode positioning law in all transducers. The layouts of the PE-LN and PC-LN filters are shown in Figures 2.4-9 and 2.4-10, respectively. The upper portion in each case shows the 4x22 die layout on the photomask while the lower portion shows a single filter.

The principal difference between the lithium niobate and quartz filter designs is that shunt (rather than series) inductive tuning is used in the lithium niobate filters. The relatively high dielectric and electromechanical coupling ($k^2$) constants of lithium niobate are such that either the series radiation resistance or shunt radiation conductance can be designed for an impedance match yielding 30 dB insertion loss with reasonable apertures. However, when a filter operates with 30 dB insertion loss, there is a possibility of unacceptable distortion (yielding time sidelobes higher than -25 dB) caused by interaction between the transducer and an improperly designed electric load. It has been established[16] that the minimum spurious reflections and regenerated signals are found when the electric load approaches a short circuit, a property that is predicted by Hughes' crossed-field circuit model analysis. Both series-tuned and shunt-tuned designs were investigated with circuit model analysis for the PE-LN and PC-LN filters. It was found that series-tuned loads lead to unacceptable signal distortions that result in one sidelobe higher than -25 dB.

[16] W.R. Smith, "Experimental Distinction between Crossed-Field and In-Line Three-Port Circuit Models for Interdigital Transducers," IEEE Trans. MTT-22, pp. 960-964, November 1974.

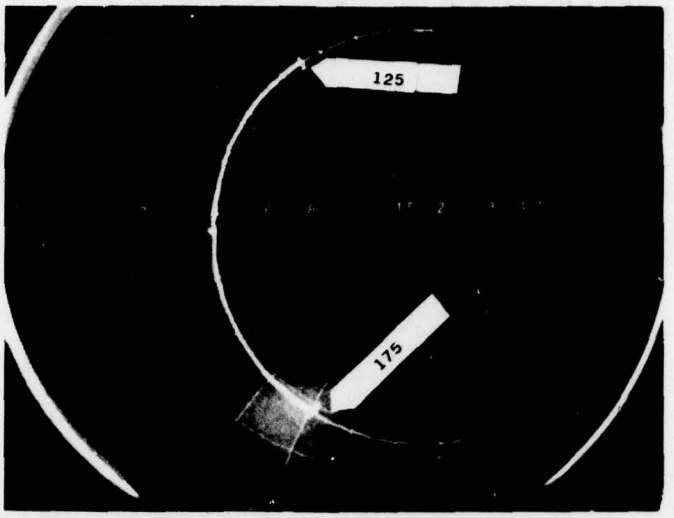


(a) IMPEDANCE OF INPUT TRANSDUCER SWEPT OVER 100 MHz CENTERED AT 150 MHz

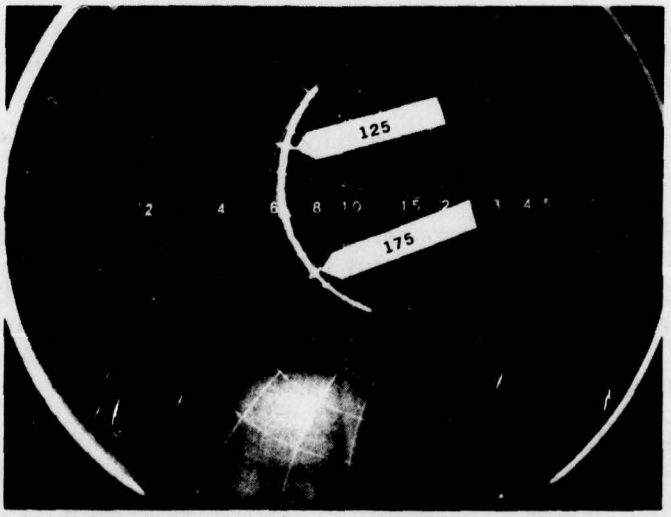


(b) IMPEDANCE OF OUTPUT TRANSDUCER SWEPT OVER 100 MHz CENTERED AT 150 MHz

92509-15R

Figure 2.4-6. Smith Chart Impedance Plots for the PC-Q #2 Transducers with Series Tuning Inductors

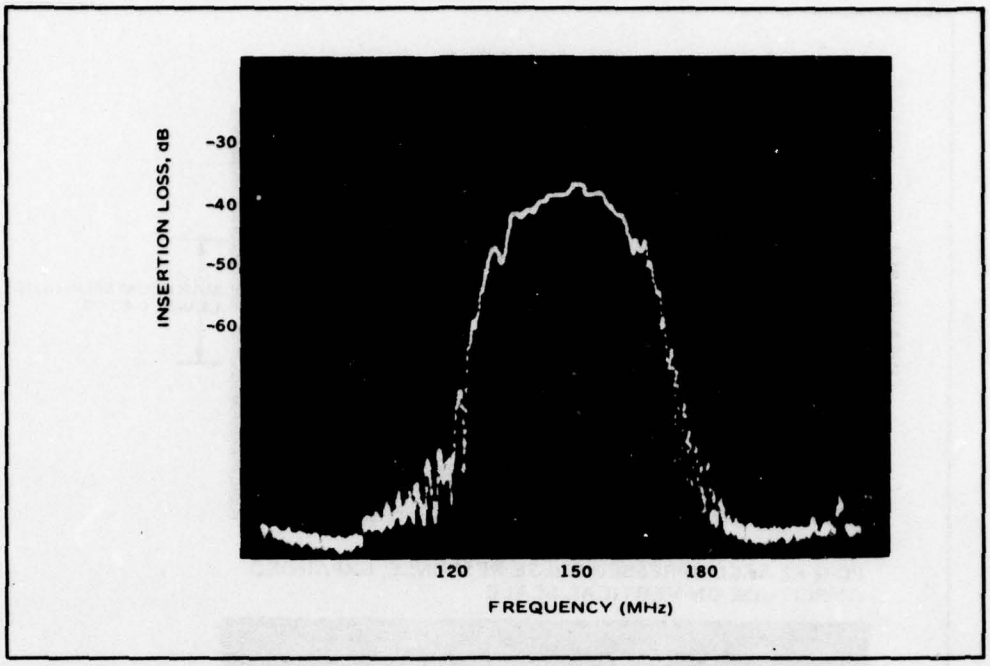


Figure 2.4-7. Swept Frequency Response of Tuned PC-Q #1. Minimum Insertion Loss was 39 dB.

For this reason, the shunt tuned load was adopted; a resistor in parallel with the tuning inductor serves to lower the load impedance to reduce signal distortion, while a separate series resistor is used to lower the VSWR. A tight, four-way tradeoff exists among diffraction loss, insertion loss, VSWR, and signal distortion which raises the sidelobes. A wide aperture is desirable to reduce acoustic diffraction (important because of the extreme apodization in the Hamming-weighted transducer). However, a wide aperture is detrimental to the simultaneous realization of 30 dB insertion loss and low time sidelobes.

Initially, an aperture of 0.016 in. (about 18 wavelengths at 150 MHz) was investigated and it was found that 30 dB insertion loss, better than -25 dB sidelobes, and a VSWR of less than 1.5 could be achieved with a single shunt padding resistor. Although the two transducers would be operating well under near-field conditions if all electrodes had the maximum aperture of 18 wavelengths at 150 MHz, some of the electrodes in the Hamming-weighted transducer have an aperture of only about 1.4 wavelengths. For this reason, it was decided to increase the maximum aperture to 0.025 in., or about 28 wavelengths at 150 MHz. This is the largest aperture for which an insertion loss of 30 dB, time sidelobes below -25 dB and a VSWR of less than 1.5 can be realized simultaneously according to circuit model analysis.

The insertion loss functions of the PE-LN and PC-LN filters are shown in Figures 2.4-11 and 2.4-12, respecively. The compressed pulse is shown in Figure 2.4-13. The insertion loss is just under 30 dB for the PC-LN and there is one trailing time sidelobe at -26 dB below midband. The VSWR of all transducers is just under 1.5. Diffraction is not included in the circuit model analysis and the principal uncertainty to be resolved experimentally is whether diffraction effects will degrade the performance of the heavily apodized, Hamming weighted

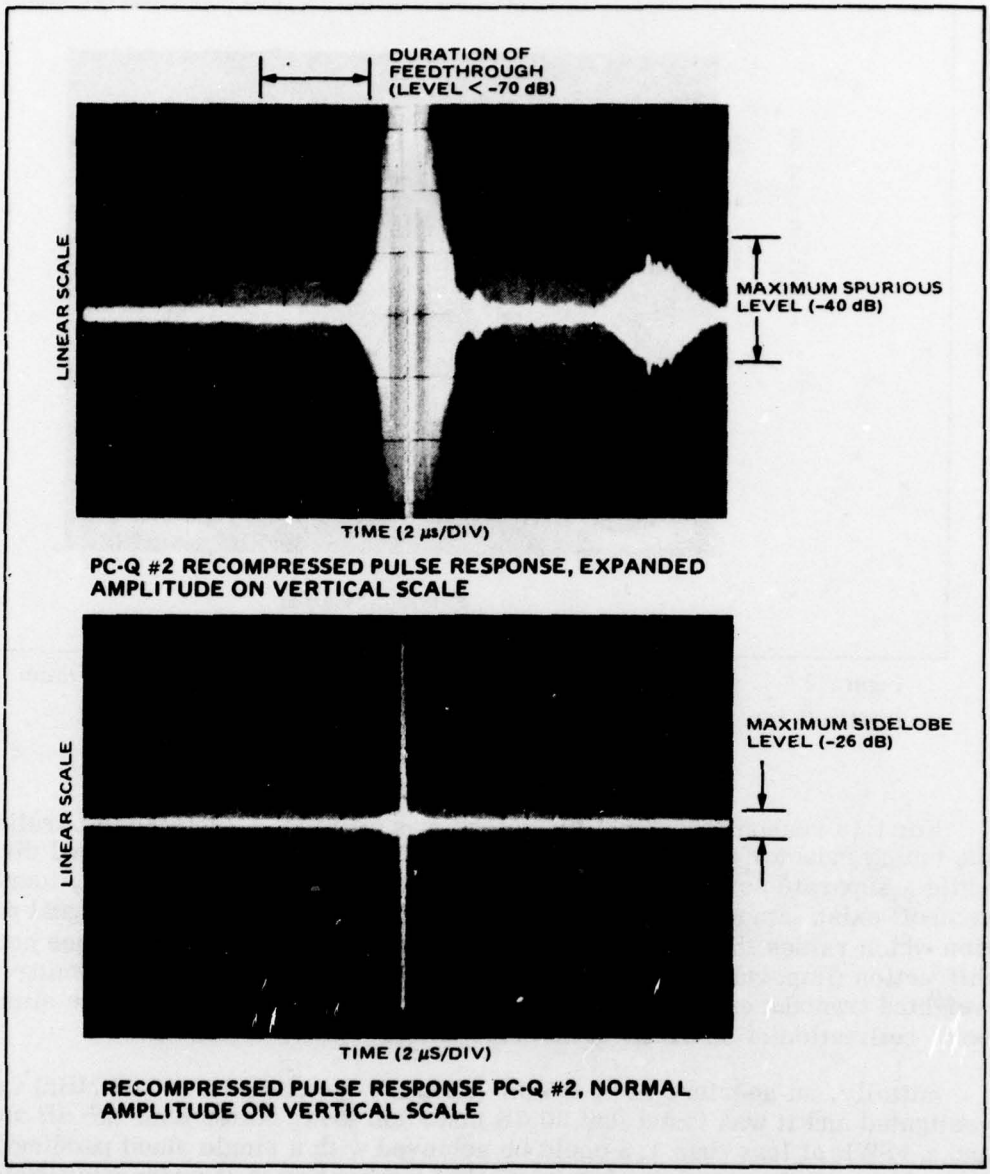


Figure 2.4-8. Recompressed Pulse Response for PC-Q #2 on Normal and Expanded Amplitude Scales. Vertical linear scale determined by attenuation measurement.

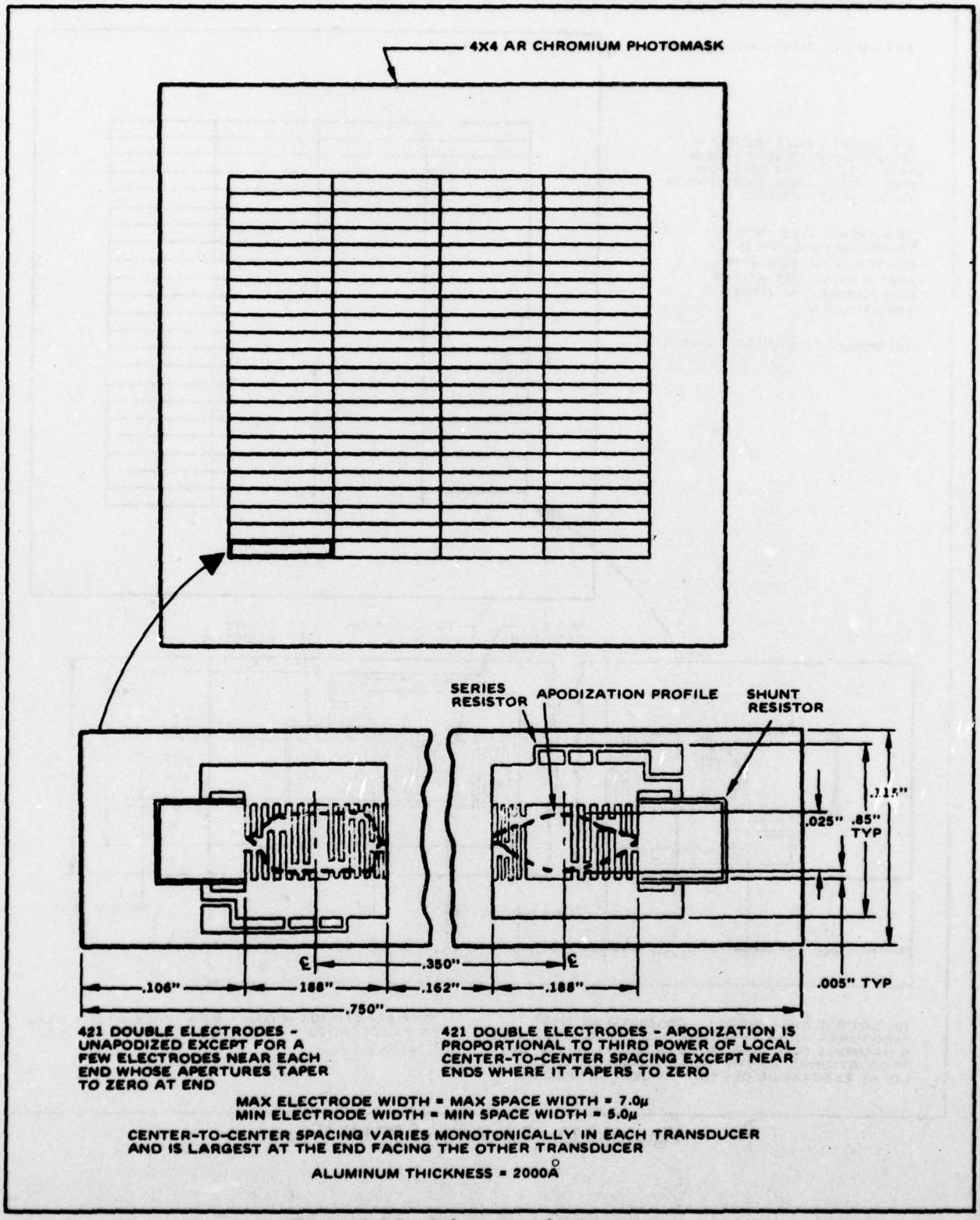


Figure 2.4-9. Schematic of PE-LN Layout

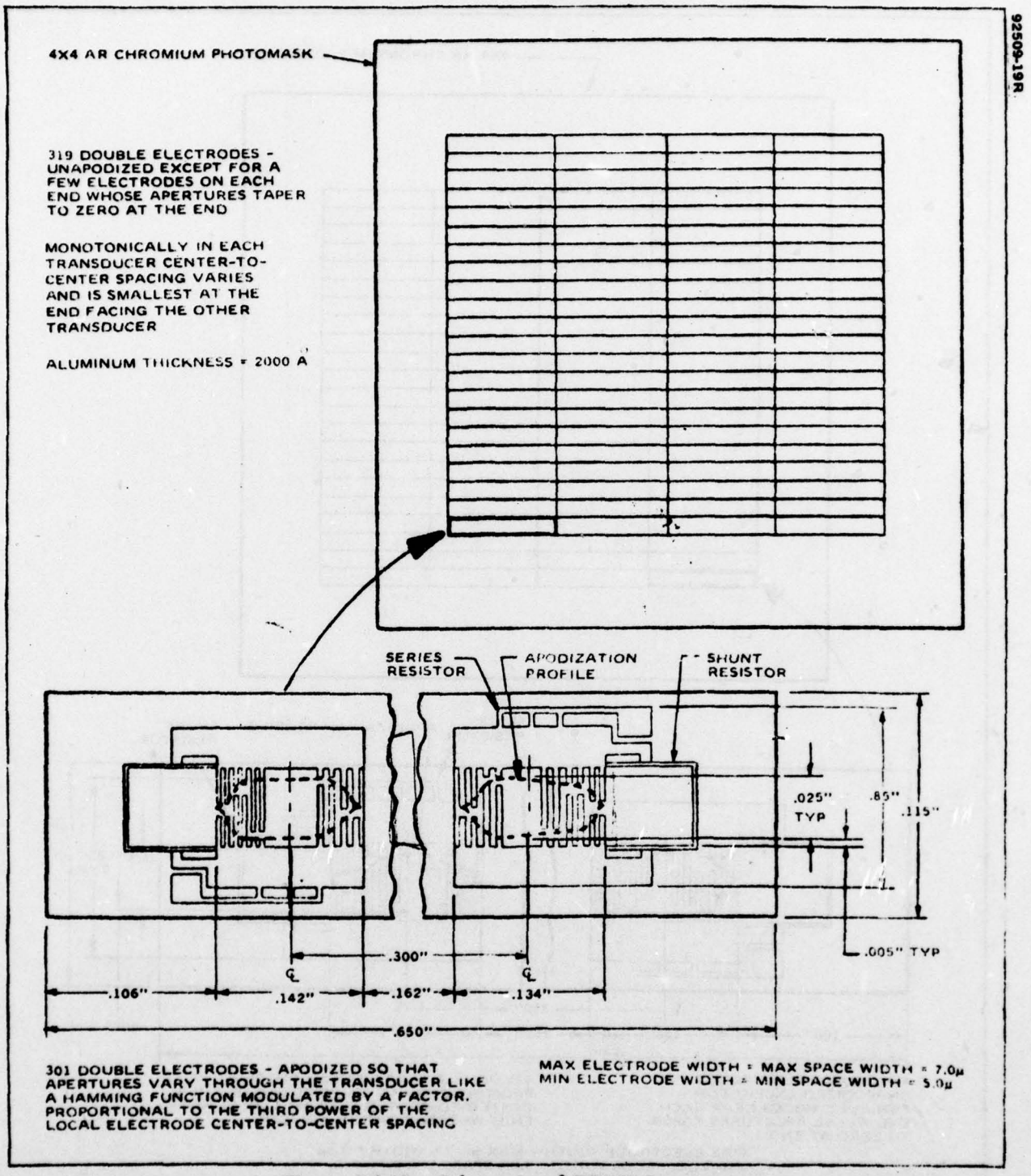


**Figure 2.4-10. Schematic of PC-LN Layout**

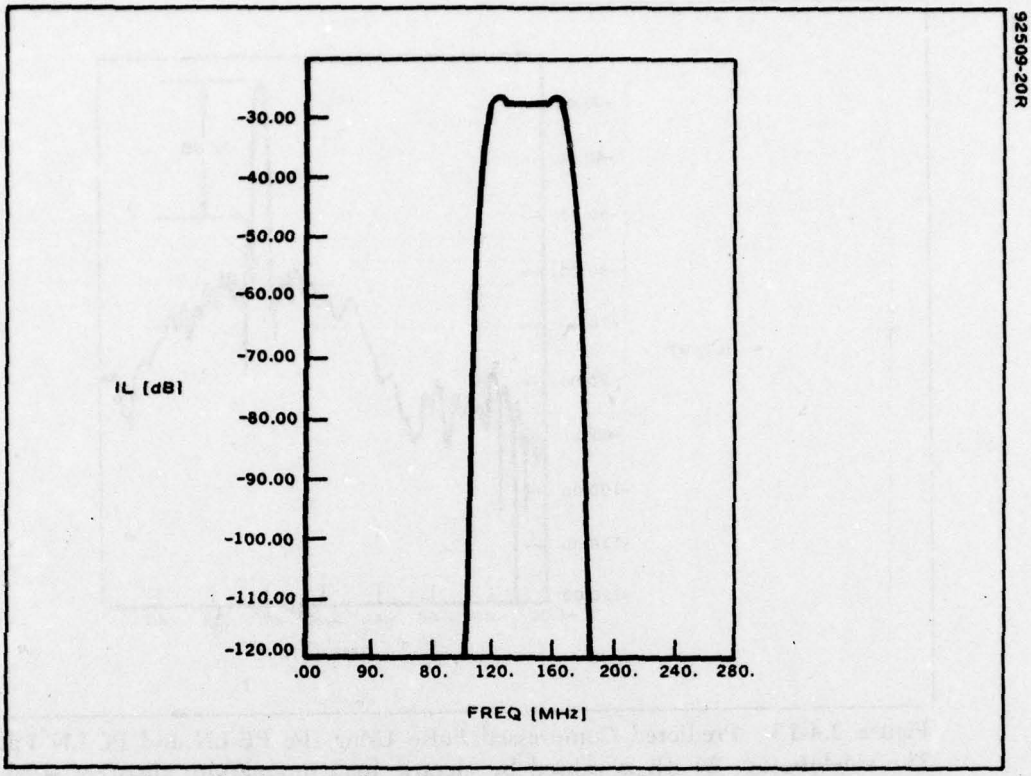


Figure 2.4-11. Predicted Insertion Loss of the PE-LN Filter

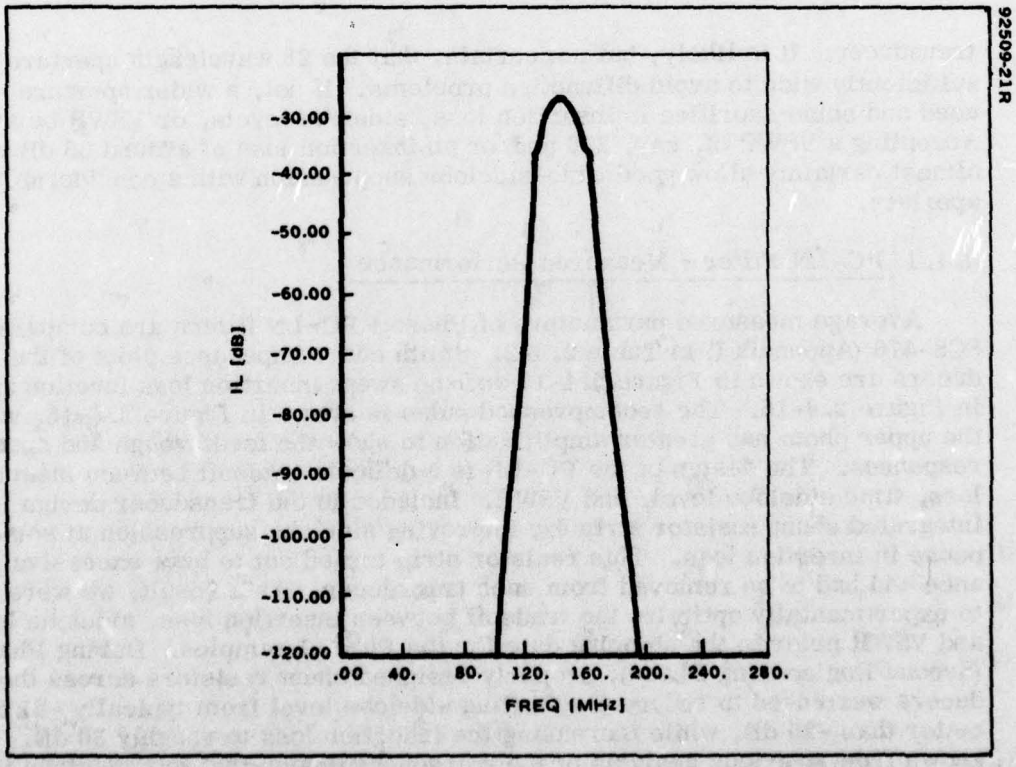


Figure 2.4-12. Predicted Insertion Loss of the PC-LN Filter

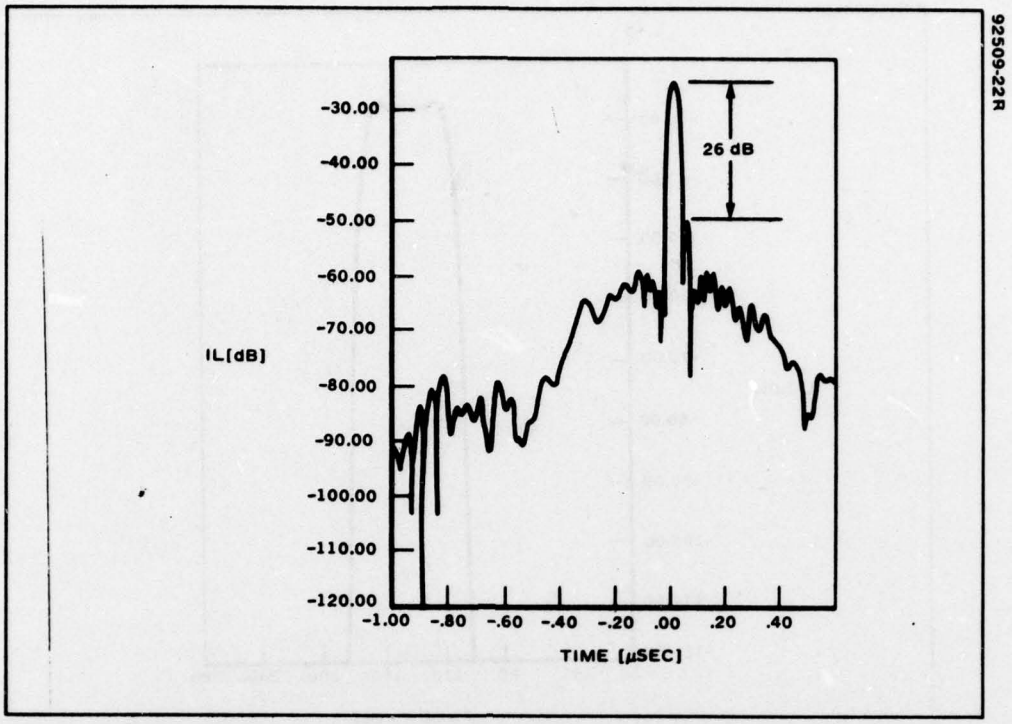


Figure 2.4-13. Predicted Compressed Pulse Using the PE-LN and PC-LN Filters. The sidelobe at -26 dB is caused by electric load interaction; all other sidelobes are below -35 dB.

transducer. It is likely, but not certain, that the 28 wavelength aperture will be sufficiently wide to avoid diffraction problems. If not, a wider aperture should be used and some sacrifice in insertion loss, sidelobe levels, or VSWR be tolerated. Accepting a VSWR of, say, 2.0 and/or an insertion loss of around 35 dB would almost certainly allow good time-sidelobe suppression with a considerably wider aperture.

### 2.4.4 PC-LN Filter – Measured Performance

Average measured parameters of Phase I PC-LN filters are compared with SCS-476 (Appendix I) in Table 2.4-2. Smith chart impedance plots of the transducers are shown in Figure 2.4-14 and the swept insertion loss function appears in Figure 2.4-15. The recompressed pulse is shown in Figure 2.4-16, where the upper photo has greater amplification to show the feedthrough and spurious responses. The design of the PC-LN is a delicate tradeoff between insertion loss, time sidelobe level, and VSWR. Included in the transducer design is an integrated shunt resistor strip for improving sidelobe suppression at some expense in insertion loss. This resistor strip turned out to have excessive inductance and had to be removed from each transducer. As a result, we were unable to experimentally optimize the tradeoff between insertion loss, sidelobe level, and VSWR prior to the shipping date for the Phase I samples. During Phase II (Second Engineering Phase), properly designed shunt resistors across the transducers were used to reduce the trailing sidelobe level from typically -21 dB to better than -25 dB, while increasing the insertion loss to roughly 30 dB. It is known from previous analysis of the transducer design that this sidelobe is due

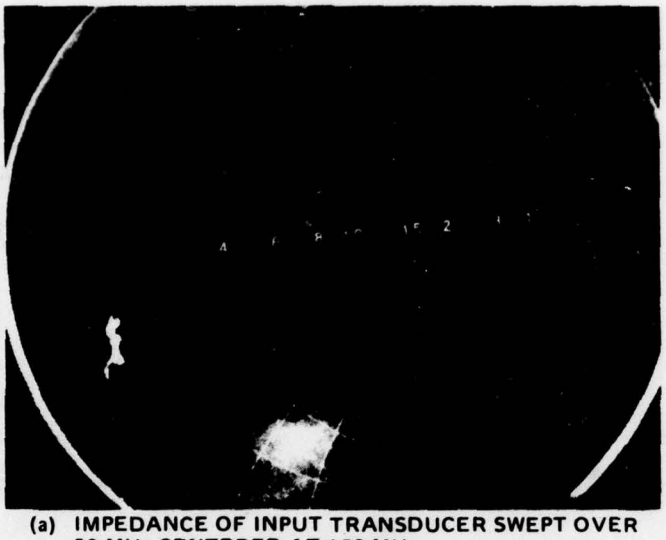

(a) IMPEDANCE OF INPUT TRANSDUCER SWEPT OVER 50 MHz CENTERED AT 150 MHz

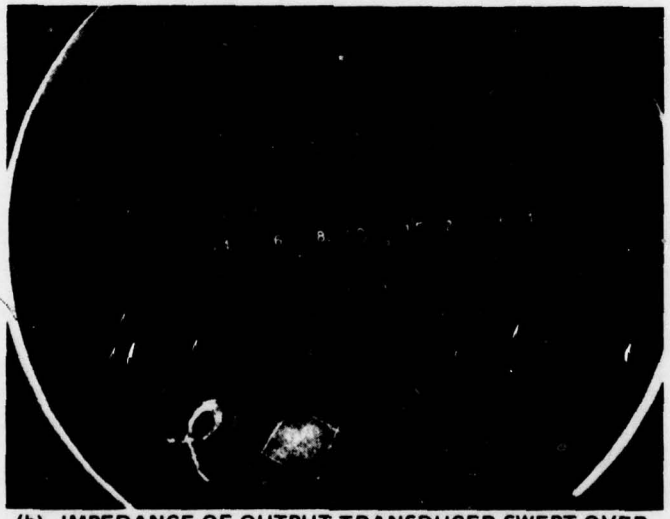

(b) IMPEDANCE OF OUTPUT TRANSDUCER SWEPT OVER 50 MHz CENTERED AT 150 MHz

92509-23R

Figure 2.4-14. Smith Chart Impedance Plots for the PC-LN #1 Transducers, with No Tuning

to regeneration resulting improper matching of the transducer to the external circuit impedance. As part of Phase II investigation, it was determined if sufficient series resistance could be added to reduce VSWR to less than 1.5:1 over the operating band without incurring excessive loss.

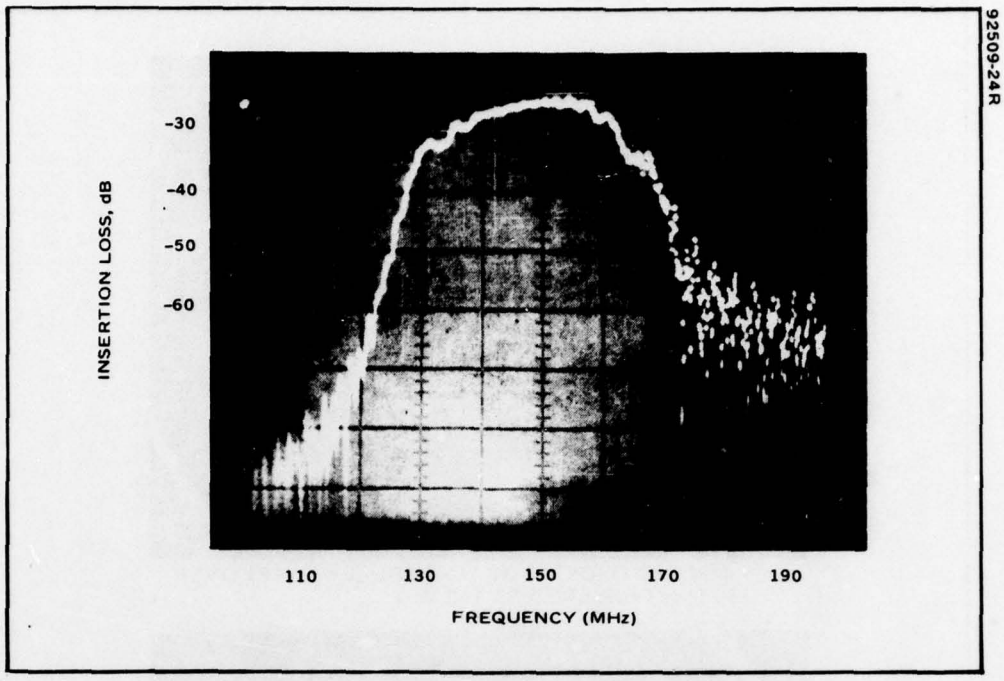


Figure 2.4-15. Swept Frequency Response of Tuned PC-LN #1. Minimum insertion loss was 24 dB.

TABLE 2.4-2. COMPARISON OF MEASURED PARAMETERS WITH SPECIFICATIONS FOR PC-LN FILTER

| SCS-476 Para No. | Parameter | SCS-476 Dec. 9, 74 | Average of Measured Parameter |
|---|---|---|---|
| 3.10.1.1b | fc (MHz) | 150 ± 3 | 150 |
| 3.10.2.1b | $\beta$ (MHz) | 50 ± 1* | 50 |
| 3.10.3.1b | $\tau$ ($\mu$sec) | 2 ± 0.01 | 2 |
| 3.10.4.1b | $\tau$ x $\beta$ | 100 | 100 |
| 3.10.5.1b | Insertion loss (dB) | 30 ± 3 | 24 - 28 |
| 3.10.6.1b | Sidelobe supp. (dB) | ≥25 | 19 - 28 |
| 3.10.7 | Feedthrough supp. (dB) | >50 | 65 |
| 3.10.8 | Spurious supp. (dB) | >35 | 45 |
| 3.10.9 | VSWR | <1.5:1 | >10:1 |

*Interpreted to be -6 dB bandwidth of unweighted linear FM waveform and the -28 dB bandwidth of the Hamming-weighted pulse compression filter. See Appendix V.

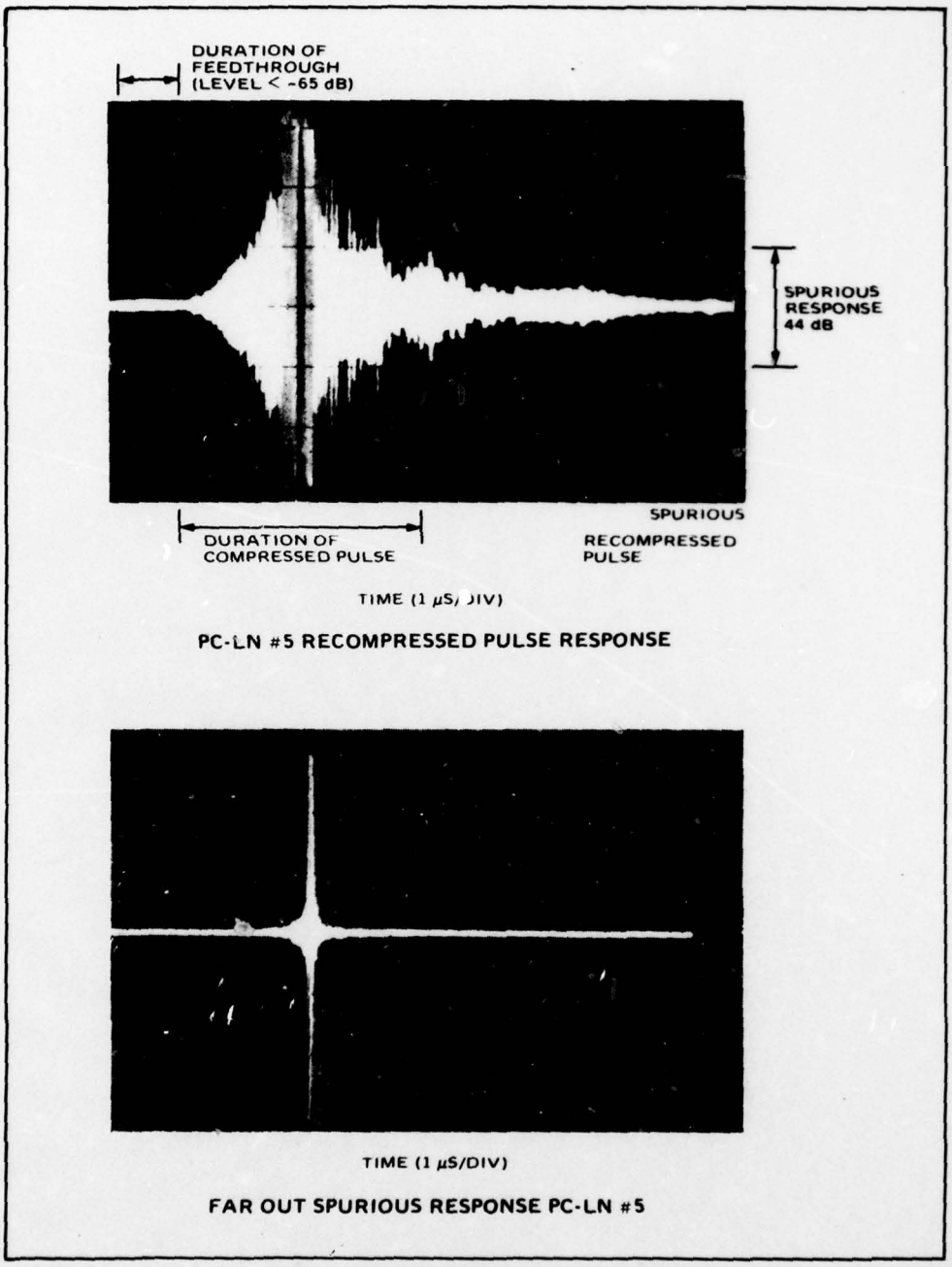


Figure 2.4-16. Recompressed Pulse Response of PC-LN #5 on Normal and Expanded Amplitude Scales

# 2.5.0
# MATERIALS AND PROCESSES CONSIDERATIONS FOR PHASE I DEVICE CONSTRUCTION

## 2.5.0 MATERIALS AND PROCESSES CONSIDERATIONS FOR PHASE I DEVICE CONSTRUCTION

### 2.5.1 Wafer Fabrication

Device processing for Phase I was essentially that documented in the Process Specification Volume of this report. Specific problems unique to Phase I will be outlined below.

Substrates were not procured to a specification at this point in the program. A unique orientation problem occurred with the quartz vendor, and is discussed in the following section. Essentially, substrate materials were ordered to the following specification:

ST-quartz plates, (±15 min. orientation to X axis) 3 x 0.75 x 0.25 inch were obtained from Valpey-Fisher Corp.[17] Lithium niobate wafers (±6 min. orientation to Z axis) 2 (dia.) x 0.020 inch were supplied by Crystal Technology Inc.[18] Both items are stated to be standard product by their respective vendors.

Cleaning, evaporation and photolithographic/etch procedures were identical to those outlined in the Process Specification Volume. A summary of these procedures is outlined below.

Both materials were cleaned with an acetone soak and scrub and a detergent scrub. Intermediate steps involved a deionized water rinse. The substrates were dried under a dry nitrogen stream. These substrates were then metallized with aluminum to a thickness appropriate to the design requirement (2000 A ±10% except TDL, 1250 ±10%). The metallized substrates were spun at 5000 rpm in order to achieve a positive resist thickness (Shipley AZ-1350B) of 3000 A ±10%. A prebake schedule of 10 min at 90°C was utilized.

Transducer patterns were exposed at from 3-6 sec. using a Kasper Alligner, (Model 1800). Development of the resist involved a 50% dilution of commercial developer. Exposure and development times were adjusted to give the proper line-to-space ratios for a given filter pattern. The patterns were then defined in the aluminum using a nitric acid, phosphoric acid, water (2:40:9) etchant. The photoresist was stripped in acetone prior to visual inspection at 200X magnification. In the majority of cases to date, the predice yield has exceeded fifty percent. The criterion for this yield is based on the number of good die vs. the number of die printed. A good die is defined as having no shorts and less than 5 opens.

Prior to dicing, the substrates were recoated with resist and baked for protective purposes. They were then mounted with optical pitch and diced using a 6 mil diamond blade. Dice were then recleaned and inspected at 220X individually prior to packaging. At this point, excessive chipping and pin holing was noted on some die. This was attributed to the use of a bad lot of resist for the protective coating, and the fact that the "streets" on the mask were too narrow for the kerf produced by the 6 mil diamond blade.

Die were mounted in the slotted aluminum chassis using Dow Corning 3140 RTV, cured for 24 hours in air. Thermocompression wire bonding was effected using a Hughes pulse tip wire bonder Model 360. After precap electrical tune and test, the chassis lids were screwed on. It should be noted that the machined nonhermetic chassis and SMA connectors were utilized in Phase I to eliminate elec-

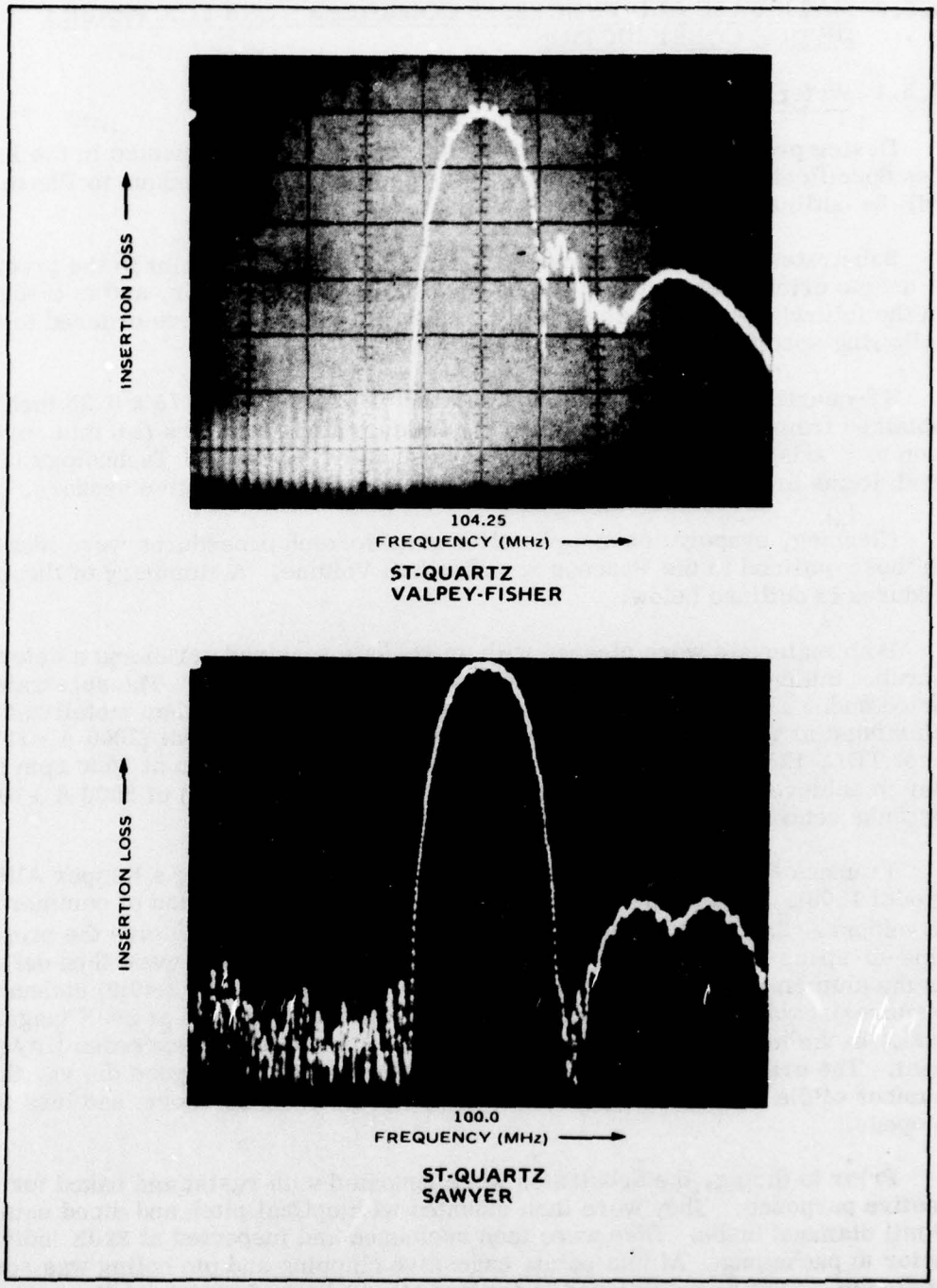


Figure 2.5-1. Insertion Loss Spectra for BP-Q Design on Quartz Supplied by Two Vendors

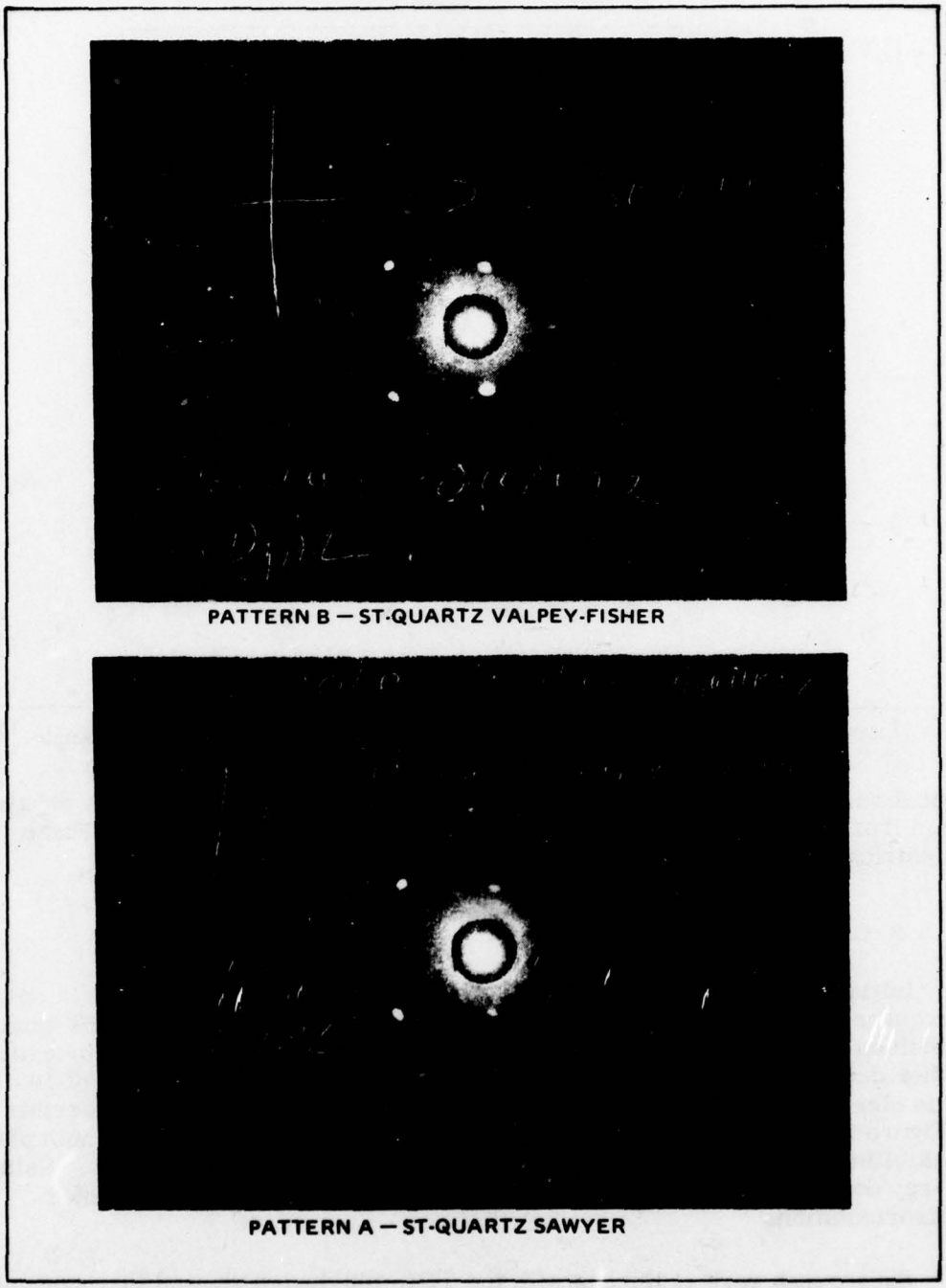


Figure 2.5-2. Comparison of Laue Back Reflection X-Ray Photograph of Two Sources of Quartz

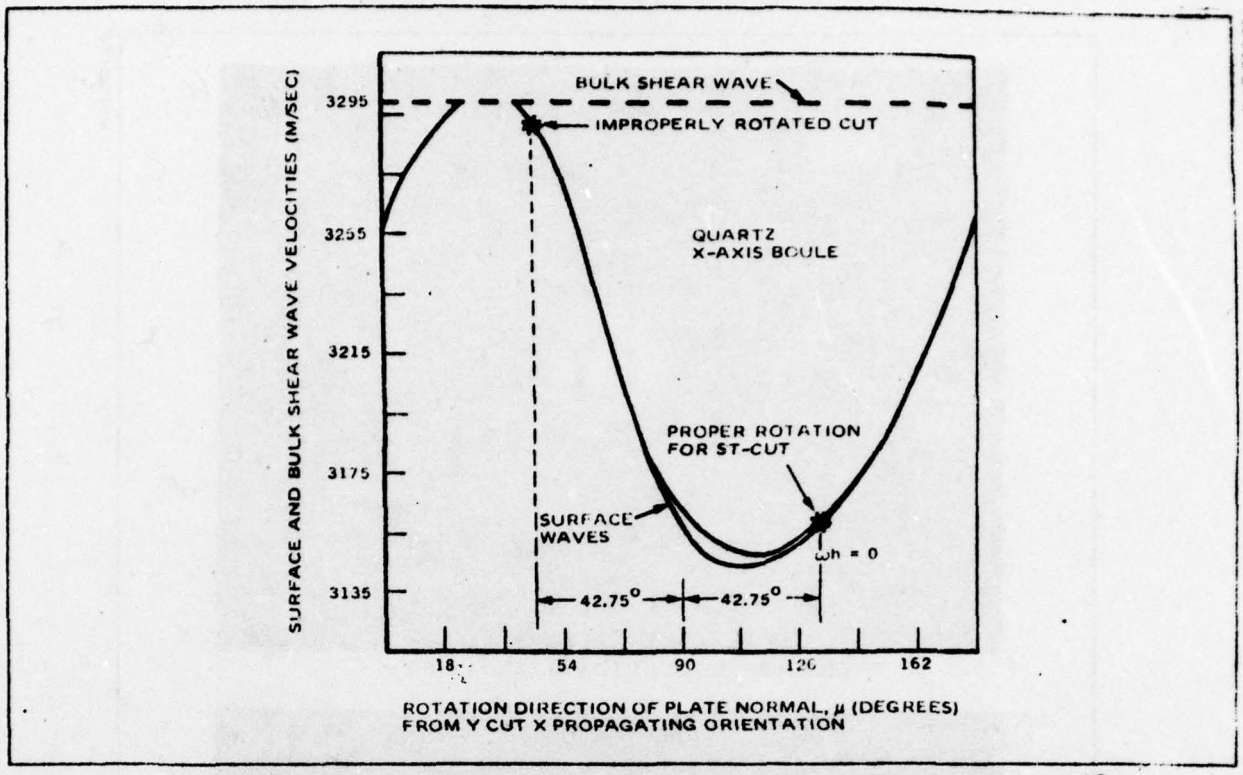


Figure 2.5-3. Acoustic Velocity of Quartz as a Function of Cutting Angle [19]

trical variables, such as feedthrough, in order to distinguish a faulty crystal design from a packaging phenomena. Package sealing is discussed in Phase II. Electrical data has been discussed previously.

## 2.5.2 Crystal Orientation Problem

Initial results on BP-Q devices indicated a four percent increase in operating frequency (Figure 2.5-1). This same design was then fabricated on ST-quartz obtained from another vendor and of proven quality relative to the fabrication of other device designs. In this case, the center frequency design goal of 100 MHz was obtained. Laue Back Reflection x-ray photographs of the two materials (Figure 2.5-2) indicated an apparent misorientation problem. A sample plate exhibiting the misorientation was returned to the vendor for analysis. Using the x-ray double diffraction technique, he was unable to confirm the alleged misorientation.

Subsequent work at Hughes with the TDL-100 design showed that supposedly identical plates from the same shipment were capable of producing devices at zero and plus four percent of the design frequency. With reference to Figure

---

[17] Valpey-Fisher Corp., 75 South St., Hopkington, MA 01748.

[18] Crystal Technology, 2510 Old Middlefield Way, Mountain View, CA 94040.

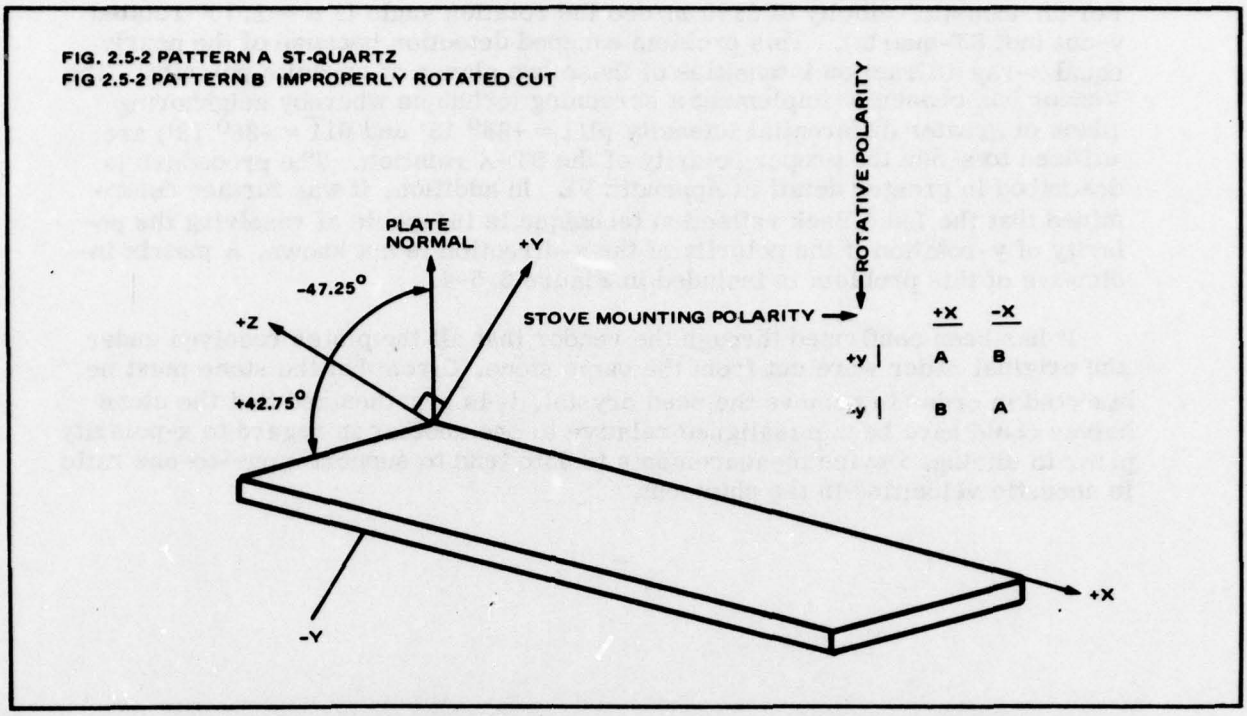


Figure 2.5-4. X-Ray Pattern Matrix as a Function of Orthogonal Polarity

2.5-3, this frequency difference can be accounted for by an equivalent acoustic velocity difference according to:

$$f_o = \frac{V}{2S}$$

where

$f_o$ = center frequency
V = acoustic velocity
S = center-to-center transducer spacing.

This acoustic velocity difference can be related to the polarity of the y-axis rotation relative to the z axis (Figure 2.5-4). Here, for the proper acoustic velocity of 3158 m/sec, the rotation angle is a + 42.75° rotated y-cut (ST-quartz).

---

[19] A.J. Slobodnik, Jr., E.D. Conway and R.T. Delmonico, "Microwave Acoustics Handbook," p. 119 1A 1973 (AFCRL-TR-73-0597).

For an acoustic velocity of 3290 m/sec the rotation angle is a -42.75° rotated y-cut (not ST-quartz). This problem escaped detection because of the nearly equal x-ray diffraction intensities of these two planes of opposite polarity. The vendor has chosen to implement a screening technique whereby neighboring plans of greater differential intensity (011 = +38° 13' and $01\bar{1}$ = -38° 13') are utilized to sense the proper polarity of the ST-X rotation. The procedure is described in greater detail in Appendix VI. In addition, it was further determined that the Laue Back reflection technique is incapable of resolving the polarity of y-rotation if the polarity of the x-direction is not known. A matrix indicative of this problem is included in Figure 2.5-4.

It has been confirmed through the vendor that all the plates received under the original order were cut from the same stone. Given that the stone must be bisected in order to remove the seed crystal, it is hypothesized that the stone halves could have been misaligned relative to one another in regard to x-polarity prior to slicing. Device measurements to date tend to support a one-to-one ratio in acoustic velocities in the shipment.

## 2.6.0
## CONCLUSIONS FROM PHASE I

## 2.6.0 CONCLUSIONS FROM PHASE I

At the conclusion of Phase I, 60 devices of six differing SAW designs were built, tested and shipped. Evaluation of the test results demonstrated that two of the designs (BP-LN and TDL-100) suffered major deviations from the insertion loss specification. Further reevaluation of these designs was undertaken in Phase II.

Three of the remaining designs, TDL-200, PC-LN, and PC-Q suffered only minor deviation from specification. Further testing was performed during Phase II in order to determine the adjustments necessary to make these designs conform fully to the specification. The BPQ devices met all design goals in Phase I.

Conclusions and recommendations from Phase I discrepant designs are listed below:

BP-Q: Because the midband insertion loss is at the maximum of the specified range of 20 ±2 dB, a small decrease in series resistance was to be exercised, at the expense of VSWR, in order to more comfortably meet specification incorporated in the design during Phase II.

BP-LN: A redesign would be evaluated in Phase II elminating the MSC.

TDL-100: It was concluded that the design of the TDL-100 should be thoroughly examined during the Phase II, and a new performance specification would be developed. The following areas of change were envisaged:

1. VSWR should be increased to optimize the insertion loss versus waveform distortion tradeoff. (See Appendix IV.)

2. Insertion loss should be redefined in terms of the correlation peak level of the compressed pulse.

3. Metallization of less than the specified minimum value of 1000 A should be allowed.

4. Maximum time sidelobe level should be increased from -19 dB to as high as -17 dB.

TDL-200: The recommendations applicable to the TDL-100 apply to the TDL-200. However, due to the lower fractional bandwidth of this device, the VSWR of the input transducer could be achieved.

PC-Q: Add series resistance to decrease VSWR (see Appendix IV).

PC-LN: Redesign the shunt resistor in order to reduce the trailing sidelobe level to specification tolerance and add series resistance to reduce VSWR (see Appendix IV). While both of these changes will increase insertion loss, it is felt that there is enough latitude between the measured and specified level to accomplish both goals.

Crystal orientation problems encountered with Valpey-Fisher during Phase I were resolved with the incorporation of a new Insepction procedure. Difficulties with lower than expected yeilds after dicing were eliminated by restepping photomasks for Phase II.

# APPENDIX I
# ELECTRONICS COMMAND TECHNICAL REQUIREMENTS
# SCS 476, DATED 9 DECEMBER 1974

# APPENDIX I

ELECTRONICS COMMAND
TECHNICAL REQUIREMENTS

SCS-476

## PHOTOLITHOGRAPHICALLY PRODUCED ACOUSTIC SURFACE WAVE PULSE COMPRESSION, BAND-PASS AND PHASE-CODED FILTERS

### 1. SCOPE

1.1 Scope. This specification covers the requirements for photolithographic and batch fabrication techniques necessary for the low-cost production of acoustic, surface-wave pulse compression, band-pass, and phase-coded filters.

### 2. APPLICABLE DOCUMENTS

2.1 The following documents, of the issue in effect on date of invitation for bids or request for proposal, form a part of this specification to the extent specified herein.

SPECIFICATIONS

MILITARY

| | |
|---|---|
| MIL-C-39012 | Connector, Coaxial, Radio Frequency, General Specification For. |

STANDARDS

MILITARY

| | |
|---|---|
| MIL-STD-105 | Sampling Procedures and Tables for Inspection by Attributes. |
| MIL-STD-130 | Identification Marking of US Military Property. |
| MIL-STD-202 | Test Methods for Electronic and Electrical Component Parts. |
| MIL-STD-883 | Test Methods and Procedures for Microelectronics. |

(Copies of specifications, standards, drawings, and publications required by suppliers in connection with specific procurement functions should be obtained from the procuring activity or as directed by the contracting officer. Both title and identifying number or symbol should be stipulated when requesting copies.)

## 3. REQUIREMENTS

3.1 General Description. The filters shall be photolithographically fabricated on lithium niobate or ST quartz substrates.

3.2 Processing.

3.2.1 Metallization. An aluminum film shall be deposited on the piezoelectric substrates using high vacuum or radio frequency sputtering systems. The resistivity shall be less than 0.5 ohms per square.

3.2.1.1 Uniformity of metallization. The absolute thickness of the aluminum film may vary between 1000 and 2000 angstrom ($A^{o}$); the uniformity of the thickness shall be controlled to ±5 percent.

3.2.1.2 Adhesion of metallic film. The adhesion of the aluminum film to the substrate shall remain intact on the surface of the substrate (see 4.6.2).

3.2.2 Photoresist application. Photoresist shall be applied to the lithium niobate and ST quartz substrates resulting in a thin uniform coating capable of resolving 2 micron lines.

3.2.3 Photolithographic processing. Contact printing (etching), "lift-off" or "wet contact" printing techniques shall be used, whereby photomasks are applied over the photoresist.

3.2.4 Visual inspection.

3.2.4.1 Wafer. Circuits on the undiced wafer shall be checked using a government approved prototype comparison standard to check the sameness of each circuit pattern using 1000K magnification.

3.2.4.2 Filter package (device). The circuit chip shall be examined after placement in package (without cover) for broken wire bonds, dirt, scratches or other circuit imperfections under 20X magnification.

3.2.5 Dicing of wafer into circuit chips. When required to separate the multiple identical circuits fabricated on the same waver, a diamond-tipped precision cutting tool shall be used.

3.2.6 Wire bonding. Wire bonding techniques shall be performed so that reliable electrical connections between the surface acoustic wave circuit and the package connectors are made.

3.2.7 Device packaging. Packaging and sealing techniques shall be used so that the resultant hermetically sealed filters shall be capable of meeting all the environmental requirements as specified herein.

3.3 Classes of devices. The required filter type devices are identified as follows:

| Devices | Substrate Materials | Center Frequency |
|---|---|---|
| a. Linear FM Pulse Compression Filter | ST Quartz | 150 MHz |
| | Lithium Niobate | 150 MHz |
| b. Linear Phase Band-Pass Filter | ST Quartz | 100 MHz |
| | Lithium Niobate | 150 MHz |
| c. Biphase-Coded Tapped Delay Line Filter | ST Quartz | 100 MHz |
| | ST Quartz | 200 MHz |

3.3.1 Linear FM pulse compression filters. In-line configuration shall be used with internal weighting for sidelobe suppression. Conjugate matched filter pairs shall be fabricated from each substrate material and used to demonstrate pulse compression in each case.

3.3.2 Linear-phase band-pass filters. Multistrip couplers shall be used on lithium niobate to couple the two apodized transducers which effect the weighted filter response.

3.3.3 Biphase-coded tapped delay line filters. Phase-coded tapped delay line filters with center frequencies of 100 and 200 MHz shall use uniform aperature for the phase-coded array. Conjugate matched filter pairs shall be fabricated and used to demonstrate autocorrelation.

3.4 Number of circuit chips per wafer.

3.4.1 Linear-FM pulse compression filters.

3.4.1.1 ST quartz. At least 10 circuit chips shall be fabricated on a single piezoelectric wafer.

3.4.1.2 Lithium niobate. At least 10 circuit chips shall be fabricated on a single piezoelectric wafer.

3.4.2 Linear-phase band-pass filters.

3.4.2.1 ST quartz. At least 15 circuit chips shall be fabricated on a single piezoelectric wafer.

3.4.2.2 Lithium niobate. At least 15 circuit chips shall be fabricated on a single piezoelectric wafer.

3.4.3 Biphase-coded tapped delay line filters.

3.4.3.1 At least 7 circuit chips shall be fabricated on a single piezoelectric ST quartz wafer.

3.5 Construction.

3.5.1 Connections (external). The basic filter shall employ two or three parts, depending on the type of filter device with connectors or strip leads. (The precise location should be finalized prior to the confirmatory sample phase).

3.5.1.1 Connectors. When connectors are used with these filter devices, they shall be series SMA and shall conform to the requirements of MIL-C-39012.

3.5.1.2 Strip leads (lead integrity). When strip leads are used, they shall show no physical or mechanical damage when tested (see 4.6.4.2).

3.5.2 Connections (internal), wire bonding (lead integrity). Gold wire connections of two mil diameter and minimum length, shall show no evidence of loosening or rupturing from the wire bond connection (see 4.6.4.1).

3.5.3 Dimensions. The crystal and package size shall meet the maximum dimensions in inches specified in Table I (see 4.6.3).

3.6 Hermetic seal. Each filter shall be back-filled with an inert gas and shall show no evidence of leakage (see 4.6.5).

3.7 Thermal shock. Each filter shall show no evidence of mechanical or physical damage and shall exhibit no short circuits (see 4.6.6).

3.8 Solderability (strip leads) (when applicable). Strip leads shall be solderable (see 4.6.7).

TABLE I. DIMENSIONS.

| Classes of Devices | Substrate Material | Max. Circuit Chip Size Substrate (Inches) L W T | Max. Filter Package Size (Inches) L W T |
|---|---|---|---|
| Linear-FM Pulse Type Compression Filters | ST Quartz<br>Lithium Niobate | 1.00 x 0.200 x 0.050 | 2.0 x 1.0 x 0.50 |
| Linear Phase Band Pass Filters | ST Quartz<br>Lithium Niobate | 1.00 x 0.200 x 0.050 | 2.0 x 1.0 x 0.50 |
| Biphase-coded Tapped Delay Lines | ST Quartz (100 MHz)<br>ST Quartz (200 MHz) | 2.20 x 0.200 x 0.050<br>2.20 x 0.200 x 0.050 | 3.0 x 1.0 x 0.50<br>3.0 x 1.0 x 0.50 |

3.9 Short circuit test. All circuit devices shall be checked for no shorted circuits (see 4.6.8).

3.10 Electrical characteristics. Filters shall meet the electrical characteristics and tolerances as specified (see 4.6.9).

3.10.1 Center frequency of operation.

3.10.1.1 Linear FM pulse compression filters.

a. ST Quartz: 150 MHz ±3 MHz.

b. Lithium Niobate: 150 MHz ±3 MHz.

3.10.1.2 Linear-phase band-pass filters.

a. ST Quartz: 100 MHz ±2 MHz.

b. Lithium Niobate: 150 MHz ±3 MHz.

3.10.1.3 Biphase-coded tapped delay line filters.

a. ST Quartz: 100 MHz ±2 MHz.

b. ST Quartz: 200 MHz ±4 MHz.

3.10.2 Bandwidth (3db).

3.10.2.1 Linear FM pulse compression filters.

a. ST Quartz: 50 MHz ±1 MHz.

b. Lithium Niobate: 50 MHz ±1 MHz.

3.10.2.2 Linear-phase band-pass filters.

a. ST Quartz: 2 MHz ±40 MHz.

b. Lithium Niobate: 30 MHz ±0.6 MHz.

3.10.2.3 Biphase-coded tapped delay line filters.

a. ST Quartz: 10 MHz ±0.2 MHz (100 MHz) center frequency.

b. ST Quartz: 10 MHz ±0.2 MHz (200 MHz) center frequency.

3.10.3 Time-delay.

3.10.3.1 Linear FM pulse compression filters (dispersive delay).

a. ST Quartz: 2 microsec ±0.01 microsec.

b. Lithium Niobate: 2 microsec ±0.01 microsec.

3.10.3.2 Linear-phase band-pass filters (nondispersive delay).

a. ST Quartz: 2 microsec ±0.01 microsec.

b. Lithium Niobate: 2 microsec ±0.01 microsec.

3.10.3.3 Biphase-coded tapped delay line filters.

a. ST Quartz: 12.7 microsec ±10 nanosec (100 MHz) center frequency.

b. ST Quartz: 12.7 microsec ±10 nanosec (200 MHz) center frequency.

3.10.4 Time-bandwidth product.

3.10.4.1 Linear FM pulse compression filters.

a. ST Quartz: 100:1

b. Lithium Niobate: 100:1

3.10.4.2 Linear-phase band-pass filters.

a. ST Quartz: 4:1

b. Lithium Niobate: 60:1

3.10.4.3 Biphase-coded tapped delay line filters.

a. ST Quartz: 127:1 (100 MHz) center frequency.

b. ST Quartz: 127:1 (200 MHz) center frequency.

3.10.5 Insertion loss.

3.10.5.1 Linear FM pulse compression filters.

a. ST Quartz: 55db ± 5 db.

b. Lithium Niobate: 30db ± 3db.

3.10.5.2 Linear-phase band-pass filters.

a. ST Quartz: 20db ± 2db.

b. Lithium Niobate: 15db ± 1.5db.

3.10.5.3 Biphase-coded tapped delay line filters.

a. ST Quartz: 30db ± 3db (100 MHz) center frequency.

b. ST Quartz: 30db ± 3db (200 MHz) center frequency.

3.10.6 Time-sidelobe suppression level.

3.10.6.1 Pulse compression filters.

a. ST Quartz: ≥ -25db.

b. Lithium Niobate: ≥ -25db.

3.10.6.2 Linear-phase band-pass filters.

a. ST Quartz: ≥ -35db.

b. Lithium Niobate: ≥ -35db.

3.10.6.3 Biphase-coded tapped delay line filters.

a. ST Quartz: ≥ -19db (100 MHz) center frequency.

b. ST Quartz: ≥ -19db (200 MHz) center frequency.

3.10.7 Feedthrough suppression. The feedthrough suppression shall be greater than -50db for all types of filters.

3.10.8 Spurious echo suppression. The spurious echo suppression shall be greater than -35db for all types of filters.

3.10.9 Voltage standing wave ratio (VSWR). The VSWR shall be less than 1.5:1 for all types of filters over the operating band with a 50 ohm impedance ($Z_o$).

3.11 High temperature storage. Filters shall show no evidence of physical or mechanical damage and no electrical short circuits after subjection to a temperature of 75°C (see 4.6.10 and 4.6.8).

3.12 Shock (specified pulse). Filters shall show no evidence of mechanical or physical damage and no electrical short circuits (see 4.6.11 and 4.6.8).

3.13 Vibration (low frequency). Filters shall show no evidence of mechanical or physical damage and no electrical short circuits (see 4.6.12 and 4.6.8).

3.14 Moisture resistance. Filters shall show no evidence of mechanical or physical damage and no short circuits. All of the electrical characteristics (final) shall be met in accordance with the limits provided in the government approved contractor's plan (see 4.6.13 and 4.6.8).

3.15 Life. After 500 hours of life, the filters shall show no evidence of mechanical or physical damage; and shall meet all of the electrical characteristics (final) in accordance with the limits provided in the government approved contractor's plan (see 4.6.14).

3.16 Marking. All markings shall remain legible throughout processing and testing in accordance with MIL-STD-130.

3.16.1 Wafer. Identification shall be provided on each chip on the substrate to indicate the manufacturer; crystal type; batch or lot; crystal cut and orientation.

3.16.2 Filter. Identification of the type of device along with a descriptive identifying number indicating operating frequency and bandwidth.

3.17 Workmanship. Chips and filters shall be processed in such a manner as to be uniform in quality and shall be free from cracks or other defects that will affect life, serviceability and appearance.

4. QUALITY ASSURANCE PROVISIONS

4.1 Responsibility for inspection. The contractor is responsible for the performance of all inspections specified herein. The contractor may utilize his own facilities or any commercial laboratory acceptable to the government. Tests shall be performed under the supervision of a government representative. Inspection records of the examinations and tests shall be kept complete and available to the government as specified in the contract.

4.2 Classification of inspection. Inspection shall be classified as follows:

a. First article inspection (does not include preparation for delivery) (see 4.4).

b. Quality conformance inspection.

4.3 Inspection condition. Unless otherwise specified herein, all inspections shall be in accordance with the test conditions specified in general requirement of MIL-STD-202.

4.4 First article inspections. This inspection shall consist of all the tests in Tables III and IV including the use of the contractor submitted government-approved plan on test methods and procedures for determining the electrical characteristics and the electrical characteristics final limits. No failures in excess of those indicated shall be permitted.

4.4.1 Sample.

4.4.1.1 Wafers. (See Table II.)

4.4.1.2 Circuit chips. The wafers shall be diced into discrete circuit chips with the exclusion of one wafer for each type of substrate and shall be submitted for inspection as indicated in Table II.

4.4.2 Test routine.

4.4.2.1 Wafer submission. Sample units shall be subjected to the inspection specified in Table III, in the order shown prior to dicing into discrete circuit devices. Ten (10) each of the first four categories in Table II shall be tested and seven (7) each of the last two categories (ST Quartz 100 and 200 MHz, respectively).

4.4.2.2 Circuit devices. Eighty-four (84) operable filter circuit devices shall be submitted to the inspections specified in Table IV, in the order shown. Twelve sample units shall be used for group II inspection only. The remaining units shall be subjected to group I inspection and subdivided into the remaining groups for their particular examination or test.

TABLE II. CLASS OF DEVICES WITH MINIMUM NUMBER OF WAFERS, CIRCUITS PER WAFER AND TOTAL NUMBER OF OPERABLE FILTER CIRCUIT DEVICES.

| Class of devices | Minimum Nr. of wafers | Minimum Nr. of circuits per wafer | Operable filter circuit devices |
|---|---|---|---|
| Linear FM pulse compression filters | 10-ST Quartz | 10 | 84 |
| | 10-Lithium Niobate | 10 | 84 |
| Linear band-pass filters | 10-ST Quartz | 15 | 84 |
| | 10-Lithium Niobate | 15 | 84 |
| Biphase-coded tapped delay line filters | 7-ST Quartz (freq 100 MHz) | 7 | 42 \| 84 |
| | 7-ST Quartz (freq 200 MHz) | 7 | 42 \| |

TABLE III. FIRST ARTICLE INSPECTION OF EACH TYPE OF WAFER.

| Examination or test | Requirement paragraph | Test paragraph |
|---|---|---|
| Marking | 3.16.1 | |
| Visual check (using a standard for reference under magnification) (1000X) | 3.2.4.1 | 4.6.1.1 |
| Adhesion of metallic film | 3.2.1.2 | 4.6.2 |
| Short circuit | 3.9 | 4.6.8 |

TABLE IV. FIRST ARTICLE INSPECTION OF EACH CLASS OF FILTER DEVICES (CIRCUIT DEVICES).

| Examination or test | Requirement paragraph | Test paragraph | Number of Samples | Number of Defects |
|---|---|---|---|---|
| Group I | | | | |
| Visual check (20X magnification) | 3.2.4.2 | 4.6.1.2 | 72 | 0 |
| Marking | 3.16.2 | | | |
| Dimensions | 3.5.3 | 4.6.3 | | |
| Strip lead (lead integrity) | 3.5.1.2 | 4.6.4.2 | | |
| Internal wire bonding (lead integrity) | 3.5.2 | 4.6.4.1 | | |
| Electrical characteristics | 3.10 | 4.6.9 | | |
| Group II | | | | |
| Solderability (when applicable) | 3.8 | 4.6.7 | 12 | 0 |
| Group III | | | | |
| High temperature storage | 3.11 | 4.6.10 | 18 | 0 |
| Electrical characteristics | 3.10 | 4.6.9 | | |
| Center frequency | 3.10.1 thru 3.10.1.3, incl. | | | |
| Insertion loss | 3.10.5 thru 3.10.5.3, incl. | | | |
| Group IV | | | | |
| Life | 3.15 | 4.6.14 | 18 | 1 |
| Short circuit test | 3.9 | 4.6.8 | | |
| Electrical characteristics (Final) | 3.10 | 4.6.9 | | |
| Group V | | | | |
| Hermetic seal | 3.6 | 4.6.5 | 12 | 0 |
| Short circuit test | 3.9 | 4.6.8 | | |

TABLE IV. FIRST ARTICLE INSPECTION OF EACH CLASS OF FILTER DEVICES (CIRCUIT DEVICES) (Continued).

| Examination or test | Requirement paragraph | Test paragraph | Number of Samples | Number of Defects |
|---|---|---|---|---|
| Group VI | | | | |
| Vibration | 3.13 | 4.6.12 | | |
| Short circuit test | 3.9 | 4.6.8 | | |
| Shock | 3.12 | 4.6.11 | | |
| Short circuit test | 3.9 | 4.6.8 | | |
| Thermal shock (10 cycles) | 3.7 | 4.6.6 | 24 | 2 |
| Short circuit test | 3.9 | 4.6.8 | | |
| Moisture resistance | 3.14 | 4.6.13 | | |
| Short circuit test | 3.9 | 4.6.8 | | |
| Electrical characteristics (Final) | 3.10 | 4.6.9 | | |

4.4.3 Defectives.

4.4.3.1 Wafers. No defects shall be allowed in Table III; any defects shall be cause for refusal to grant first article inspection approval.

4.4.3.2 Filter circuit devices. Defects in excess of those allowed in Table IV shall be cause for refusal to grant first article inspection approval.

4.5 Quality conformance inspection.

4.5.1 Inspection of product for delivery. Inspection of products for delivery shall consist of groups A, B and C inspection.

4.5.1.1 Inspection lot. An inspection lot shall be as specified in MIL-STD-105.

4.5.1.2 Group A inspection. Group A inspection shall consist of the examinations and tests in Table V in the order shown. Subgroup I examination and tests are on wafers and subgroup II on the filter circuit devices.

TABLE V. GROUP A INSPECTION.

| Examination or test | Requirement paragraph | Method paragraph |
|---|---|---|
| Subgroup I | | |
| Marking | 3.16.1 | |
| Adhesion of metallic film | 3.2.1.2 | 4.6.2 |
| Short circuit | 3.9 | 4.6.8 |
| Subgroup II | | |
| Visual (magnification 20X) | 3.2.4.2 | 4.6.1.2 |
| Marking | 3.16.2 | |
| Hermetic seal | 3.6 | 4.6.5 |
| Strip lead (lead integrity) | 3.5.1.2 | 4.6.4.2 |
| Internal wire bonding (lead integrity) | 3.5.2 | 4.6.4.1 |

4.5.1.2.1 Sampling plan. 100 percent inspection shall be performed on subgroup I on the wafers which shall then be diced into discrete circuits; and subgroup II inspection shall be performed using 100 percent inspection.

4.5.1.2.2 Rejected samples. If during the 100 percent inspection of subgroup II, screening requires that over 30 percent of the wafers be discarded, the lot shall be rejected.

4.5.1.3 Group B Inspection. Group B inspection shall consist of the tests specified in Table VI, in the order shown and shall be made on sample units which have been subjected to and have passed group A, subgroup II inspection.

TABLE VI. GROUP B INSPECTION.

| Examination or test | Requirement paragraph | Method paragraph |
|---|---|---|
| Electrical characteristics | | |
| Center frequency of operation | 3.10.1, 3.10.1.1, 3.10.1.2, 3.10.1.3 | 4.6.9 |
| Bandwidth | 3.10.2, 3.10.2.1, 3.10.2.2, 3.10.2.3 | 4.6.9 |
| Time delay | 3.10.3, 3.10.3.1, 3.10.3.2, 3.10.3.3 | 4.6.9 |
| Time-bandwidth product | 3.10.4, 3.10.4.1, 3.10.4.2, 3.10.4.3 | 4.6.9 |
| Insertion loss | 3.10.5, 3.10.5.1, 3.10.5.2, 3.10.5.3 | 4.6.9 |
| Time-sidelobe suppression level | 3.10.6, 3.10.6.1, 3.10.6.2, 3.10.6.3 | 4.6.9 |
| Feedthrough suppression | 3.10.7 | 4.6.9 |
| Spurious echo suppression | 3.10.8 | 4.6.9 |
| Voltage standing wave ratio (VSWR) | 3.10.9 | 4.6.9 |

4.5.1.3.1 Sampling plan. Sampling plan shall be in accordance with special procedures for small sample inspection of MIL-STD-105. The AQL shall be 6.5 percent defective using inspection level S-4.

4.5.1.3.2 Test routine. The samples specified in 4.5.1.3 shall be subjected to the tests in Table VI in the order shown.

4.5.1.3.3 Rejected lots. If an inspection lot is rejected, the contractor may withdraw the particular lot once, screen out defectives, and reinspect once. Such lots shall be kept separate from new lots and shall be clearly identified as reinspected lots. Rejected lots shall be reinspected using tightened inspection.

4.5.1.3.4 Disposition of samples. Sample units which have passed all the group B inspections may be delivered on the contract, if the lot is accepted and the sample units are still within the electrical tolerances.

4.5.1.4 Group C inspection. Group C inspection shall be performed once each month and shall consist of the tests specified in Table VII, in the order shown. Group C inspection shall be made on sample units selected from inspection lots which have passed groups A and B inspections.

4.5.1.4.1 Sampling plan. Six sample units shall be selected for each of subgroups, 1, 2 and 3 at random from each lot as specified in 4.5.1.1.

4.5.1.4.1.1 Test routine. The samples selected in accordance with 4.5.1.3 shall be subjected to the tests shown in Table VII. Not more than one defect shall be allowed for a single group of six samples.

4.5.1.4.2 Disposition of samples. Filter circuit devices subjected to group C inspection shall not be delivered on the contract or order.

TABLE VII. GROUP C INSPECTION.

| Examination or test | Requirement paragraph | Test paragraph |
|---|---|---|
| Group I | | |
| High temperature storage | 3.11 | 4.6.10 |
| Short circuit | 3.9 | 4.6.8 |
| Hermetic seal | 3.6 | 4.6.5 |
| Short circuit | 3.9 | 4.6.8 |
| Subgroup II | | |
| Solderability (strip leads) (when applicable) | 3.8 | 4.6.7 |
| Life | 3.15 | 4.6.14 |
| Electrical characteristics (final) | 3.10 | 4.6.9 |
| Subgroup III | | |
| Vibration | 3.13 | 4.6.12 |
| Short circuit | 3.9 | 4.6.8 |
| Shock | 3.12 | 4.6.11 |
| Short circuit | 3.9 | 4.6.8 |
| Thermal shock (10 cycles) | 3.7 | 4.6.6 |
| Short circuit | 3.9 | 4.6.8 |
| Moisture resistance | 3.14 | 4.6.13 |
| Electrical characteristics (final) | 3.10 | 4.6.9 |

4.5.1.4.3 Noncompliance. If a sample fails to pass group C inspection, the contractor shall take corrective action on the materials or processes, or both, as warranted, and on all units of product which can be corrected and which were manufactured under essentially the same materials, processes, and so forth, and which are considered subject to the same failure. Acceptance of the product shall be discontinued until corrective action, acceptable to the government, has been taken. After the corrective action has been taken, group C

inspection shall be repeated on additional sample units (all inspections or the inspection which the original sample failed at the option of the government). Groups A and B inspection may be reinstituted; however, final acceptance shall be withheld until the group C reinspection has shown that the corrective action was successful. In the event of failure, action shall be furnished to the contracting officer.

4.6 Methods of examination and test.

4.6.1 Visual.

4.6.1.1 Wafer (see 3.2.4.1 and 3.17). A government approved comparison standard shall be utilized using 1000X magnification.

4.6.1.2 Filter device (see 3.2.4.2 and 3.17). An examination for circuit inspections shall be performed under 20X magnification.

4.6.2 Adhesion of metallic film (see 3.2.1.2). A one-inch strip of pressure sensitive cellophane tape, conforming to type I, class A of Federal Specification L-T-90, shall be applied to the metallized surface, adhesion side down, employing firm hand pressure. The tape shall then be removed with one abrupt motion, and the adhesive side examined for detached particles of metallic film.

4.6.3 Dimensions (see 3.5.3). Dimensions shall be measured using a micrometer.

4.6.4 Lead integrity (internal wire bonding and strip lead). Filter devices shall be tested in accordance with method 2004 of MIL-STD-883, method 4.6.4.1 or 4.6.4.2 as applicable.

4.6.4.1 Internal wire bonding. The following details shall apply:

a. Test condition A - Tension.
b. Weight to be attached to lead - 2 grams.
c. Length of time weight is to be attached - A minimum of 10 seconds.

4.6.4.1.2 Strip lead. Test condition A - Tension.

4.6.5 Hermetic seal (see 3.6). Filter devices shall be tested in accordance with method 112B, MIL-STD-202. The following details shall apply:

a. Test condition - C.
b. Leak-rate sensitivity - $10^{-8}$ atm cc/sec.
c. Procedure IV, test for gross leaks using test condition A.

4.6.6 Thermal shock (see 3.7). Filter devices shall be tested in accordance with method 107, MIL-STD-202, test condition A (10 cycles).

4.6.7 Solderability (strip leads only, when applicable) (see 3.8). Filter devices shall be tested in accordance with method 2003 of MIL-STD-883. Each strip lead on a filter device shall be tested.

4.6.8 Short circuit (see 3.9). Chip and filter devices shall be tested for short circuits by any suitable means.

4.6.9 Electrical characteristics (see 3.10). The government approved contractor's plan of electrical test methods, procedures and limits of degradation (electrical characteristics final) shall be used.

4.6.10 High temperature storage (see 3.11 and 3.9). Filter devices shall be tested in accordance with method 1008 of MIL-STD-883. The following details shall apply:

a. Test condition - A (75°C).
b. Test duration - 72 hours.
c. At the end of the exposure period, the devices shall be allowed to stabilize at room temperature and the filter device tested for short circuits.

4.6.11 Shock (specified pulse). Filter devices shall be tested in accordance with method 213 of MIL-STD-202. The following details shall apply:

a. Test condition - I
b. Method of mounting - Filter devices shall be rigidly mounted by their normal mounting means.

4.6.12 Vibration (low frequency) (see 3.13). Filters shall be tested in accordance with method 201 of MIL-STD-202. The filters shall be rigidly mounted by their normal mounting means.

4.6.13 Moisture resistance (see 3.14). Filters shall be tested in accordance with method 106D of MIL-STD-202. The following details shall apply:

a. Polarizing voltage - 50 Vdc
b. Final measurements - Before measurements, all units shall be removed from the test chamber and stabilized at room temperature. The filters shall be visually inspected and all electrical characteristics shall be performed and degradation

limits shall be as indicated in the government approved contractor's plan.

4.6.14 Life (at elevated ambient temperature) (see 3.15). Filters shall be tested in accordance with method 108 in MIL-STD-202. The following details and exceptions shall apply:

a. Mounting - Normal mounting means as used in a system or sub-system.

b. Distance between filter devices - 6 inches.

c. Test temperature and tolerance - $85^{\circ}C \begin{smallmatrix} + 10^{\circ} \\ - 5^{\circ} \end{smallmatrix} C$.

d. Final measurements - Before measurements are made, all units shall be removed from the test chamber and stabilized at room temperature. All electrical characteristics shall be performed and degradation limits shall be as indicated in the government approved contractor's plan.

5. PREPARATION FOR DELIVERY.

The substrates, circuit chips and filters shall be in accordance with best commercial practices.

6. NOTE

Normally the filter device will be employed in a system or sub-system as a plug-in device, hence, soldering will not normally be required.

# *Errata Sheet on SCS-476
# Photolithographically Produced Acoustic Surface Wave Pulse Compression, Band Pass and Phase-Coded Filters

1. Page 1-4, paragraph 3.6 Hermetic seal. Delete "leakage" and substitute "leakage".

2. Page 1-5, paragraph 3.9 Short circuit test. Delete and substitute:

   "3.9 Short circuit and open circuit tests. All chips and filter circuit devices, as applicable, shall be checked for no shorted circuits. A continuity check shall be made to determine that no open circuits exist between the external connection and the surface wave circuit."

3. Page 1-15, paragraph 4.6.8 Short circuit. Delete and substitute:

   "4.6.8 Short circuit and open circuit tests. All chips and filter circuit devices, as applicable, shall be tested for short circuits by any suitable means including the open circuit test between the external connection and the surface wave circuit."

4. Page 1-9, paragraph 4.4.2.1 Wafer submission. Add this sentence to this paragraph: "There shall be no failures."

   Page 1-9, paragraph 4.4.2.2 Circuit devices. Add this sentence to this paragraph:

   "Forty-two sample units of each substrate material (100 MHz and 200 MHz) of the operable biphase-coded tapped delay line filter circuit devices shall be submitted to the inspections specified in Table IV, in the order shown, using 36 sample units for group I; 6 sample units for group II; 9 sample units for groups III and IV; 6 sample units for group V, and 12 sample units for group VI. The number of defects shall remain as indicated for each group excluding group VI, where only 1 defect shall be allowed.

5. Page 1-11, paragraph 4.5.1.1 Inspection lot. Delete and substitute:

   "An inspection lot shall be as specified in MIL-STD-105 and applies to each of the six types of wafers or filter circuit devices, as applicable".

   Page 1-11, paragraph 4.5.1.2.2 Rejection samples. Delete and substitute:



*Negotiated at post award conference

"If during the 100 percent inspection of subgroup I, screening indicated that over 30 percent of the total filter circuit devices on the wafer (undiced) be discarded, the lot (wafers) shall be rejected".

6. Page 1-12, paragraph 4.5.1.3.4 Disposition of samples. Delete this paragraph in its entirety.

Page 1-12, paragraph 4.5.1.4 Group C inspection. In the first sentence, delete the following:

"shall be performed once each month and"

Page 1-12, paragraph 4.5.1.4.1 Sampling plan. After six sample units, add the following:

" of each type of tiler circuit device"

Page 1-12, paragraph 4.5.1.4.2 Disposition of samples. Add the following sentence:

"Samples emanating from lots which have passed groups A, B and C inspection may be delivered on the contract".

AD-A065 566 HUGHES AIRCRAFT CO FULLERTON CALIF GROUND SYSTEMS GROUP F/G 9/5
PHOTOLITHOGRAPHIC TECHNIQUES FOR SURFACE ACOUSTIC WAVE (SAW) DE--ETC(U)
DEC 78 A W DOZIER, W R SMITH DAAB07-75-C-0044
UNCLASSIFIED FR-79-12-40-VOL-2 DELET-TR-75-0044-F-V-2 NL

2 OF 2
AD
A065566

END
DATE
FILMED
5-79
DDC

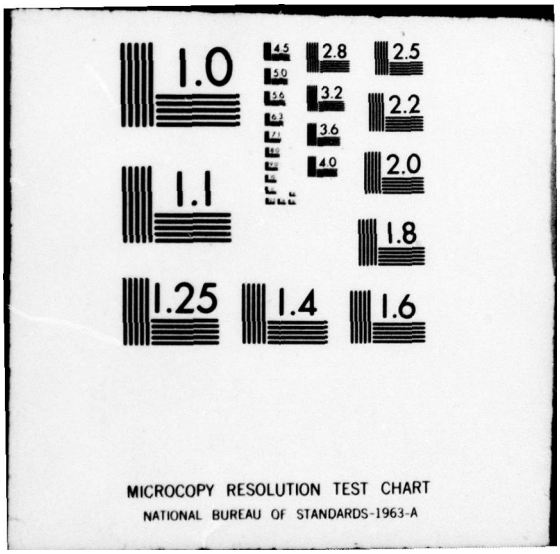
1.0
1.1
1.25
1.4
1.6
1.8
2.0
2.2
2.5
2.8
3.2
3.6
4.0
4.5
5.0
5.6
MICROCOPY RESOLUTION TEST CHART
NATIONAL BUREAU OF STANDARDS-1963-A

# APPENDIX II
# A SIMPLE TECHNIQUE FOR MAKING PI-POINT DELAY MEASUREMENTS ON SAW DELAY LINES

# APPENDIX II

## A SIMPLE TECHNIQUE FOR MAKING PI-FOINT DELAY MEASUREMENTS ON SAW DELAY LINES

As described by E.H. Young[1] the most accurate method of measuring the time delay characteristics of an acoustic delay line is to first determine its transfer phase characteristics in the frequency domain. For our purposes, let this function be:

$$\phi_{DEG}(f) = -360\, A_1 f - \phi_{err}(f) \tag{1}$$

Where $A_1$ is some constant that gives the best linear fit to actual phase response and $\phi err(f)$ is the difference between that estimate and the measured phase response. Once this phase characteristic is known, the group delay, $\tau_g$, of the line can be calculated by taking the derivative of the phase response which yields:

$$\tau_g(f) = -\left[\frac{1}{360}\,\frac{d\phi(f)}{df}\right] = A_1 + \frac{1}{360}\,\frac{d\,\phi err^f}{df} \tag{2}$$

For an ideal nondispersive delay line, the phase error term in (1) would be zero and thus the $A_1$ constant would be equal to the group delay of the line for all frequencies. In an actual device the error term is nonzero which means that the group delay will vary with frequency about this $A_1$ value as a function of phase error derivative term given in (2).

In its simpler form, the derivative in (2) is approximated by noting the change in frequency required to give some incremental phase shift. This means the group delay function is set equal to:

$$\tau_g(f) = -\frac{1}{360}\,\frac{\phi_2-\phi_1}{f_2-f_1} = -\frac{1}{360}\,\frac{\Delta\phi}{\Delta f} \tag{3}$$

Where the measurement frequency, f, is taken to be the average of $f_1$ and $f_2$. When $\Delta\phi$ is set equal to some multiple of $360^\circ$ or $2\pi$ radians, the delay is calculated by evaluating:

$$\tau_g(f) = \frac{1}{360} \frac{N(360)}{\Delta f} = \frac{N}{\Delta f} \qquad (4)$$

Where N is the number of $2\pi$ resolutions or "pi-points" used in making the measurement. For an ideal nondispersive line, the derivative of the $\phi(f)$ function is exactly equal to the finite difference approximation given in (3), which means that the group delay could be determined with a single measurement. However, in a practical situation where higher order phase error terms are present, numerous pi-point measurements must be taken to accurately determine a device group delay characteristics. As an aid to making these measurements on a semi-automatic basis, Hughes has developed a simple measurement technique that utilizes the discrete frequency stepping increment capabilities of the HP 8660B frequency synthesizer. The frequency synthesizer has been designed so that it takes 1000 discrete steps to cover a specified sweep range. This means the $\Delta f$ frequency change in (3) is equal to $\Delta F/1000$, where $\Delta F$ is the desired sweep range about some specified center frequency. This discrete stepping increment can be used to quickly determine the $A_1$ constant giving the best linear fit to a given delay line phase response as described below.

The key to making group delay measurements with the synthesizer is to pick some $\Delta F$ sweep range so that $\Delta f$ step size between measurements will result in a $\Delta\phi$ phase change of some desired value. In some cases, it is practical to set $\Delta f$ so that $\Delta\phi$ is equal to $-360^\circ$. Under this condition, the measured phase response for an ideal line would be displayed as a constant straight line, and the group delay would be found by solving (3) for the specified test conditions given by:

$$\tau_g = \frac{\Delta\phi}{360\ \Delta f} = -\frac{-360}{360\ \Delta F/1000} = \frac{1000}{\Delta F}$$

If the $\Delta F$ sweep range picked for this ideal line was smaller than the best fit value, then the phase change between measurements would be smaller than $-360^\circ$, and the resulting phase measurements would be displayed as a straight line having a positive slope. If the step size was too large, then the slope of displayed phase would be negative. With these characteristics, the step size required to achieve the best linear fit to the lines phase response can be determined quite accurately in a short period of time.

In cases where a device has a short time delay and a narrow frequency response, only a few pi-points may occur over its passband. In these situations, a step size corresponding to an integral fraction of a 360° phase change may be used to attain a reasonable degree of resolution in the lines amplitude and phase response. An example of this type of measurement is shown for the BPQ lines developed for this program. In this case, the step size was picked such that the phase change between measurements was 10° as shown in the data of Figure IA-1. Under these conditions, the phase response will return to the same value on every 36th measurement. Consequently, the phase response is displayed as a series of repetitive phase error curves reported by 10° increments. If desired, the discrete nature of the resulting curves can be filled in by taking multiple measurements of the lines using different phase offsets. The step size in this example was picked to obtain a flat phase error response at the center of the lines passband response. Using equation (4) the corresponding group delay was computed to be:

$$\tau_g = \frac{-\Delta\phi}{360\ \Delta f} = -\frac{-10^\circ}{360\ \Delta F/1000} = \frac{(10)\,(1000)}{360(13.92\ \text{MHz})} = 1.995\mu\text{sec}$$

The residual nonlinear phase error shown for this linear fit estimate indicated that this group delay tended to become larger near the skirts of its passband. The magnitude of this group delay change could be computed by fitting a function to the error curve and then taking the derivative of that function as noted in equation (2).

(1) E.H. Young, "Discussion of Time Delay in Reference to Electrical Waves," IRE Trans. on Ultrasonics Engineering, Vol. UE-9, No. 1, pp 13-21, July 1962.

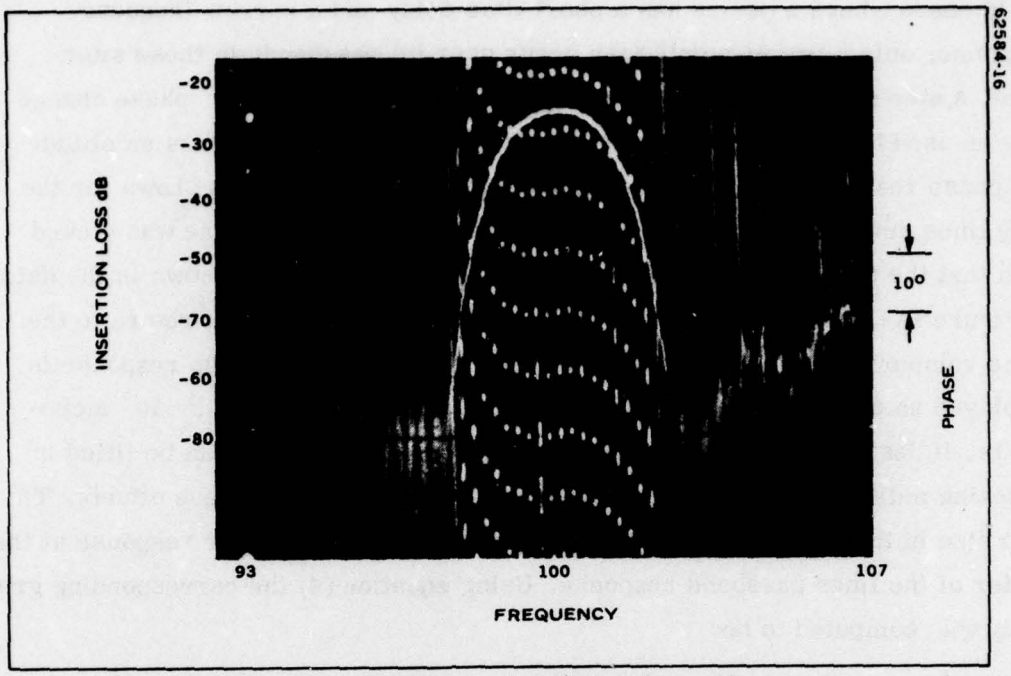


**Figure I-A-1. Insertion Loss and Phase of a BP-Q Filter. Phase component shown is the residual nonlinear component after removing a linear term corresponding to the 1.995 $\mu$sec delay.**

# APPENDIX III
# IMPEDANCE MATCHING TO HIGH-Q SAW TRANSDUCERS

# APPENDIX III

## IMPEDANCE MATCHING TO HIGH-Q SAW TRANSDUCERS

Broadband coupling between a resistive source and a SAW transducer on ST-quartz is complicated by the inherent high-Q impedance characteristic of the transducer. In particular, this limits the maximum bandwidth for which both low insertion loss and low VSWR can be achieved. In this section the design tradeoffs made in selecting the matching network for the TDL-100 and TDL-200 input transducers will be described. Estimates of fundamental limitations on broadband coupling based on the Bode-Fano network theorem will be reviewed. The specific problem of matching the TDL input transducers will then be discussed and the selected approach will be analyzed with emphasis on the tradeoff among insertion loss, VSWR, and deviation from the desired response.

### Fundamental Limitations

The equivalent circuit of a SAW transducer illustrated in Figure IC-1a, consists of the static interelectrode capacitance in parallel with the radiation admittance parameters which represent the electric-to-acoustic conversion process. If it is assumed that $B_a = o$ and $G_a = \hat{G}_a$ = constant over the frequency band of interest, the problem illustrated in Figure IC-1b reduces to the classical one of matching a resistive source to a parallel R-C load. Following the analysis of Reeder and Sperry[1], one can invoke the theorem of Bode[2] and Fano[3] for ideal coupling networks which relates reflection coefficient, $\Gamma(f)$, the load parameters and the frequency, f, according to

$$\int_0^\infty \ln\left|\Gamma(f)\right|^{-1} df = \pi/RC \qquad (1)$$

In order to evaluate theoretical limits, one considers the most efficient possible network; that is, one which provides constant coupling ($\left|\Gamma(f)\right| = \left|\Gamma_m\right|$) over the desired bandwidth, $\Delta F$, but which totally reflects incident energy ($\Gamma(f) = 1$) at all other frequencies. In this case, (1) reduces to

$$\left|\Gamma_m\right| = \exp\left[-\frac{\pi}{(\Delta F)RC}\right] \qquad (2)$$

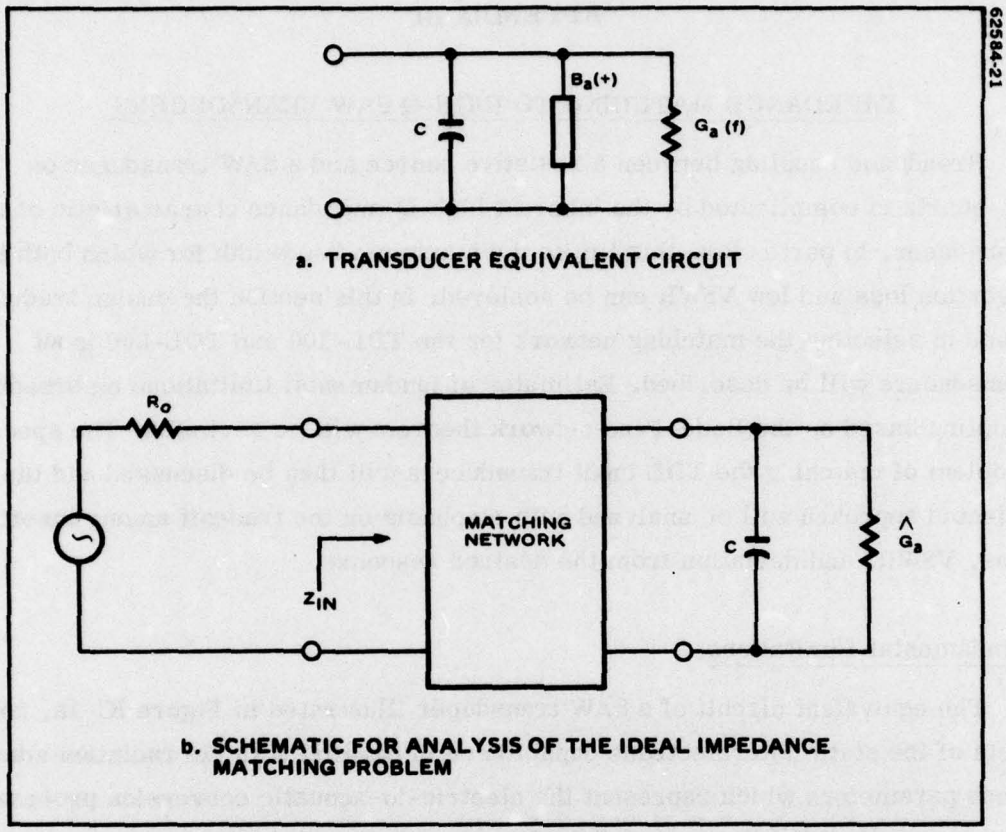


Figure I-C-1. Equivalent Circuits for the Transducer Impedance Matching Problem

which can be expressed in terms of the Q of the RC load as

$$\left|\Gamma_m\right| = \exp\left[-\frac{\pi}{\beta Q}\right] \tag{3}$$

where $\beta$ is the desired fractional bandwidth. The corresponding input VSWR and reflection loss can now be expressed as

$$\text{VSWR} = \frac{1+\left|\Gamma_m\right|}{1-\left|\Gamma_m\right|} \tag{4}$$

and

$$\text{LOSS} = 10\log_{10}\frac{1}{1-\left|\Gamma_m\right|^2} = -10\log_{10}\left(1-\exp\left[\frac{-2\pi}{\beta Q}\right]\right) \tag{5}$$

These results clearly identify the fractional bandwidth -Q product ($\beta Q$) as the primary parameter in determining the minimum achievable insertion loss and VSWR. Equations (4) and (5) are plotted in Figure IC-2 to illustrate these relationships.

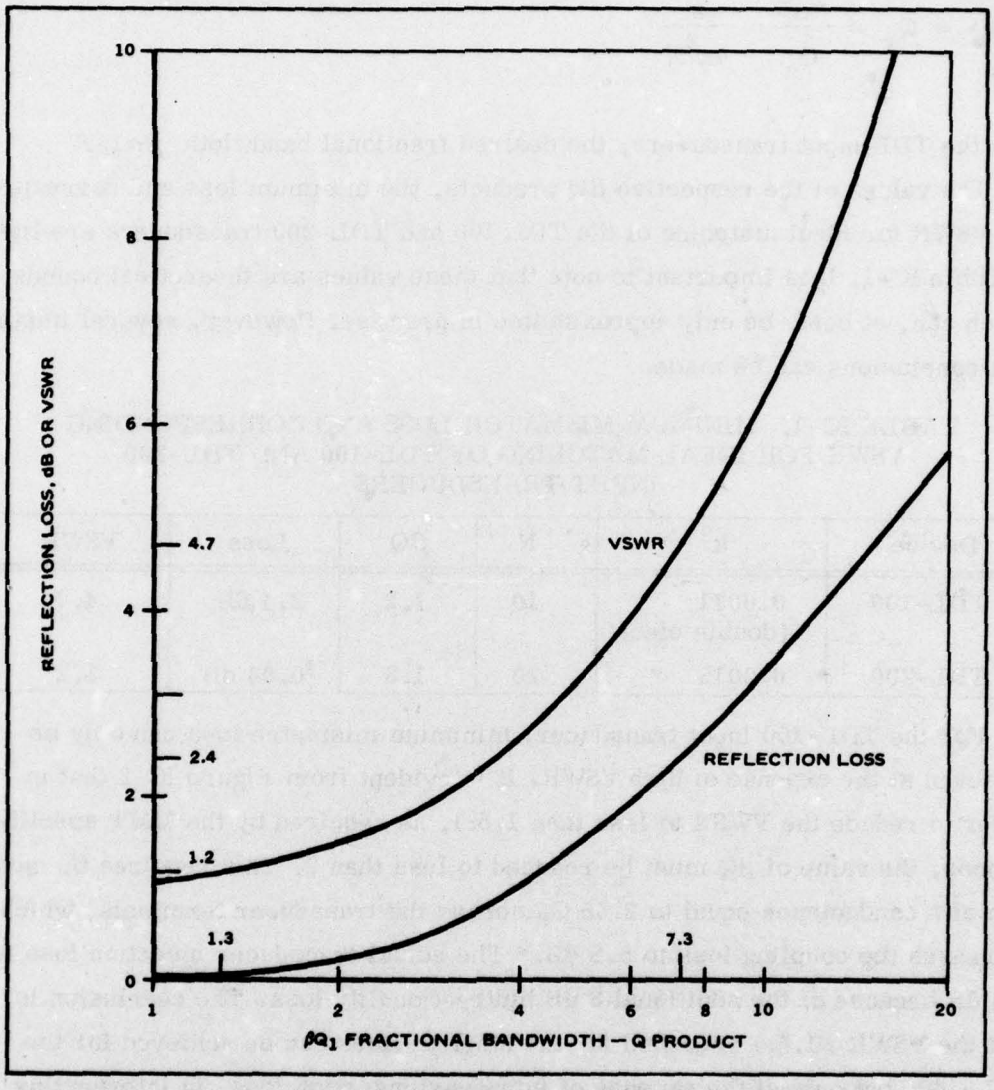


Figure I-C-2. Reflection Loss and VSWR for the Assumed Ideal Matching Network

This theory can be applied approximately to uniform, periodic SAW transducers. The equivalent circuit parameters are given by:

$$\hat{G}_a = 8k^2 f_o CN$$

$$\omega C = 2\pi f_o C$$

where $f_o$ is the center frequency, $k^2$ is the electromechanical coupling constant, and N is the number of pairs of active interelectrode gaps. The load Q assumed in (3) corresponds to the acoustic radiation Q; that is,

$$Q = Q_r = \frac{\omega_o C}{\hat{G}_a} = \frac{\pi}{4k^2 N} \tag{6}$$

For the TDL input transducers, the desired fractional bandwidth $\beta \alpha 1/N$

The values of the respective $\beta Q$ products, the minimum loss and corresponding VSWR for ideal matching of the TDL 100 and TDL-200 transducers are listed in Table IC-1. It is important to note that these values are theoretical bounds which can, at best, be only approximated in practise. However, several important conclusions can be made.

TABLE IC-1. MINIMUM MISMATCH LOSS AND CORRESPONDING VSWR FOR IDEAL MATCHING OF TDL-100 AND TDL-200 INPUT TRANSDUCERS

| Device | $k^2$ | N | $\beta Q$ | Loss | VSWR |
|---|---|---|---|---|---|
| TDL-100 | 0.0011 (double elec) | 10 | 7.2 | 2.4 dB | 4.7 |
| TDL-200 | 0.0015 | 20 | 1.3 | 0.04 dB | 1.2 |

For the TDL-100 input transducer, minimum mismatch loss can only be achieved at the expense of high VSWR. It is evident from Figure IC-2 that in order to reduce the VWSR to less than 1.5:1, as required by the MMT specifications, the value of $\beta Q$ must be reduced to less than 2. This requires the addition of a conductance equal to $2.65\ \hat{G}_a$ across the transducer terminals, which increases the coupling loss to 5.8 dB.* The actual transducer insertion loss is 8.8 dB because of the additional 3 dB bidirectionality loss. The conclusion is that the VSWR $\leq$1.5:1 specified for the MMT devices can be achieved for the TDL-100, but only at the expense of increased insertion loss. In interpreting this result, it should be recalled that the theory assumes an ideal matching

*This is calculated as follows: For $\beta Q = 2.0$, the coupling loss to the total load is 0.2 dB. However, the power splits between the added conductance and the transducer so that the latter receives the fraction $10 \log_{10} (\hat{G}_a / 2.65\ \hat{G}_a + \hat{G}_a) = -5.6$ dB. Therfore, the net loss is 5.6 + 0.2 = 5.8 dB.

network which cannot be realized in practice. Good approximations can be implemented using impedance transformers such as the lowpass impedance inverter networks described by Reeder and Speery[1]. However, at least a single-section $\pi$ network is involved and usually up to 4 sections are required to achieve near-optimum performance. For simpler series or shunt-tuned transducers, considerably higher insertion loss can be expected.

For the TDL-200 transducer, minimal loss and VSWR can simultaneously be achieved, but the practical problem of matching network realization must also be solved in this case.

## Design Considerations for Matching the TDL Input Transducers

Section 2.3.1 describes the design of the TDL-100 and TDL-200 devices. In both cases, the number of electrodes in the tap transducers was chosen to suppress tap reflections by at least 25 dB and the acoustic aperture was then chosen to minimize tap array insertion loss. In both designs, the resulting aperture was roughly 100 acoustic wavelengths. It was concluded that the multi-element matching networks required to optimize the couplings of the input transducers to the source were not feasible because of thier cost, size and complexity. Instead the simple series R-L matching circuit shown in Figure IC-3 was selected. The inductor resonates the transducer reactance at the center frequency, $f_o$, and minimizes the reactance at the ±5 MHz bandedges. The series resistance value is selected to minimize the input VSWR over the operating bandwidth. For the remainder of this analysis, it will be assumed that $R_S$ is chosen so the total input resistance at midband equals $R_o$, the source resistance. The resistor can be implemented as part of the transducer summing bar structure, leaving the series inductor as the only separate tuning component.

Figures IC-4 and IC-5 present the calculated input transducer insertion loss, maximum VSWR and bandedge distortion as a function of the acoustic aperture of the TDL-100 and TDL-200 input transducers, respectively. The bandedge distortion is assessed by calculating the increase in insertion loss from midband to the $f_o$ ±5 MHz bandedges, and denoting the result as $\Delta$IL (±5 MHz) in Figures 4 and 5. This parameter is then compared with the ideal value of $\Delta$IL = 3.92 dB to obtain a measure of amplitude distortion produced by the matching network. The results for the TDL-200 are acceptable because the VSWR is less than the required value of 1.5, while the midband insertion loss is only 4.2 dB higher than the ideal value computed earlier, and the insertion loss at the

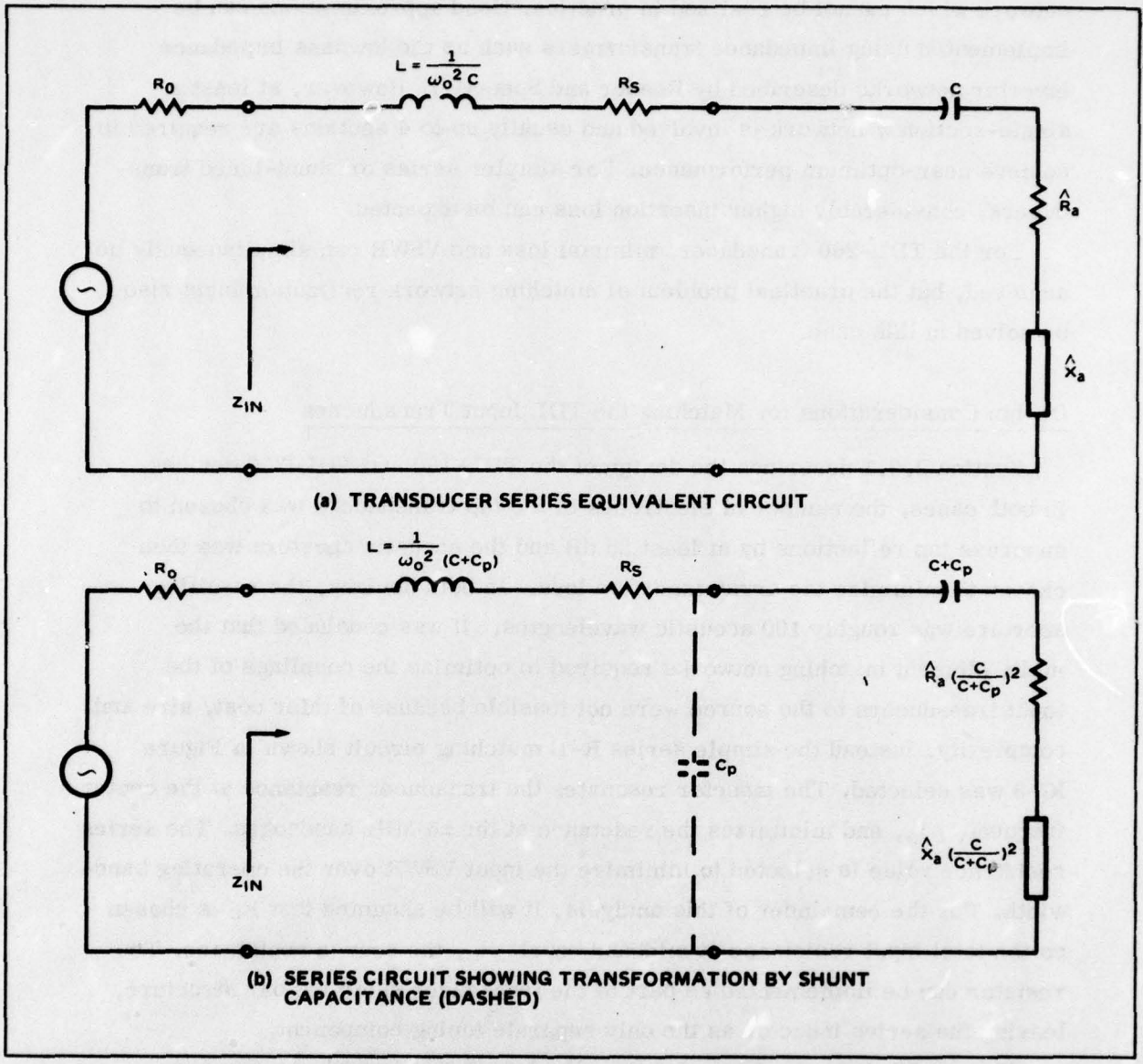


Figure I-C-3. Transducer Series Equivalent Circuits with Series R-L Tuning

bandedges is within 0.91 dB of the theoretical value. In constrast, the results for the TDL-100 are not acceptable, and it is evident that the electrical network narrowbands the input transducer response. This explains the experimental observation described in Section 2.3.2.2 where signal cancellation near phase reversals of the TDL-100 impulse response occurred when series tuning was applied. The narrowbanding spreads the impulse response of the input transducer so that adjacent chips in the TDL-100 output waveform overlap, and thereby tend to cancel when phase reversals occur.

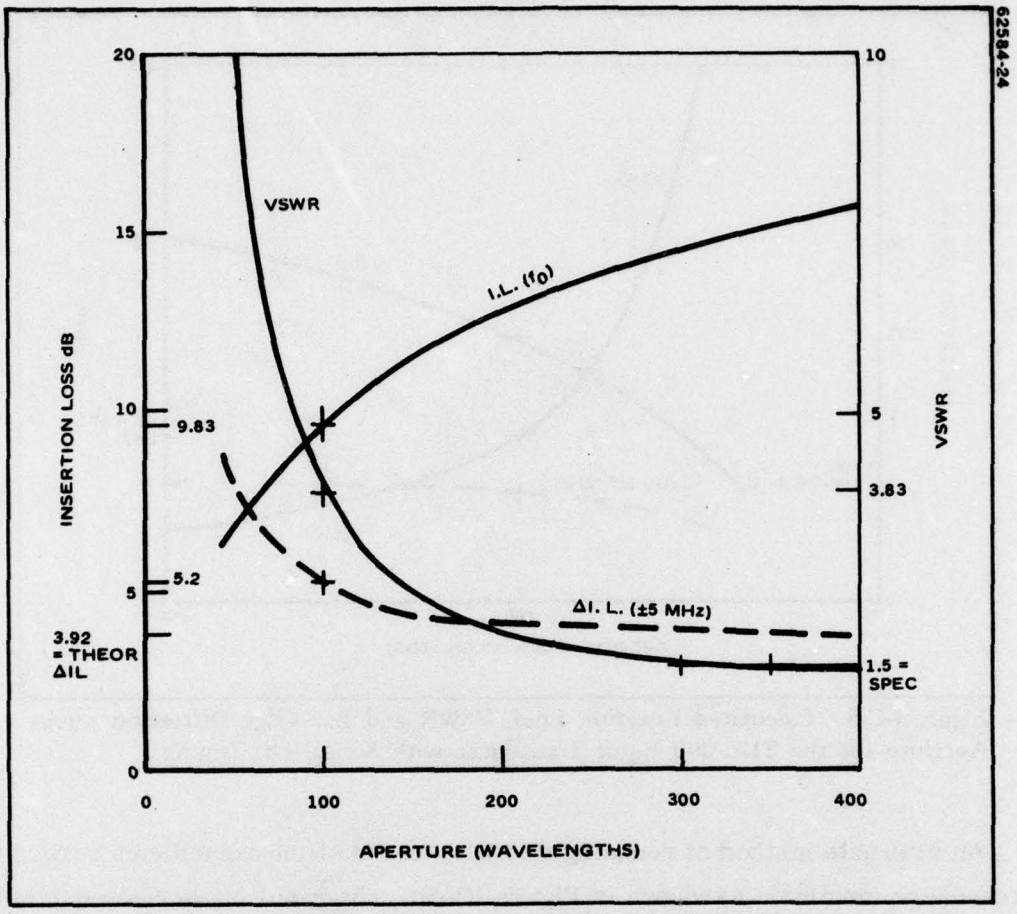


Figure I-C-4. Calculated Insertion Loss, VSWR and Bandedge Distortion versus Aperture for the TDL-100 Input Transducer with Series R-L Tuning

## Improvements to the TDL-100 Matching Network

It is evident from Figure IC-4 that if the input transducer aperture was a design variable (which it is not), then the required VSWR limit of 1.5:1 could be met with an aperture of 350 wavelengths, at the expense of 5.5 dB additional insertion loss. This amounts to reducing the Q of the input impedance at the source terminals, which is given by

$$Q_{in} = \frac{1}{\omega_o(R_s + \overset{A}{R}_A)C} = \frac{1}{\omega_o R_o C} \qquad (7)$$

where C is now larger because of the increased aperture size.

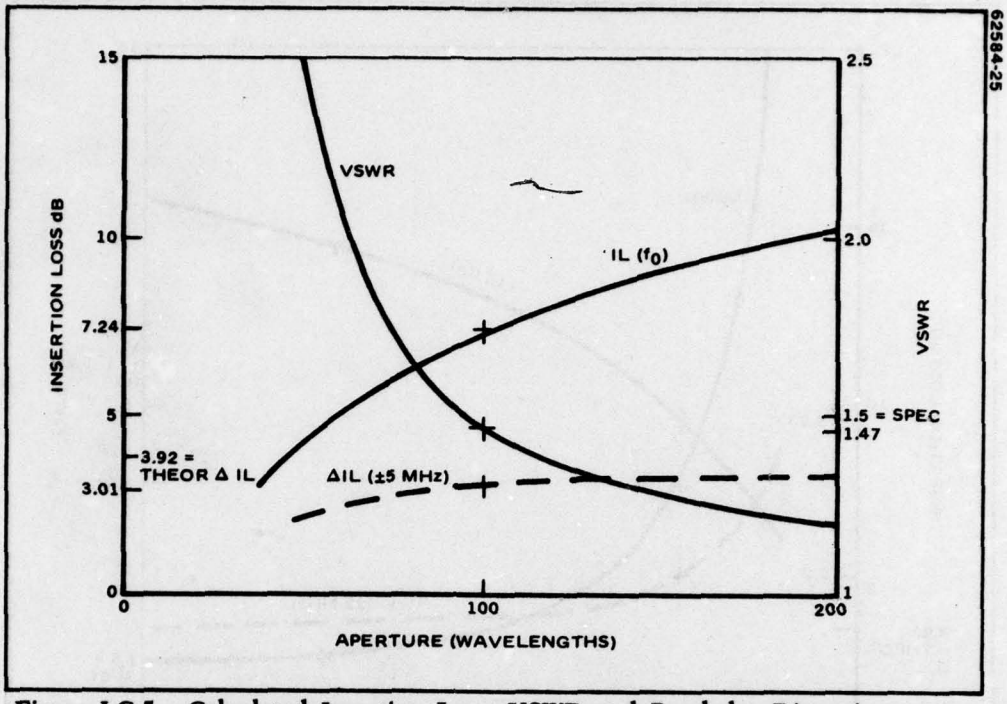


Figure I-C-5. Calculated Insertion Loss, VSWR and Bandedge Distortion versus Aperture for the TDL-200 Input Transducer with Series R-L Tuning

An alternate method of reducing this Q is to add shunt capacitance across the transducer terminals as shown in Figure IC-3b. The resulting series equivalent circuit illustrates that the acoustic radiation impedance is reduced while the net series capacitance is increased. By again increasing $R_s$ so that the net input resistance at center frequency equals $R_o$, the Q of the input impedance becomes

$$Q_{in} = \frac{1}{\omega_o R_o (C + C_p)} \tag{8}$$

Figure IC-6 illustrates the dependence of the TDL-100 insertion loss and VSWR on the ratio Cp/C. In order to achieve a maximum VSWR ≤ 1.5:1 the ratio Cp/C = 2.5 which results in a minimum insertion loss of 21 dB. When this loss is added to the estimated 25 dB loss of the tap array, the minimum TDL-100 insertion loss is 46 dB compared to the specification of 30 ± 3 dB. Even if the theoretical limit of 8.8 dB, derived previously for the TDL-100 input transducer, could be achieved, the VSWR and insertion loss requirements could not be met simultaneously. This confirms the presumptions made in the Hughes proposal.

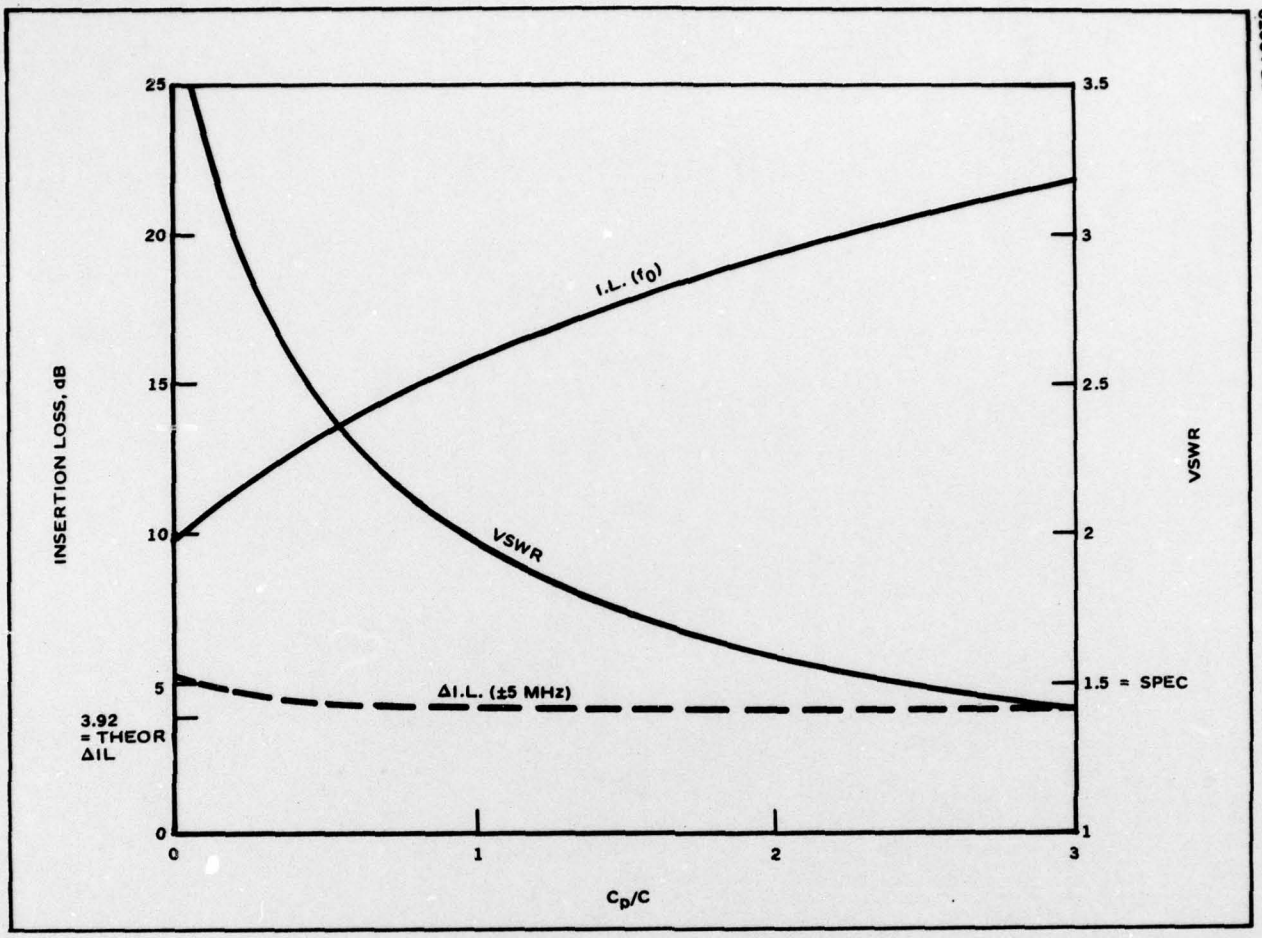


Figure I-C-6. Calculated Insertion Loss, VSWR and Bandedge Distortion versus $C_p/C$ for the Current TDL-100 Input Transducer with Series R-L Tuning

Obviously, the specifications must be modified, and Hughes recommends that the insertion loss be increased to 40 ± 3 dB and the VSWR ≤ 2.5:1 over the operating band. This will allow the use of shunt capacitance values in the range of $0.5 \leq Cp/C \leq 1.5$. (See Figure IC-6.)

## REFERENCES

(1) T.M. Reeder and W.R. Sperry, "Broad-Band Coupling to High-Q Resonant Loads", IEEE Trans Microwave Theory and Tech. Vol. MTT-20, No. 7, pp. 453-458, July 1972.

(2) H.M. Bode, Network Analysis and Feedback Amplifier Design, New York, Van Nostrand, 1945, pp. 360-371.

(3) R.M. Fano, "Theoretical Limitations on Broadband Matching of Arbitrary Impedances", J. Franklin Inst., Vol. 249, pp. 57-84 and 139-154, Jan.-Feb. 1950.

# APPENDIX IV
# EFFECTS OF IMPEDANCE MISMATCH ON SYSTEM PERFORMANCE

# APPENDIX IV

## EFFECTS OF IMPEDANCE MISMATCH ON SYSTEM PERFORMANCE

Appendix III contains an analysis of impedance matching to Surface Acoustic Wave (SAW) transducers. There, it is pointed out that the input impedance of most SAW transducers has an inherently high-Q characteristic, and that optimum coupling to an external circuit results in a tradeoff between VSWR and insertion loss. Generally, insertion loss must be increased substantially in order to reduce VSWR to below 1.5:1. However, SAW devices operate in the VHF and UHF ranges where the deleterious effects of impedance mismatches are often minimal. It is therefore important to characterize these effects and to determine the design constraints which can make high VSWR acceptable in an electronic system.

The problem to be analyzed is depicted in Figure ID-1. The SAW device, including its transducer matching networks, is characterized by impedances $Z_2$ and $Z_3$ at its input and output ports, respectively. It is driven by a source with a port impedance, $Z_1$ through a transmission line of length, $L_1$, and characteristic impedance $Z_o$. The load network is connected with a similar transmission line of length, $L_2$. It will be assumed that the transmission lines are lossless, in which case $Z_o$ is real and perfect matching occurs when

$$Z_i = Z_o, \qquad i = 1, 2, 3, 4 \tag{1}$$

The voltage reflection coefficients, given by

$$\Gamma_i = \frac{Z_i - Z_o}{Z_i + Z_o} \tag{2}$$

are then zero, the corresponding VSWR, given by

$$\rho_i = \frac{1 - |\Gamma_i|}{1 + |\Gamma_i|} \tag{3}$$

are unity, and power transfer is maximized. In practice, (1) cannot be satisfied at all frequencies which results in the following potential problems

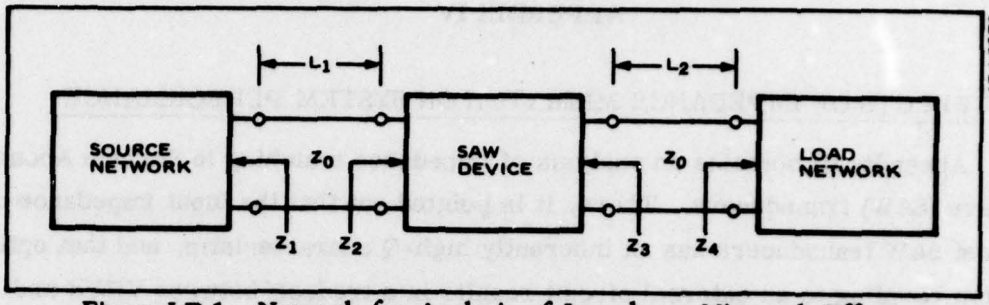


Figure I-D-1. Network for Analysis of Impedance Mismatch Effects

- impedance mismatch loss
- distortion due to "transmission line effects"
- instability and increased noise figure of active source and load networks

Each of these problems will now be analyzed and shown to be tolerable in most SAW device applications.

Impedance Mismatch Loss

The power transfer efficiency at a port is given by

$$\eta_i = 1 - |\Gamma_i|^2 \qquad (4)$$

Hence, insertion loss results from impedance mismatch. Aside from bidirectionality loss, the insertion loss of a SAW device is predominantly mismatch loss because the acoustic propagation loss is generally negligible. The transducer impedance mismatch is often a result of its high Q characteristic, but in many cases, mismatch is intentionally incorporated to minimize distortions due to acoustic reflections and external circuit effects (regeneration). In either event, minimization of the impedance mismatch at the SAW device ports requires the addition of padding resistance to the matching network which increases the device insertion loss.

The conclusion is that high VSWR in a SAW device does not necessarily imply maximum insertion loss, and in fact, insertion loss must generally be increased to minimize VSWR. Therefore, impedance mismatch loss is not an

important consideration in determining the tolerable VSWR for most practical SAW devices.

Transmission Line Effects

Whenever the electrical length of the transmission line interconnecting two networks is an appreciable fraction of the wavelength, multiple transit electromagnetic echos due to port reflections can result in significant amplitude and phase distortions. To analyze this effect, consider the driving network of the SAW device depicted in Figure ID-1. When $Z_1$, $Z_2 \neq Z_o$, multiple reflections of the original incident signal occur, and the total excitation at the SAW device input port is given by

$$S_2(f) = S(f)(1-\Gamma_2)\left|1+\Gamma_1\Gamma_2 \exp\left[i4\pi fT_1\right]\right. \tag{5}$$

$$\left. + (\Gamma_1\Gamma_2)^2 \exp\left[i8\pi fT_1\right] + \ldots .\right|$$

where S(f) is the Fourier transform of incident excitation signal and $T_1$ is the electromagnetic time delay for the transmission line of length, $L_1$. A convenient closed form expression for (5) is

$$S_2(f) = S(f)(1-\Gamma_2)\left(\frac{1}{1-\left|\Gamma_1\right|\left|\Gamma_2\right| \exp\left[i(4\pi fT_1+(\theta_1+\theta_2))\right]}\right) \tag{6}$$

where $\theta_1$ and $\theta_2$ are the phases of the reflection coefficients, $\Gamma_1$ and $\Gamma_2$, respectively. Equation (6) can be manipulated into the polar form:

$$S_2(f) = S(f)(1-\Gamma_2)\left[\frac{1}{1+(\left|\Gamma_1\right|\left|\Gamma_2\right|)^2-2\left|\Gamma_1\right|\left|\Gamma_2\right|\cos\left[4\pi fT_1+(\theta_1+\theta_2)\right]}\right]$$

$$\exp\left(-i\left[\frac{\left|\Gamma_1\right|\left|\Gamma_2\right|\sin\left[4\pi fT_1+(\theta_1+\theta_2)\right]}{1-\left|\Gamma_1\right|\left|\Gamma_2\right|\cos\left[4\pi fT_1+(\theta_1+\theta_2)\right]}\right]\right) \tag{7}$$

The term, $S(f)(1-\Gamma_2)$, is the excitation at the SAW device terminals in the absence of any echos. Therefore, the term in brackets accounts for amplitude distortions due to the multiple electromagnetic echos while the exponent contains the phase distortion. Several conclusions can be derived from (7).

- If either $|\Gamma_1|$ or $|\Gamma_2| = 0$, all distortions vanish. In practice, this can only be approximated. For example, sources and loads for SAW devices are usually amplifiers. General purpose, broadband amplifiers are specified to have VSWR <2:1 for which $|\Gamma| < 0.33$, while custom narrowband amplifiers can be designed for maximum VSWR as small as 1.2:1 ($|\Gamma| < 0.1$).

- The effects of reflections depend strongly on the time delay, $T_1$, of the interconnection cable. When $T_1$ is comparable to the frequency period, the amplitude distortion is oscillatory with a peak-to-peak value given by

$$\Delta|S_2(f)| = \frac{1+|\Gamma_1||\Gamma_2|}{1-|\Gamma_1||\Gamma_2|} \tag{8}$$

which is plotted in Figure ID-2. From Figure ID-2, it is evident that when $T_1$ is large, impedance mismatches must be minimized to eliminate unacceptable distortions. However, SAW devices are more typically used in IF circuits where they are in close proximity to the source and load networks. The delay, $T_1$, is then sufficiently small that the frequency dependence of the trigonometric function arguments in (7) is due primarily to $\theta_1$ and $\theta_2$. Assuming that $\theta_1, \theta_2 = 0$, the amplitude distortion is given by

$$\Delta|S_2(f)| = \frac{1}{1-|\Gamma_1||\Gamma_2|} \tag{9}$$

which is plotted in Figure ID-3. In practice $|\Gamma_1|$ and $|\Gamma_2|$ vary slowly with frequency so that this effect can be either neglected, or it can be compensated in the SAW device design. The important conclusion here is that although impedance mismatch results in loss due to reflections, short interconnecting transmission lines minimize the frequency dependence of the loss. Moreover, as discussed earlier, it is often undesirable to minimize impedance mismatch because the commensurate increase in SAW device insertion loss more than offsets the reduction in mismatch loss.

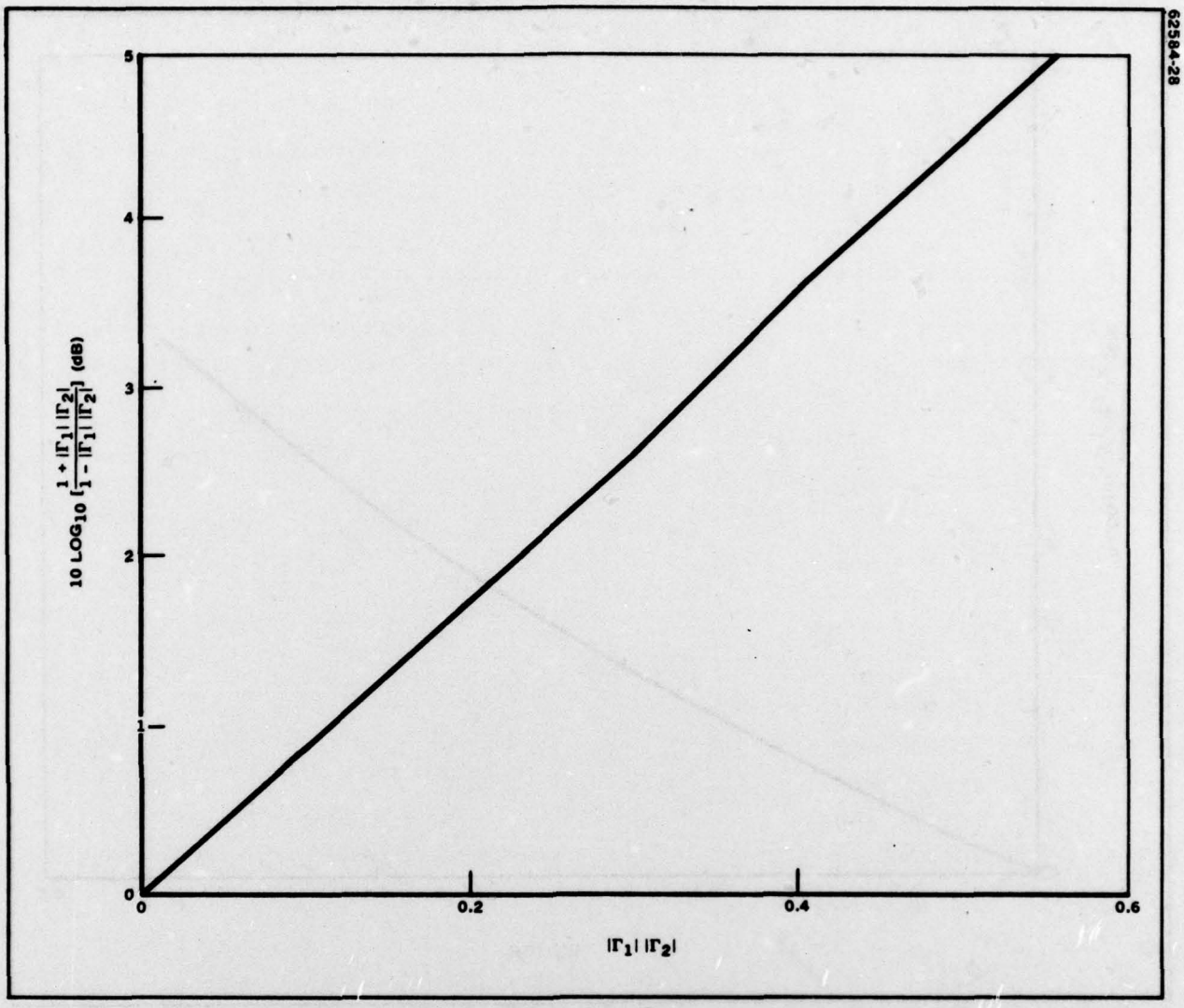


Figure I-D-2. Excitation Amplitude Ripple $\Delta|S_2(f)|$ (eqn 8) versus $|\Gamma_1|\ |\Gamma_2|$ for Large $T_1$

## Effects on Active Networks

Formerly, input and output impedance mismatches could affect both the stability and noise figure of amplifiers. However, nearly all commercially available amplifiers are designed to have characteristics which are independent of external impedances, i.e., they are unconditionally stable. One exception is the noise figure which can vary by as much as 1 to 2 dB as a function of termination impedances. This is seldom an important factor, however, because the reduced SAW device insertion loss associated with the mismatch can produce a net increase in signal/noise. In cases where signal/noise must be

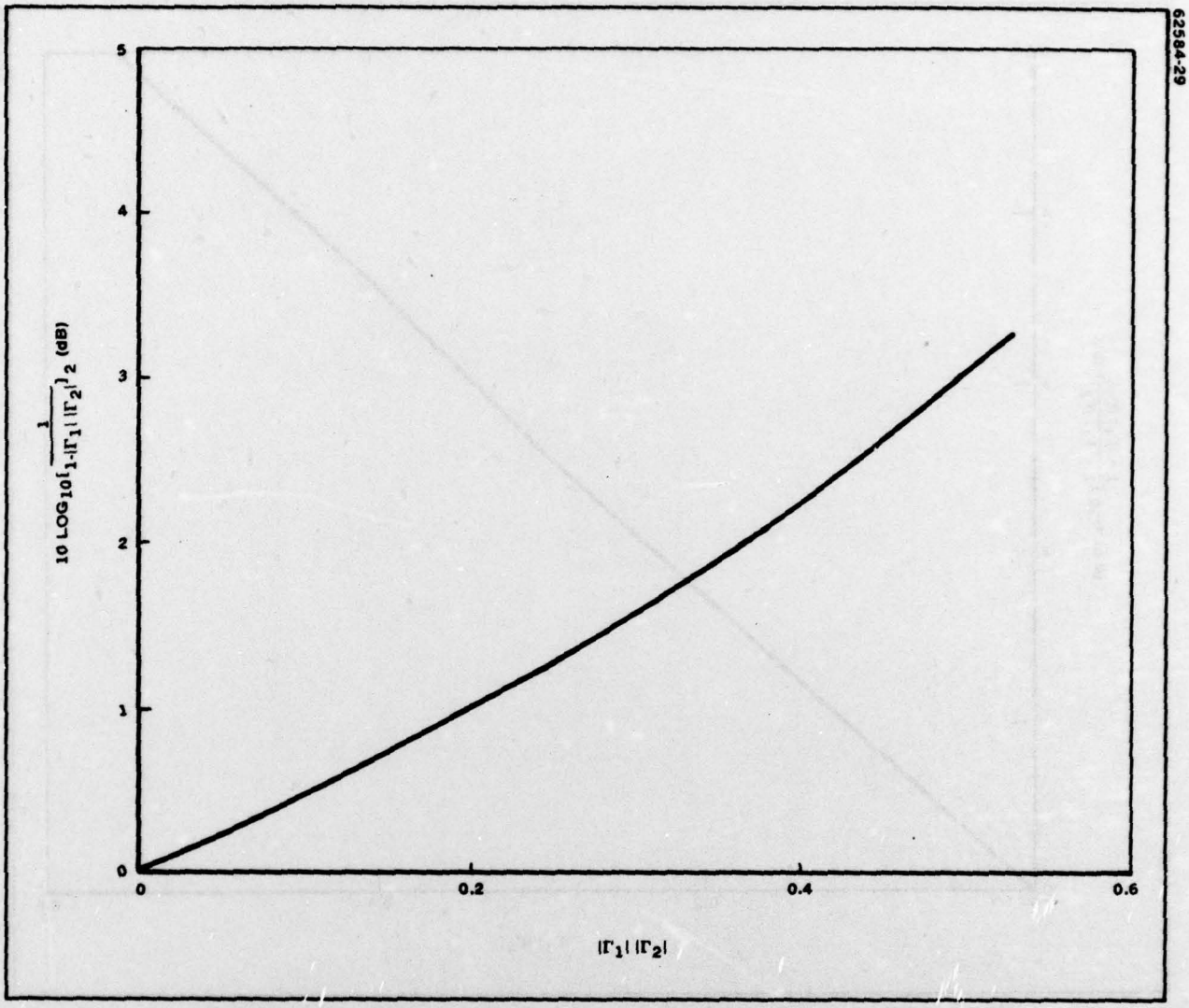


Figure I-D-3. Mismatch Loss (eqn 9) versus $|\Gamma_1|\ |\Gamma_2|$ for $T_1 \rightarrow 0$

**maximized, an amplifier can be designed to have its optimum noise figure for an arbitrary impedance level.**

# APPENDIX V
# OPERATING CHARACTERISTICS OF LINEAR FM CHIRP SYSTEMS

*HUGHES-FULLERTON*
*Hughes Aircraft Company*
*Fullerton, California*

## APPENDIX V

## OPERATING CHARACTERISTICS OF LINEAR FM CHIRP SYSTEMS

The generally accepted method of defining the operating parameters of a linear FM chirp system is to specify the instantaneous operating bandwidth and differential time delay of the transmitted signal. The time and frequency domain characteristics of a waveform having a bandwidth, $\beta$, and a differential delay, T, are shown in Figure IB-1.

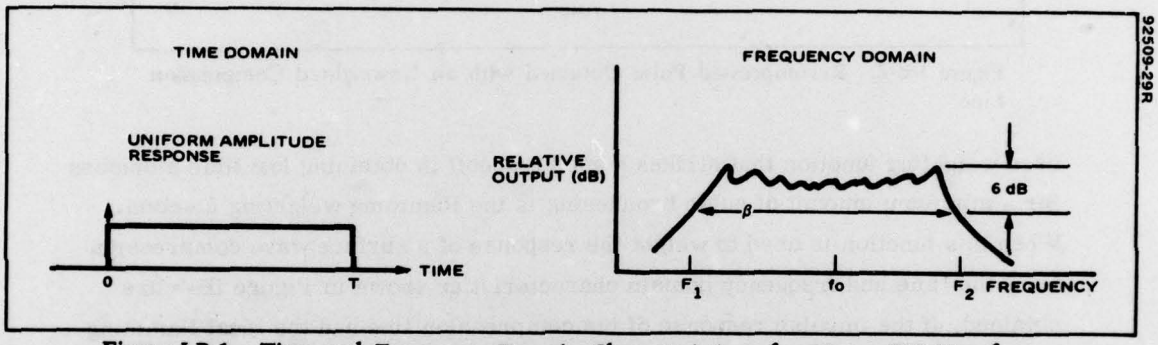


Figure I-B-1. Time and Frequency Domain Characteristics of a Linear FM Waveform

As shown in the figure, the time domain response is assumed to be flat over the pulse length, T. The instantaneous frequency of the carrier varies linearly between the extremes $F_1$ and $F_2$ which define the characteristic bandwidth to be $\beta$ $(F_2 - F_1)$. The spectrums of this waveform has a nominally rectangular envelope response whose -6 dB bandwidth is equal to $\beta$. If this waveform were correlated in a matched unweighted compression line having the opposite chirp slope, the recompressed pulse shown in Figure IB-2 would be obtained. With no weighting, the close in sidelobes would be 13 dB down from the peak output response. The -4 dB width of the recompressed pulse would be equal to $1/\beta$ while its null width would equal $2/\beta$. The ratio of the transmitted pulse length to the -4 dB width of the recompressed pulse would be $T/(1/\beta)$ or $T\beta$. Thus the pulse compression ratio of an unweighted chirp system is equal to the product of the transmitted pulse length times its instantaneous operating bandwidth.

In most systems, it is desirable to reduce the amplitude of the time sidelobes in the recompressed pulse by including some form of weighting in the receiver. This weighting also broadens the width of the recompressed pulse and thus some range resolution must be sacrificed to obtain low time sidelobes. A commonly

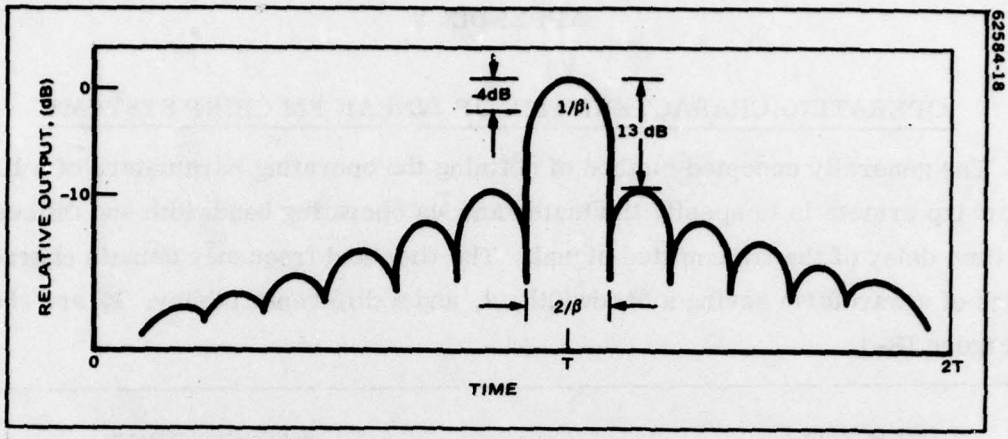


Figure I-B-2. Recompressed Pulse Obtained with an Unweighted Compression Line

used weighting function that strikes a good tradeoff in obtaining low time sidelobes for a minimum amount of pulse broadening is the Hamming weighting function. When this function is used to weight the response of a surface wave compression line, the time and frequency domain characteristics shown in Figure IB-3 are obtained. If the impulse response of the compression line had the ideal Hamming weighted envelop response, then its spectrum would have a -28dB width equal to the instantaneous bandwidth, $\beta$, of the compression line.

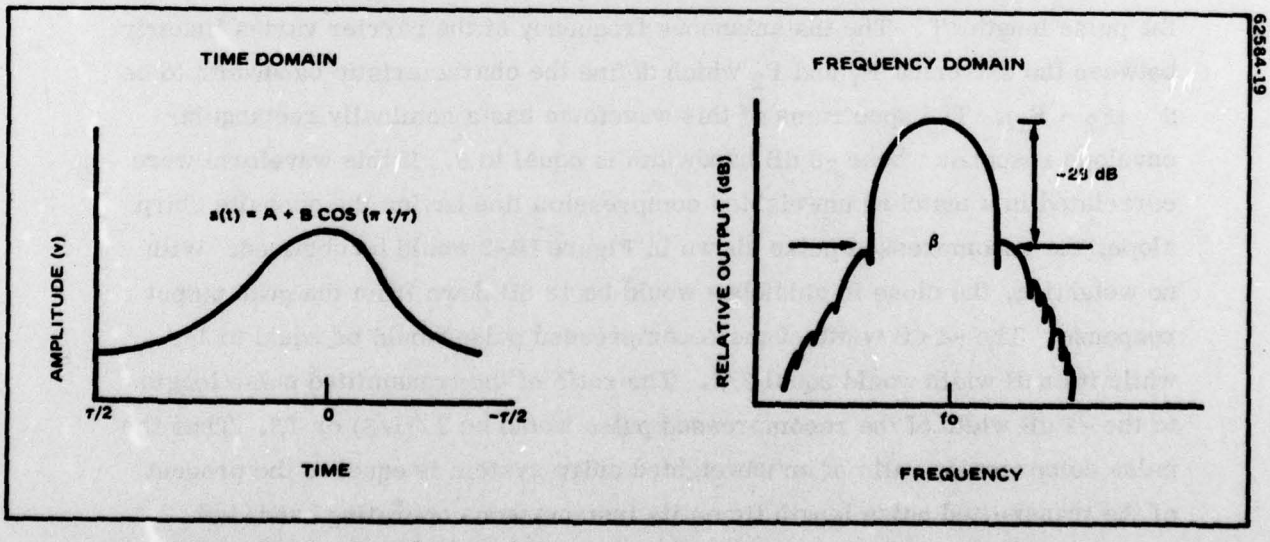


Figure I-B-3. Waveform and Spectrum of a Hamming Weighting Function

The ideal recompressed pulse that would be obtained in a large time bandwidth (>100) chirp system using this type of weighting in the receiver is shown in Figure IB-4. The peak output response obtained with this weighting would be about 5.4dB down from the peak level obtained in an unweighted chirp system. The noise level at the output of the weighted line would be 4dB down from the noise level expected for an unweighted line. Consequently, the signal to noise ratio obtained with the weighted line is about 1.4dB smaller than the level that would be achieved with a matched filter (unweighted line) in the receiver.

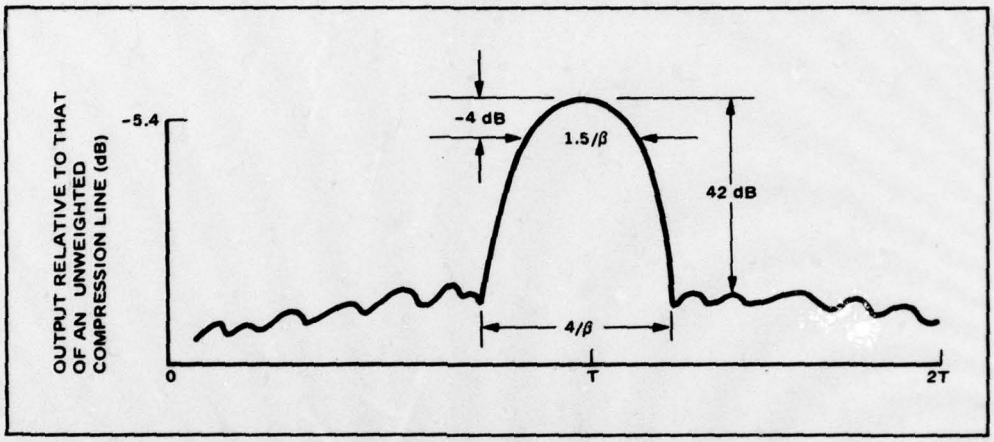


**Figure I-B-4. Ideal Recompressed Pulse that would be Obtained with Hamming Weighting in a Large Time – Bandwidth Product Chirp System**

With no amplitude or phase errors in the system, the close in time sidelobes would be 42dB down from the peak output response. The -4dB pulse width would be 1.5 times wider than the $1/\beta$ width obtained with an unweighted line. Consequently, the ratio of the transmitted pulse length to the -4dB width of the recompressed pulse would be $T\beta/1.5$ which means that the pulse compression ratio of a weighted system is about 33% smaller than the time bandwidth product of the transmitted pulse.

# APPENDIX VI
# PROCEDURE FOR CHECKING THE SENSE OF THE Y-ROTATION FOR ST-CUT QUARTZ

# APPENDIX VI

## PROCEDURE FOR CHECKING THE SENSE OF THE Y-ROTATION FOR ST-CUT QUARTZ*

1. The ST-cut (+42 3/4° rotated Y-cut) is near the (011) reflection (+38° 13')
2. The $(01\bar{1})$ reflection is rotated in the opposite direction (-38° 13' rotated Y)
3. X-ray intensity from the (011) is 2 to 4 times more intense than from the $(01\bar{1})$, using copper radiation at $2\theta = 26.65^{\circ}$, i.e.,

$$^{ie}I_{(011)} = 2 \text{ to } 4\ I_{(01\bar{1})}$$

Procedure:

1. Rotate blank (about X) 38° 13' from Y toward Z and measure intensity.
2. Then rotate in opposite direction 38° 13' from Y to opposite Z and measure intensity.
3. The higher intensity plane is within a few degrees of the ST-cut.

*S. Roth, Valpey-Fisher Corp., Hopkinton, MA

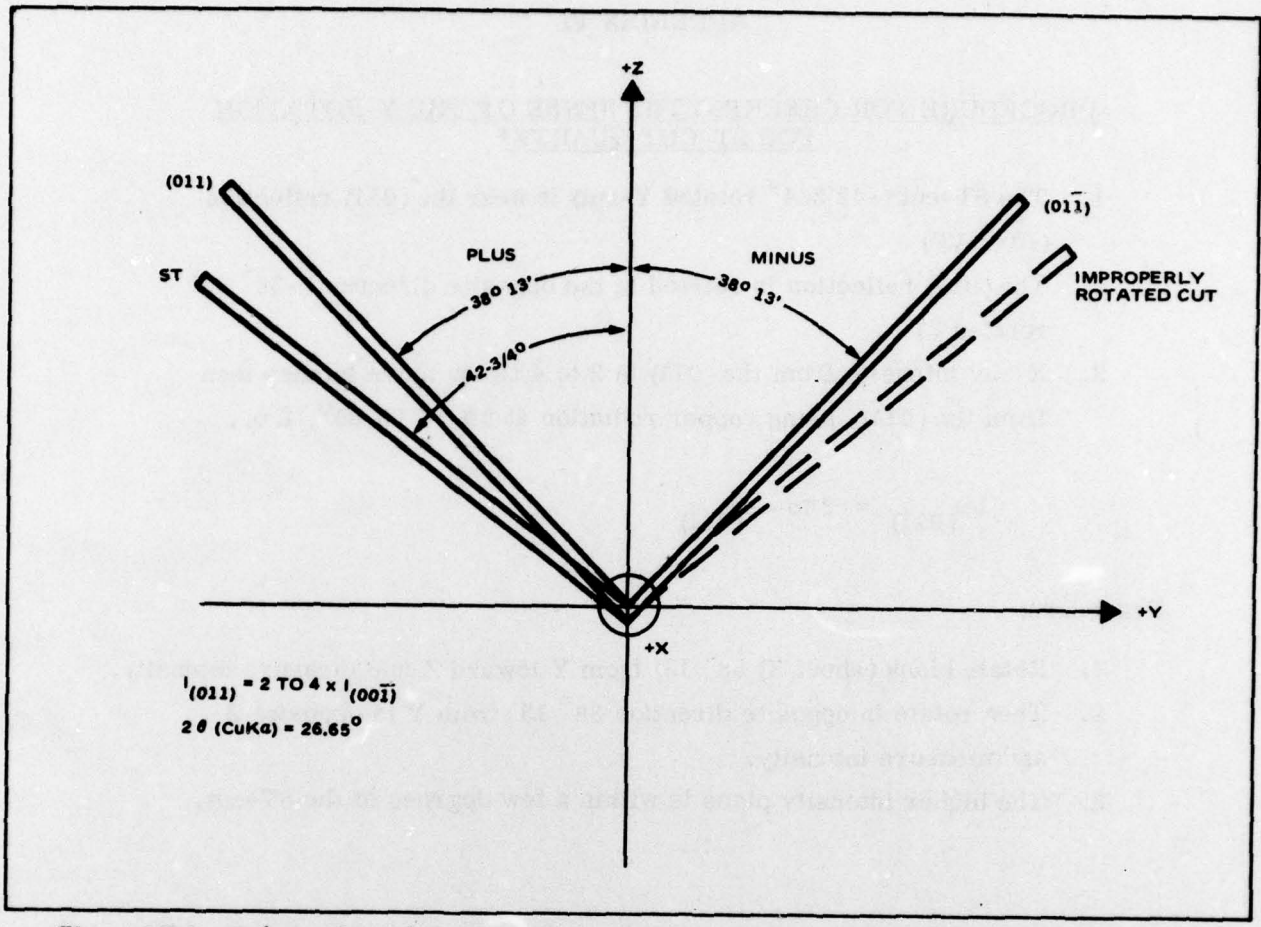


**Figure I-E-1. Relationship of the 011 Plane of Quartz to the Proper ST-Y Rotation of Quartz**

## DISTRIBUTION LIST

101 Defense Documentation Center
Attn: DDC-TCA
Cameron Station (Bldg 5)
*012 Alexandria, VA 22314

Naval Research Laboratories
Code 5237
Washington, D.C. 20375
001 Attn: Dr. D. Webb

307 HQ ESD (DRI)
L.G. Hanscom AFB
001 Bedford, MA 01731

Army Materials and Mechanics
Research Center (AMMRC)
Watertown, MA 02172
001 Attn: DMXMR-EO

437 Deputy For Science & Technology
Office, Assist Sec Army (R&D)
001 Washington, DC 20310

481 Harry Diamond Laboratories,
Dept of Army
Attn: Mr. S. Lieberman
2800 Powder Mill Road
001 Adelphi, MD 20783

511 Commander, Picatinny Arsenal
Attn: SARPA-FR-S
Bldg. 350
001 Dover, NJ 07801

680 Commander
US Army Electronics R&D Command
000 Fort Monmouth, NJ 07703

1 DELEW-D
2 DELCS-D
1 DELSD-AS
1 DELET-DD
1 DELET-DT
1 DELET-P
1 DELSD-L (Tech Lib)
1 DELSD-D
1 Originating Office DELET-MM

*Decrease to 2 copies if report is not releasable to public. See ECOMR 70-31 for types of reports not to be sent to DDC.

703 NASA Scientific & Tech Info Facility
Baltimore/Washington Intl Airport
001 P.O. Box 8757, MD 21240

705 Advisory Group on Electron Devices
201 Varick Street, 9th Floor
002 New York, NY 10014

Commanding General
US Army Electronics Research and
Development Command
2800 Powder Mill Road
Adelphi, MD 20783

ATTN: DRDEL-CT - 2 copies
ATTN: DRDEL-PAO
ATTN: DRDEL-LL/DRDEL-SB/DRDEL-EA
ATTN: DRDEL-AP - 2 copies
ATTN: DRDEL-PR
ATTN: DRDEL-PA/DRDEL-ILS/
DRDEL-E'

Mr. E. Stern
MIT
Lincoln Laboratories
P.O. Box 73
001 Lexington, Massachusetts 02173

Dr. R. La Rosa
Hazeltine Corporation
001 Greenlawn, New York 11740

General Electric Co.
Electronics Lab
Electronics Park
Syracuse, N.Y. 13201
001 ATTN: Dr. S. Wanuga

Air Force Cambridge Labs
ATTN: CRDR (Dr. P. Carr
& Dr. A. J. Slobodnik)
001 Bedford, MA 01730

Mr. H. Bush CORC
RADC
Griffiss Air Force Base,
001 NY 13440

Commander, AFAL
ATTN: Mr. W. J. Edwards, TEA
001 Wright-Patterson AFB, Ohio 45433

DISTRIBUTION LIST (Continued)

Andersen Laboratories, Inc.
1280 Blue Hills Ave.
ATTN: Tom A. Martin
001 Bloomfield, Conn. 06002

Mr. Henry Friedman
RADC/OCTE
001 Griffiss AFB, N.Y. 13440

Autonetics, Division of North American Rockwell
P.O. Box 4173
3370 Miraloma Avenue
Anaheim, California 92803
001 ATTN: Dr. G. R. Pulliam

General Dynamics, Electronics Division
P.O. Box 81127
San Diego, CA 92138
001 ATTN: Mr. E. D. Bowen

Texas Instruments, Inc.
P.O. Box 5936
13500 N. Central Expressway
Dallas, Texas 75222
001 ATTN: Mr. L. T. Clairborne

Raytheon Company
Research Division
28 Seyon Street
Waltham, Massachusetts 02154
001 ATTN: Dr. M. B. Schulz

Sperry Rand Research Ctr
100 North Road
Sudbury, Massachusetts 01776
001 ATTN: Dr. H. Van De Vaart

Westinghouse Electric Corp.
Research & Development Ctr
Beulah Road
Pittsburgh, PA 15235
001 ATTN: Dr. J. DeKlerk

International Business Machines Corp.
Research Division
P.O. Box 218
Yorktown Heights, NY 10598
001 ATTN: Dr. F. Bill

TRW
Defense and Space Systems Group
One Space Park
Redondo Beach, CA 90278
001 ATTN: Dr. R. S. Kagiwada

Tektronix Inc.
P.O. Box 500
Beaverton, OR 97077
001 ATTN: Dr. R. Li

Dr. Fred S. Hickernell
Integrated Circuit Facility
Motorola Govt.
Electronics Div.
8201 East McDowell Road
001 Scottsdale, Arizona 85257

United Aircraft Research Labs
ATTN: Dr. Thomas W. Grudkowski
001 East Hartford, Conn. 06108

Science Center
Rockwell International
Thousand Oaks, CA 91360
001 ATTN: Dr. T. C. Lim

SAWTEK, Inc.
P.O. Box 7756
2541 Shader Rd.
Orlando, FL 32854
001 ATTN: Mr. S. Miller